

Dissertation on
TIME VARIATION OF COSMIC RAY INTENSITY
AND OF GEOMAGNETIC FIELD

Presented
by
K. NARAYANAN NAIR
for the degree of
DOCTOR OF PHILOSOPHY
of the
University of Kerala

043



B4200

June 1971

Physical Research Laboratory
Ahmedabad
India.

STATEMENT

The electromagnetic state of the interplanetary medium is a subject of great interest. Studies of cosmic ray time variations and geomagnetic field perturbations provide excellent means of probing the spatial and temporal variations of the plasma in interplanetary space.

The investigations reported in this thesis cover: (a) A study using crossed East-West cosmic ray telescopes at an equatorial station. A comparison of the daily variation of the intensity measured by the two telescopes, as they scan the celestial sphere provides a clue to the relative contributions of the anisotropy of primary cosmic rays and of a source due to an uncorrected meteorological effect or of other local origin. Chapters 1 and 2 deal with this study. (b) Using the records of magnetometers from low latitude stations, the extent to which the features of the daily variation of H can be related to the characteristics of the interplanetary plasma impinging on the magnetosphere are investigated. Chapters 3 and 4 summarise these investigations. (c) In Chapter 5 the summary and the conclusions of the above studies are reported. Therein it is also pointed out how ΔH , the daily range of the horizontal component of the earth's magnetic field at a low latitude station away from the effects of the equatorial electrojet, can be used for probing the electromagnetic state of interplanetary space, in the neighbourhood of the earth.

In April 1963 the author undertook the construction of directional counter telescopes pointing to east and west at

Trivandrum (Geographic latitude 8.4° N and geographic longitude 76.9° E) close to the dip equator. The unit functioned from January 1964 to December 1966. The author also maintained vertical meson telescopes which were already in operation at Trivandrum. The author was closely associated with the construction of all the Geiger counters used in the units. Data for the period January 1964 to December 1966 is analysed.

For the study of the solar wind-magnetosphere interaction, the author used geomagnetic field data from Alibag (Geomagnetic latitude 9.5° N), Honolulu (Geomagnetic latitude 21.3° N), Guam (Geomagnetic latitude 4.0° N) and Trivandrum (Geomagnetic latitude 1.1° S) along with solar wind plasma data from IMP-1 satellite and interplanetary magnetic field data from satellites IMP-1, IMP-3 and Explorer-33.

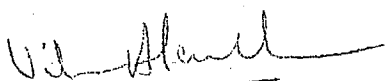
The material presented in the thesis covers the following investigations:

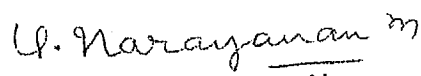
- (a.1) Computation of the variational coefficient for deriving the effect related to the primary component of cosmic-ray, from the observed variations of the secondary intensity, by directional telescopes.
- (a.2) Patel et al (1968) have reported the direction and amplitude in space of the diurnal and semi-diurnal anisotropy and β , the exponent of the variational part of the energy spectrum of the primary anisotropy on a day-to-day basis. Using their values, the expected

amplitude and phase of the diurnal and semi-diurnal components due to primary anisotropy at the respective instruments (along east, vertical and west directions) at Trivandrum on a day-to-day basis for the period 1964 to 1966 are evaluated. The modulation of ~~M~~meson intensity, probably due to temperature variations in the atmosphere is studied through a comparison of the observed pressure-corrected daily variation and the computed daily variation.

- (b.1) The question whether ΔH , the daily range of the horizontal component of the earth's magnetic field at a low latitude station away from the effects of the equatorial electrojet represents primarily an increase on the day side over a base level H_{minimum} or alternatively it is a decrease on the night side from a base level at H_{maximum} is investigated.
- (b.2) The ionospheric and magnetospheric contributions to ΔH are estimated.
- (b.3) Investigation of the strength of the equatorial electrojet in relation to the drift speeds of the irregularities in the E and F regions of the ionosphere at Trivandrum is carried out
- (b.4) A study of the enhancement of the equatorial electrojet during equinoxes is made.

- (b. 5) The deformation of the magnetosphere by the impact of the solar plasma and its effects on ΔH are studied.
- (b. 6) The effects caused by the fluctuations of the north-south component of the interplanetary magnetic field, on ΔH are looked into.
- (b. 7) The experimentally observed shift of the time of minimum of H from morning hours during quiet days to evening hours during disturbed days is examined on the basis of the drift motion of charged particles, injected through the tail of the magnetosphere in the presence of a co-rotational electric field and geomagnetic field gradients.
- (c) Relative contributions of (i) the dynamo current mainly at the ionospheric E-region (ii) the surface currents at the magnetopause and (iii) the currents in the magnetosphere namely the tail currents, the eccentric ring current and the partial ring current, to ΔH are examined.


(VIKRAM A. SARABHAI)


(K. NARAYANAN NAIR)

27/6/1971.

ACKNOWLEDGEMENT

The author wishes to acknowledge with gratitude his indebtedness to Prof. Vikram A. Sarabhai for his guidance, supervision and encouragement in carrying out the work presented in this thesis.

The author is thankful to Professors R. P. Kane, N.W. Nerurkar, P.D. Bhavsar, U.R. Rao, R.G. Rastogi, P.R. Pisharoty, and to his colleagues Drs. M.S. Dhanju, P.N. Pathak, D.M. Patel and Mr. L.V. Kargathra for useful discussions. The author is thankful to Mr. S.R. Thakore, Chief of the Computing Centre, Physical Research Laboratory, for giving the computer facilities.

Thanks are due to Messrs. M.V. Bhavsar, D.K. Patel and K.C. Patel for their help in processing of the data, and to Mr. K.P.G. Nair for neat typing of the thesis.

The author is grateful to Dr. B.N. Bhargava for supplying unpublished magnetic data from Alibag, to Dr. H.S. Bridge for supplying the solar wind plasma data from IMP-1 satellite and to Dr. C.P. Sonett for making available to the author the unpublished interplanetary magnetic field data from satellite Explorer-33. Thanks are due to Dr. N.F. Ness and to the Director, World Data Centre-A, Greenbelt for supplying interplanetary magnetic field data from satellites IMP-1 and IMP-3.

The author is grateful to the Department of Atomic Energy, Government of India, for financial support.

K. NARAYANAN NAIR

The work presented in this thesis has been published in various international journals and presented in various international symposia.

- (1) Geomagnetic Plasma Probe for Solar Wind; Sarabhai, V. and K. N. Nair, Proc. of the Indian Ac. Science, Vol. LXIX, pp. 291-306, 1969.
- (2) Daily Variation of the Geomagnetic Field and the Deformation of the Magnetosphere; Sarabhai, V. and K. N. Nair, Nature, Vol. 223, No. 5206, pp. 603-605, 1969.
- (3) Daily variation of the Geomagnetic Field at the Dip Equator; Nair, K. N., R. G. Rastogi and V. Sarabhai, Nature, Vol. 226, No. 5247, pp. 740-741, 1970.
- (4) Morphology of the Geomagnetic Field Variations and a Study of the Interplanetary Magnetic Field Fluctuation in relation to the Daily Variation of the Geomagnetic Field at Low Latitudes; Sarabhai, V and K. N. Nair, In press, Cosmic Electrodynamics, 1971.
- (5) Variational Coefficients for Vertical and Inclined Meson Telescopes with Application to the Daily Variation, for Trivandrum; Nair K. N., Proc. of the X-Symposium on "Cosmic ray, Elementary Particle Physics and Astrophysics", Aligarh, pp. 149-151, 1967.
- (6) Experimental Determination of Temperature Effect on μ Mesons recorded at Trivandrum; Nair K. N. and V. Sarabhai, Proc. of the Symposium on "Cosmic rays, Elementary Particle Physics and Astrophysics", Aligarh, pp. 152-153, 1967.

- (7) Geomagnetic Field - A measure of the Kinetic Energy Density of the Solar Wind; Sarabhai, V. and K.N. Nair, Proc. of the III International Symposium on Equatorial Aeronomy, Ahmedabad, Vol. II pp. 464-466, 1969.
- (8) The Daily Variation of the Geomagnetic field and the Deformation of the Magnetosphere related to Solar Wind; Sarabhai, V and K.N. Nair, IAGA - Bulletin No.26, ed. by L.R. Alldredge, IUGG Publication Office, Paris (V), IV - 76, 1969.
- (9) Solar Wind Effects on the Daily Variation of Geomagnetic field; Sarabhai V. and K.N. Nair, IAGA - Bulletin No.26 ed. by L.R. Alldredge, IUGG Publication Office, Paris (V), V-63, 1969.
- (10) Interplanetary Magnetic Field Fluctuations and the Daily Variations of the Geomagnetic Field; Nair, K.N. and V. Sarabhai, International Symp. on Solar - Terrestrial Physics, Leningrad, M1-6, 1970.
- (11) Particles, Fields and Currents in the Magnetosphere; Nair K.N., Proc. of the Seminar on "Problems of the Equatorial Electrojet, Ahmedabad, 6, 1970.
- (12) Magnetospheric Contributions to the Geomagnetic Daily Variations; Sarabhai V.A. and K.N. Nair, Proc. of the Seminar on "Problems of the Equatorial Electrojet", Ahmedabad, 14, 1970.
- (13) Solar Wind Effects on the Daily Variation of the Horizontal Component for Low Latitudes; Nair K.N. and V. Sarabhai, Symp. on "Ionosphere-Magnetosphere Interactions", Delhi 1.3, 1971.

CONTENTS

CHAPTER-I		Page
1.1	Introduction	1
1.2	Primary cosmic rays	1
1.21	Energy spectrum	
1.22	Geomagnetic effects	
1.3	Secondary cosmic rays	4
1.31	Production	
1.32	Atmospheric effects	
1.4	Relation between primary and secondary variations	6
1.5	Experimental evidence of the time variations of cosmic ray intensity	8
1.6	Properties of interplanetary space	9
1.61	Solar wind	
1.62	Interplanetary magnetic field	
1.7	Modulation of cosmic ray intensity	15
1.71	Diffusion - convection model	
1.72	Daily variation of cosmic ray intensity	
1.73	Study of cosmic ray daily variation at Trivandrum	
CHAPTER - II		
2.1	Experimental technique	29
2.11	Introduction	
2.12	Geiger Muller Counter	
2.13	Geometry of the apparatus	
2.2	Method of analysis	36
2.21	Data Processing	

2.22	Test of self consistency of the data	
2.23	Normalisation of cosmic ray intensity	
2.24	Pressure correction to cosmic ray intensity	
2.25	Elimination of the long-term trend in cosmic ray intensity	
2.26	Harmonic analysis	
2.27	Correlation analysis	
2.3	Results and discussions	41
2.31	Introduction	
2.32	Variational coefficient and its application to the daily variation of cosmic ray intensity	
2.33	Determination of temperature effect to the daily variation of cosmic ray intensity	
2.4	Conclusions	63

CHAPTER-III

3.1	Introduction	64
3.2	Magnetosphere	65
3.21	Models of the magnetosphere	
3.211	Mead - Beard model	
3.212	Mead - Williams model	
3.213	Taylor - Hones model	
3.22	Electric fields in the magnetosphere	
3.221	Electric field in the outer magnetosphere	
3.222	Radial electric field	
3.23	Plasma-pause	
3.24	Geomagnetically trapped particles	
3.241	Motion of charged particle trapped in the geomagnetic field	
3.242	Diffusion and acceleration of charged particles in the earth's radiation belts	

	3.243	Plasma flow in the magnetosphere	
	3.25	Particles and fields in the magnetosphere	
3.3		Earth's magnetic field	88
	3.31	Sources of the magnetic field at the surface of the earth	
	3.32	Geomagnetic co-ordinate system	
3.4		Ionospheric effects	89
	3.41	Electric conductivity in the ionosphere	
	3.42	Sq. variation	
	3.43	Ionospheric current system for Sq.	
	3.44	Short comings of dynamo theory	
3.5		Geomagnetic variations in relation to interplanetary conditions	95
	3.51	Solar wind plasma and geomagnetic effects	
	3.52	Interplanetary magnetic field and geomagnetic effects	
3.6		ΔH in relation to changes in solar wind conditions	99

CHAPTER - IV

4.1		Nature of ΔH , the daily variation of H for low latitude stations	100
4.2		ΔH , as a consequence of lowering of H_{\min} , the minimum value of H , during night time.	101
4.3		Magnetospheric and ionospheric contribution to ΔH	114
4.4		Relation between $(\Delta H_T - \Delta H_A)$ and the electron drift speed at E region at Thumba	117
4.5		Variability of H at different hours related to day-to-day changes of the daily variation.	119

4.6	Equinoxial maxima in equatorial electrojet strength	120
4.7	ΔH_A in relation to changes in K. E. density of solar wind and $\overline{B_z}$ of the interplanetary magnetic field.	123
4.8	Conclusions	132

CHAPTER V

5.1	Morphology of ΔH	134
5.11	Dynamo current	
5.12	Magnetopause currents	
5.13	Magnetospheric currents	
5.131	Tail currents	
5.132	Symmetric ring current	
5.133	Eccentric ring current	
5.134	Partial ring current	
5.2	Solar wind effects on ΔH and K_p	143
5.21	ΔH_A and the deformation of the magnetosphere	
5.22	Interplanetary magnetic field fluctuations and ΔH_A .	
5.23	The relationship of V_s and $\overline{B_z}$ with $\sum K_p$.	
5.3	Recent studies on ΔH .	148
5.4	Summary of the results and the conclusions	154
5.41	Cosmic-ray studies with directional meson telescopes at Trivandrum	
5.42	Geomagnetic plasma probe for solar wind	

CHAPTER - I

1.1 Introduction

Time variations of cosmic ray intensity have proved themselves to be very powerful tools for probing the electromagnetic conditions of interplanetary plasma. This aspect has been discussed in great detail by Dorman (1963, 1969), Parker (1966, 1969) Quenby (1967), Webber (1968) and Somogyi (1969).

The present work deals with directional cosmic ray measurements and determination of the atmospheric temperature effect on the daily variation of μ meson intensity. For this directional and vertical telescopes were operated at Trivandrum (geographic latitude 8.4° -N geographic longitude 76.9° - E) near the dip equator during the period 1964 to 1966.

1.2 Primary cosmic rays

1.21 Energy spectrum

The differential energy spectrum, can be expressed in the form of a power law given by

$$N(E) dE = K.E^{-\gamma} \quad \dots(1.01)$$

where E is the energy, K is a constant and γ is the exponent which is dependent on energy. Meyer and Simpson (1958) have reported that the differential energy spectrum changed considerably from 1948 to 1956 and that the exponent γ , in equation (1.01), increased from 2 to 2.5.

1.22 Geomagnetic effects

The cosmic ray particles which arrive at any point on the earth's surface are deflected by the geomagnetic field. "Asymptotic direction of approach" is defined as the direction in which the particle was moving in space before coming under the influence of the geomagnetic field. Figure 1.01 shows the asymptotic direction of approach of a cosmic ray particle which arrives at the earth from the direction Λ and ψ in space. Evaluation of the asymptotic directions were originally made through model experiments. (Malmfors, 1945; Burnberg and Dattner, 1953). But with the advent of electronic computers, the trajectories were determined by numerical-integration (Jory, 1956; McCracken, 1962). In cosmic ray time variation studies another important concept is that of the "Asymptotic cone of acceptance of a detector", which is defined as the solid angle containing the asymptotic directions of approach which make a significant contribution to the counting rate of the detector. It has been pointed out by Rao et al, 1963 that these concepts are extremely useful in the study of anisotropic changes in cosmic ray intensity.

The motion of a charged particle in the earth's magnetic field is given by the Lorentz equation

$$m \frac{d^2 \vec{R}}{dt^2} = \frac{Ze}{c} \left(\frac{d\vec{R}}{dt} \times \vec{H} \right) \quad \dots (1.02)$$

where H is the magnetic field, m and Ze are the relativistic mass and charge of the particle and c is the velocity of light.

The components of H along r , θ and ϕ can be written as

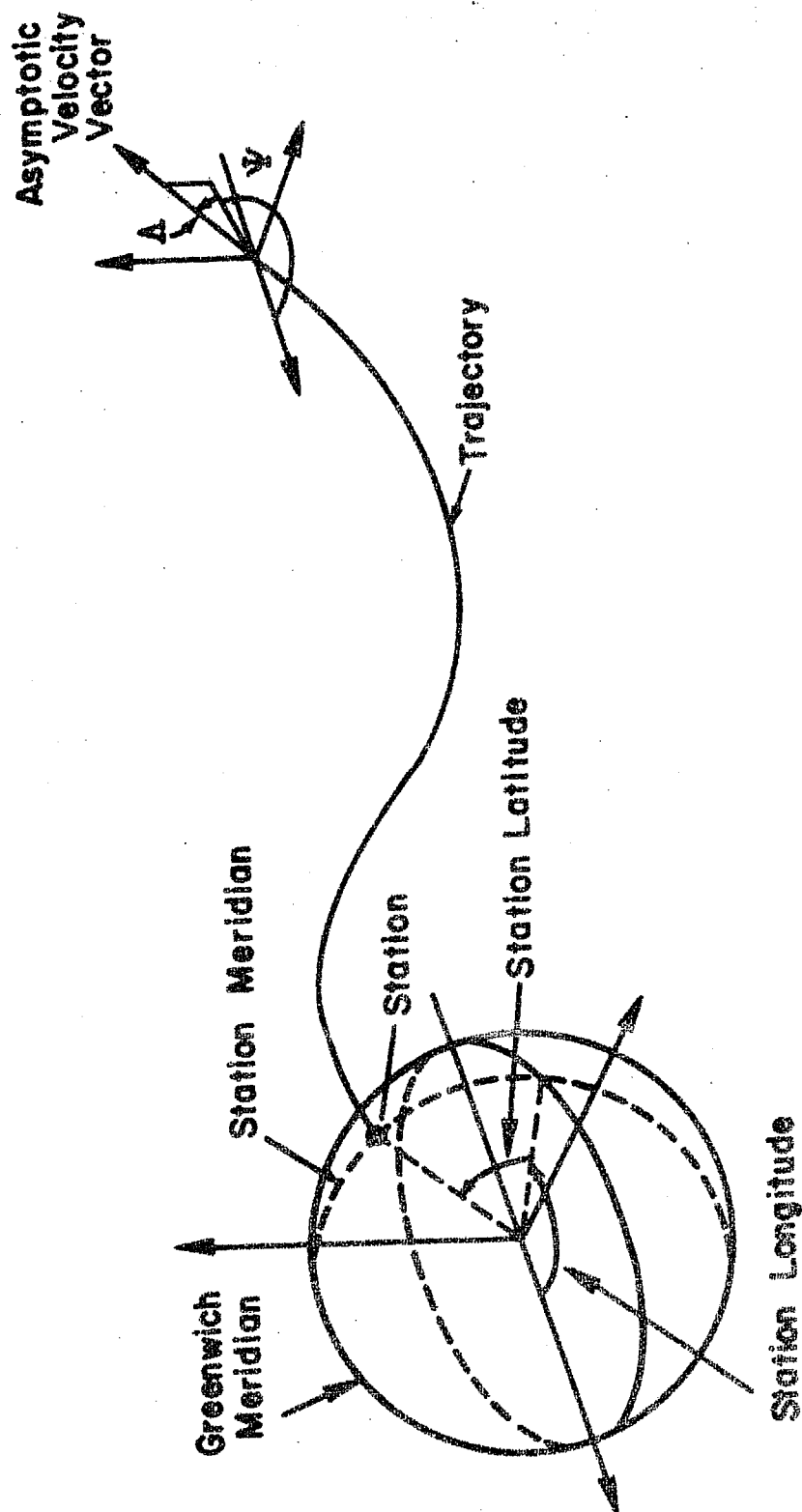


Fig. 1.01 The trajectory of a charged particle through geomagnetic field. (McCracken et al, 1965).

$$H_r = \frac{\partial V}{\partial r} \quad \dots (1.03)$$

$$H_\theta = \frac{1}{r} \frac{\partial V}{\partial \theta} \quad \dots (1.04)$$

$$H_\phi = \frac{1}{r \sin \theta} \frac{\partial V}{\partial \phi} \quad \dots (1.05)$$

Here r , θ and ϕ are respectively the radial distance co-latitude and longitude and V is the magnetic potential at the point on the earth's surface.

$$V = a \sum_{n=0}^{\infty} \sum_{m=1}^n \left(\frac{a}{r}\right)^{n+1} P_n^m(\cos \theta) [g_n^m \cos m \phi + h_n^m \sin m \phi] \quad (1.06)$$

where 'a' is the average radius of the earth, $P_n^m(\cos \theta)$ are the associated Legendre polynomials of degree 'n' and order 'm' and g_n^m and h_n^m are the Gauss coefficients. Using the sixth degree expansion of equation (1.06), Jenson and Cain (1962) have worked out the Gauss coefficients. Making use of equations (1.02) to (1.06), the cut-off rigidities along various zeniths and azimuths for a station can be calculated.

1.3 Secondary cosmic rays

1.31 Production

Primary cosmic rays while passing through the atmosphere collide with the air nuclei and the resulting nuclear interactions produce mesons (mainly π^0 , π^+ , π^-), nucleons and heavy mesons. The π^0 decays into two γ - rays which in turn generate soft cascades. π^\pm decay into μ^\pm which form the main constituents of the penetrating component at sea-level.

1.32 Atmospheric effect

The changes of the atmospheric parameters, namely the

pressure and the temperature have considerable influence on the changes of cosmic ray intensity recorded at the ground. The cosmic ray intensity as a function of atmospheric pressure can be described by an exponential law. It follows that the counting rate I , recorded at a given altitude, can be corrected for variations of pressure by the formula

$$I = I_{\text{corr.}} \exp (\beta \cdot \Delta P) \quad \dots (1.07)$$

where ΔP refers to the deviation from the mean barometric value for the given altitude and β is the pressure coefficient. For the meson component the pressure coefficient $\beta = -0.14\%/mb$ and for neutron component $\beta \approx -0.7\%/mb$ at the equator for sea level stations.

The temperature variations in the upper atmosphere mainly affect the meson component. Due to an increase in the atmospheric temperature, the height of the meson forming layer increases resulting in an increase in the path length of the mesons reaching the detector. The greater the path-length, the greater will be the probability for the μ meson to decay and hence the intensity will decrease with the increase in temperature. This effect is called the negative temperature effect. Together with the above effect there is a positive temperature effect arising from the competitive processes of $\pi \rightarrow \mu$ decay and nuclear capture of π mesons near the production level (between 100 to 200 mb). As the temperature of this region rises and the density falls, more π mesons decay and fewer interact, since the interaction distance increases. The result is that with increase in temperature at these levels more μ mesons can reach the ground detector. The temperature effect for the neutron component is less than $-0.02\%/^{\circ}C$ change of temperature near the top of the atmosphere.

Bercovitch (1968) has given a comprehensive review of the atmospheric effects on meson and nucleonic components of cosmic rays.

1.4 Relation between primary and secondary variations

Since ground stations record only secondary cosmic rays, it is necessary to find how the secondary component is related to the primary cosmic rays. Several workers have tried to establish semi-empirical relationships between primary cosmic rays and their secondary components. (Neher, 1952; Treiman, 1952; Simpson et al, 1953; Dorman, 1957).

The observed intensity $N_{\lambda}^i(h)$ of the i^{th} component of cosmic radiation (mesons, neutrons and soft components) at a station with geomagnetic latitude λ , and height h , can be written as (Dorman, 1957).

$$N_{\lambda}^i(h) = \int_{E_{\lambda}^c}^{\infty} D(E) m_i(E, h) dE \quad \dots (1.08)$$

where $D(E)$ is the differential energy spectrum of the primary particles, $m_i(E, h)$ is the multiplicity function, defined as the number of secondary particles of type 'i' at height 'h' produced by a single primary particle of energy E , and E_{λ}^c is the geomagnetic cut-off energy at the station latitude.

Variation in $N_{\lambda}^i(h)$ can result from variations in $D(E)$, $m_i(E, h)$ or E_{λ}^c . Thus differentiating equation (1.08) with respect to all the above parameters, the change in intensity can be written as

$$\begin{aligned} \frac{\delta N_{\lambda}^i(h)}{N_{\lambda}^i(h)} = & -\delta E_{\lambda}^c \cdot W_{\lambda}^i(E, h) + \int_{E_{\lambda}^c}^{\infty} \frac{\delta D(E)}{D(E)} \cdot W_{\lambda}^i(E, h) dE \\ & + \int_{E_{\lambda}^c}^{\infty} \frac{\delta m_i(E, h)}{m_i(E, h)} W_{\lambda}^i(E, h) dE \end{aligned} \quad \dots (1.09)$$

where

$$W_{\lambda}^i(E, h) = \frac{D(E) \cdot m_i(E, h)}{N_{\lambda}^i(h)} \quad \dots (1.10)$$

is called the "coupling coefficient" between the primary and secondary variation. The first term on the right hand side of equation (1.09) represents variation due to change in the geomagnetic cut-off energy which can be only a small contribution even during large geomagnetic disturbances. The last term can be accounted for by proper meteorological corrections. Thus neglecting the change in E_{λ}^c , the variation in $N_{\lambda}^i(h)$ observed, after proper meteorological correction, can be expressed as

$$\frac{\delta N_{\lambda}^i(h)}{N_{\lambda}^i(h)} = \int_{E_{\lambda}^c}^{\infty} \frac{\delta D(E)}{D(E)} \cdot W_{\lambda}^i(E, h) dE \quad \dots (1.11)$$

From the latitude survey of cosmic ray intensity variations, coupling coefficients for meson and neutron components at various heights above sea-level have been derived (Dorman, 1957; Quenby and Webber, 1969; Webber, 1962).

From the computed values of coupling constants one can relate the observed variations in the intensity of secondary cosmic rays to $\frac{\delta D(E)}{D(E)}$, which is called the energy spectrum of the variational part of the primary cosmic rays.

1.5 Experimental evidence of the time variations of cosmic ray intensity

Cosmic ray measurements on a long term basis are done mostly by ground based neutron monitors and meson monitors. These instruments measure the secondary cosmic radiation. As described in section 1.32 it is possible to correct the intensity of secondary cosmic rays for barometric effects. From the knowledge of the coupling constants it is possible to relate the secondary cosmic ray variations to the primary variations. The primary cosmic ray variations can be classified into regular and irregular variations.

The regular variations have periodicities ranging from few years to few minutes. They are (1) 11-year variation which is in phase-opposition with the 11-year variation of solar activity, (2) seasonal variations, (3) 27 day recurrence connected with the synodic rotation of the sun and (4) diurnal and semi-diurnal variations connected with the rotation of the earth and the anisotropy of cosmic ray intensity in the interplanetary space. Dhanju and Sarabhai (1967) have reported time variations in the range of a few minutes.

Among the irregular variations we have: (1) Forbush decreases, (2) day-to-day changes, and (3) sudden increase which are mostly low energy phenomena and are related to the entry of solar flare particles.

The most important cause, of these effects which are discussed in detail in section 1.7, is the modulation of cosmic ray intensity due to changes in solar wind and interplanetary magnetic

field. Thus to understand these variations in detail it becomes necessary to investigate the influence of solar activity on the electro-magnetic conditions of interplanetary space.

1.6 Properties of Interplanetary Space

1.61 Solar Wind

Geomagnetic storms have been attributed to the impact of the solar corpuscular radiation with the geomagnetic field (Chapman and Ferraro, 1930). From the observations of ionised comet tails, Biermann (1951, 1952) concluded that the solar corpuscular radiation should be present continually in the interplanetary medium. Parker (1958, 1960) showed that since the inner part of the solar corona has a temperature of the order of 10^6 degrees K, the solar corona should expand hydrodynamically against the solar gravitational force, resulting in a continuous emission of corpuscular matter called the solar wind. The initial velocity of the solar wind is few km/sec, at the photosphere and becomes supersonic beyond a distance of about 10-20 sun's radii and remains almost independent of the distance. The solar wind density falls off at the rate of $1/R^2$.

By means of satellites and space probes it has become possible to obtain direct evidence of the solar wind in the interplanetary medium. The first measurements of the solar wind were carried out by Gringauz (1961). The early measurements concerning the solar wind parameters namely velocity, density and temperature have been reported by various authors (Bridge et al, 1962; Snyder et al, 1963; Wolfe et al, 1966; Gringauz et al (1966); Neugebauer and Synder, 1966; and Pai et al, 1967 and Hundhausen et al, 1967, 1970).

The quiet day solar wind velocity is in the range 300-500 kms/sec near the orbit of the earth with a direction almost away from the sun (taking into account the appropriate correction for the aberration due to the orbital motion of the earth). Its density is nearly 5 protons cm^{-3} and temperature 10^4 to 10^5 degrees K. The high velocity solar wind streams have exhibited a pronounced tendency to recur at intervals of 27 days and this recurrence persists for several solar rotations (during Mariner-II and IMP-I periods). While it has generally been believed that the solar wind velocity would exhibit an 11-year cycle of variation, Gosling et al (1971) from satellite observations, during 1962 to 1970, have observed that the solar wind velocity does not at all change from year to year and that most of the years the average solar wind velocity was found to be $\sim 400 \text{ km/sec}$. Detailed reviews on the subject are given by Dessler (1967), Axford (1968) and Hudhausen (1968, 1970).

1.62 Interplanetary magnetic field

Parker (1958) showed that the interplanetary magnetic field is the result of the extension of the lines of force of the general solar field into space by the expanding chromosphere and corona. He has estimated the strength and directions of the interplanetary magnetic field under the assumption that this field is of solar origin and is carried along by the solar wind. The rotation of the sun and the radially moving solar wind stretch the magnetic field lines into an Archimedes spiral given by

$$\vec{r} = \frac{\vec{V}(\phi - \phi_0)}{\Omega} \quad \dots (1.12)$$

where r is the radial distance, V is the solar wind velocity, Ω is the angular velocity of the sun and ϕ is the heliographic

longitude measured from the reference longitude ϕ_0 . The Archimedes spiral structure of the interplanetary magnetic field, in the equatorial plane of the sun, resulting from extension of the general solar field by an idealised uniform 300 km/sec quiet-day solar wind is shown in figure 1.02. From the study of the arrival directions of solar flare cosmic rays McCracken (1962 a) gave experimental evidence for the spiral structure. Ahluwalia and Dessler (1962) have proposed that the spiral field, on an average should corotate with the sun so that the solar wind could move radially outward.

The streaming angle θ , often referred to as the "garden-hose angle" is defined as the angle between the field direction and the radius vector as shown in figure 1.03. At any distance r from the sun, θ is given by

$$\theta = \tan^{-1} \frac{\Omega r}{V} \quad \dots (1.13)$$

The components of the interplanetary magnetic field are given by

$$B_r = B_0 \left(\frac{R_0}{r} \right)^2 \quad \dots (1.14)$$

$$B_\theta = 0 \quad \dots (1.15)$$

$$B_\phi = B_0 \frac{\Omega R_0}{V} \left(\frac{R_0}{r} \right) \sin \theta \quad \dots (1.16)$$

along any given spiral line of force. Here, r is the radial distance, θ is the polar angle, ϕ is the azimuth measured around the sun, R_0 is the radius of the sun and B_0 is the magnetic field at the solar surface. Small-scale irregularities in the general pattern given by the above equations 1.14, 1.15 and 1.16 are to be expected, as a result of small-scale irregularities in the solar wind.

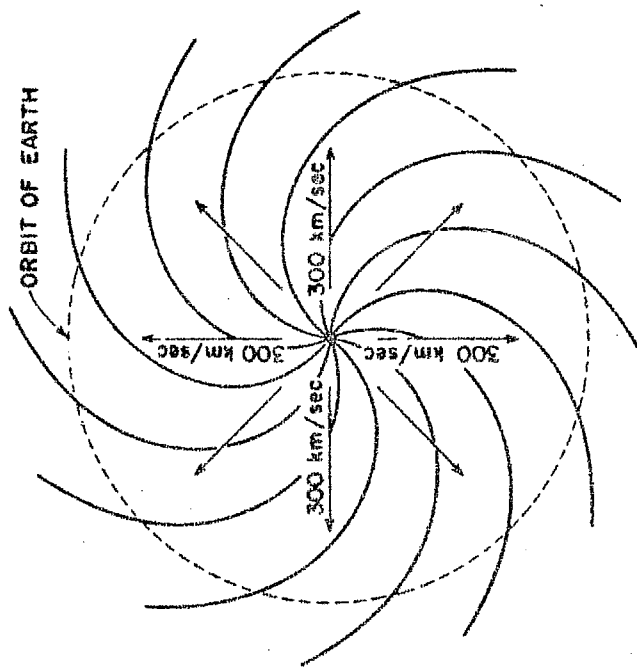


Fig. 1.02 Archimedes spiral structure of the interplanetary magnetic field for a symmetric solar wind velocity of 300 km/sec. (Parker, 1963).

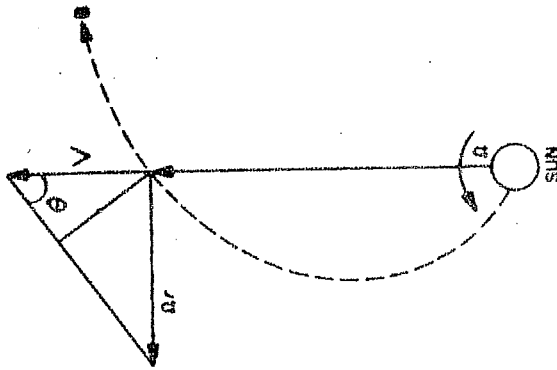


Fig. 1.03 Garden-hose geometry of the interplanetary magnetic field. (Dessler, 1967).

During recent years the magnetic field in interplanetary space has been measured in great detail and accuracy. The time resolution of the magnetic field measurements is higher than that of the plasma measurements in the interplanetary space. Even before the solar wind parameters were determined, the interplanetary magnetic field was measured by Coleman et al (1960a,b). The energy density of interplanetary magnetic field is only 1% of the solar wind kinetic energy density. The early measurements of the interplanetary magnetic field were not very reliable due to contamination by the magnetic materials in the space craft. One of the earliest reliable information on the interplanetary magnetic field comes from the work of Ness et al (1964) from magnetometers on board IMP-1 satellite. The strength of the field at the orbit of the earth was found to be about 5γ . The direction of the field on an average confirmed the predicted spiral structure. The field-component normal to the ecliptic plane was about 1 to 2γ and the direction was for most of the time towards south.

Wilcox and Ness (1965) have shown that the interplanetary magnetic field is often divided into sectors, the field direction in adjacent sectors being opposite, one away from the sun and the other towards the sun. The sectorial structure shows a 27-day recurrence equal to the synodic rotation period of the equatorial region of the sun implying that the interplanetary magnetic field co-rotates with the sun. Figures 1.04 shows the sector-structure of the interplanetary magnetic field direction for solar rotation 1784 to 1786 as observed by IMP-1 satellite.

Comprehensive reviews on the experimental and theoretical studies on this subject have been given by Lust(1967),

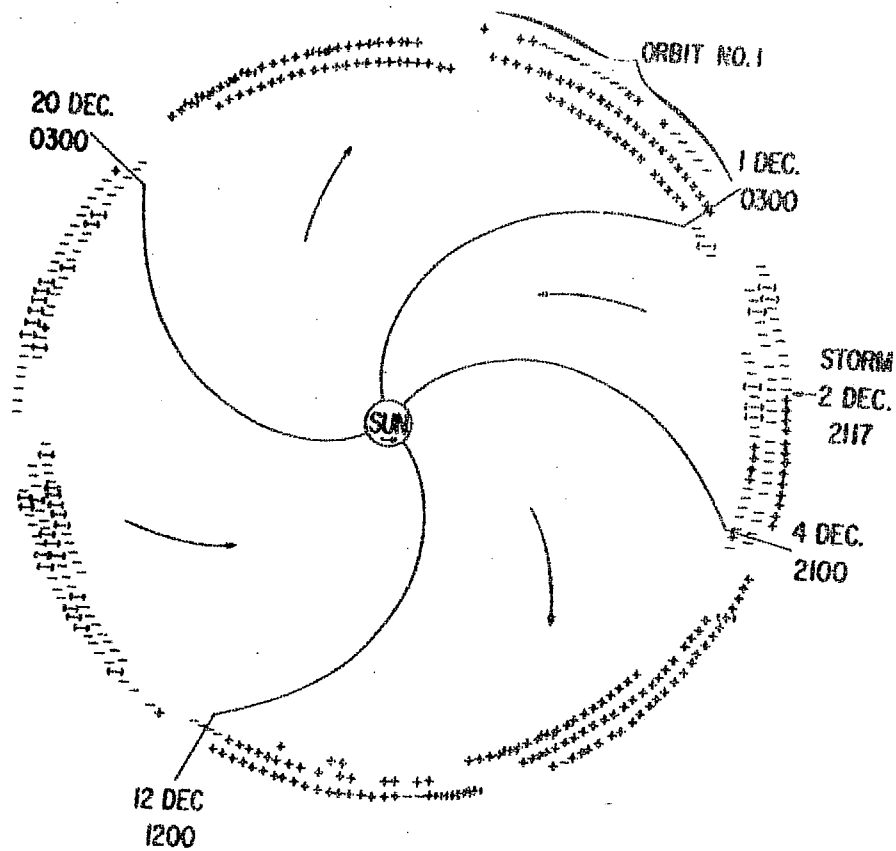


Fig. 1.04 The observed sector structure of the interplanetary magnetic field during November 1963 to February 1964. (Ness and Wilcox, 1965).

Axford (1968), Hundhausen (1968), Dessler (1967), Wilcox (1968), Parker (1967, 1969) and Hundhausen (1970).

1.7 Modulation of cosmic ray intensity

Different models have been proposed by several workers on the basis of modulation due to static and time varying electric or magnetic fields. In this connection it is worthwhile to refer to the works of Janossy (1937), Nagashima (1961), Alfven (1954), Davis (1955), Morrison (1956), Beisser (1958), Singer (1958), Parker (1958 a, 1966), Ehmert (1960), Sarabhai and Subramanian (1966), Subramanian and Sarabhai (1967), Jokipii (1967, 1968), Gleeson and Axford (1968), Jokipii (1969), Parker (1969) Fisk (1970) and Burger (1971).

1.71 Diffusion-convection model

The diffusion-convection model, originally suggested by Parker (1958 a), is now generally accepted, as it can explain most of the observed variations of cosmic ray intensity. In this model the magnitude of the modulation depends on the total number of "scattering centers" and the diffusion coefficient which is a function of energy as well as distance from the sun. Due to plasma instabilities, magnetic field irregularities are produced which act as scattering centers for the incoming cosmic ray particles. The depression of cosmic ray intensity at the orbit of the earth compared to the interstellar intensity can be understood in terms of a balance between inward diffusion and outward convection of cosmic ray particles by irregularities in the interplanetary magnetic field carried out-ward by the solar wind. The model predicts that the cosmic-ray density $U(r)$, at

a heliocentric distance 'r', can be given by

$$U(r) = U_0 \exp \left[- \int_r^R \frac{V}{K} dr \right] \quad \dots (1.17)$$

where K is the isotropic diffusion coefficient, V is the solar wind velocity which is assumed to be spherically symmetric around the sun, R is the radial size of the modulating region beyond which $V = 0$ and/or $K = \infty$, and U_0 is the unmodulated cosmic ray density in the interstellar space.

The 11-year variation of cosmic ray intensity is due to the variation of $\frac{VR}{K}$. Similarly the variation of $\frac{VR}{K}$ with the coronal and magnetic field conditions around the sun leads to the 27-day variation in cosmic ray intensity.

The isotropic diffusion coefficient

$$K = 1/3 \lambda c\beta \quad \dots (1.18)$$

where $c\beta$ is the velocity of cosmic ray particles and λ is the mean free path. λ depends on the scale length of the magnetic irregularities and the Larmor radii of the cosmic ray particles. Parker (1964) has shown that a charged particle, moving along a field line having irregularities, is most effectively scattered by the irregularities when the Larmor radius of the particle is comparable with the scale length of the irregularities. On the contrary when the Larmor radius of the particle is small, then the particle simply follows the field line and passes smoothly through the irregularity, while particles of appreciably large Larmor radius are practically unaffected. This shows that the diffusion coefficient is a function of P, the rigidity of the particle. These facts suggest that in general $K = f(r, t, P, \beta)$

where r is the radial distance from the sun, t the time and P the rigidity of the particle.

The radial size of the modulating region, R was believed to be the radial distance where the energy density of the solar wind balances the energy density of the galactic magnetic field. Sarabhai and Subramanian (1966) have suggested that the modulating region extends upto a distance where $\frac{K_{\perp}}{K_{\parallel}}$ tends to unity. Here K_{\parallel} and K_{\perp} are the diffusion coefficients, parallel and perpendicular to the interplanetary magnetic field. Jokipii and Davis (1969) have proposed that the region extends upto a distance, where the waves, responsible for scattering the cosmic rays dampen off and K_{\parallel} tends to infinity

The diffusion process is generally anisotropic since the cyclotron frequency of cosmic rays is generally more than the scattering frequency. The diffusion along the field line K_{\parallel} is more than the diffusion perpendicular to the field line K_{\perp} . For an idealized spiral interplanetary magnetic field, the cosmic ray density at a radial distance r and co-latitude θ is given by Parker, (1965).

$$U(r, \theta) = U_0 \exp \left[- \frac{V}{K_{\parallel}} (R-r) \left\{ 1 + \frac{1}{3} \left(\frac{\Omega \sin \theta}{V} \right)^2 (R^2 + Rr + r^2) \right\} \right] \quad \dots\dots(1.19)$$

where U_0 is the interstellar density, that is the density at a distance $\bar{r} = R$, Ω is the angular velocity of the sun and V is the solar wind velocity. The radial gradient for anisotropic diffusion is given by

$$\frac{1}{U} \frac{\partial U}{\partial r} = \frac{V}{K_{\parallel}} \left[1 + \frac{r^2 \Omega^2 \sin^2 \theta}{V^2} \right] \quad \dots\dots(1.20)$$

O'Gallagher (1967) has reported the radial intensity gradient for both protons and helium nuclei from 1 A. U. to 1.56 A. U., based on the data of Mariner IV during 1965. In the diffusion convection model for solar modulation, the inward transport of particles resulting from these gradients is balanced by the outward convection of particles in magnetic field irregularities carried by the solar wind. He has calculated the diffusion coefficient $K_{||}$, from the measurements of the radial gradient of the cosmic ray intensity and the velocity of solar wind. The estimated value of $K_{||} = 3.2 \times 10^{21} \text{ cm}^2/\text{sec}$ for $P \approx 1 \text{ GV}$.

Jokipii (1967) has generalized the diffusion convection processes by considering an energy dependent diffusion coefficient. Gleeson and Axford (1967, 1968) have considered the energy losses in the diffusion convection model and have shown the intensity of galactic cosmic rays within the solar system can be related to that at infinity through an energy loss parameter. Jokipii (1966, 1967) has related the power spectrum of the interplanetary magnetic field irregularities with the diffusion of cosmic rays. The scattering of cosmic rays at the magnetic field irregularities depends chiefly upon the power in the transverse component of the interplanetary magnetic field near the frequency f_0 defined by

$$f_0 = \frac{V\omega}{2\pi W} = \frac{VB_0}{2\pi P} \quad \dots (1.21)$$

where V is the solar wind velocity, ω is the cyclotron frequency of the cosmic rays, W is the velocity of cosmic rays, B_0 is the strength of the magnetic field and P is the rigidity of the cosmic ray particle. The power spectrum $M(f_0)$ can be related to frequency as

$$M(f_0) = \partial f^{-\alpha} \quad \dots (1.22)$$

and K_{\parallel} for a power spectrum of this type is given by

$$K_{\parallel} = \frac{2c B_c}{3\pi \delta} \beta P^{2-\alpha} \quad \dots (1.23)$$

where δ is the amplitude and α is the slope of the power spectrum. The rigidity dependence of K_{\parallel} is decided by the slope α (Jokipii and Parker, 1969). The observed change in cosmic ray modulation was found to be consistent with a corresponding change in magnetic field power spectra as obtained from Mariner-2 and Mariner-4 data (Jokipii, 1968). Jokipii (1971) has reviewed this subject in great detail.

1.72 Daily variation of cosmic ray intensity

Extensive analysis of data obtained from ion chambers and meson and neutron monitors have been carried out by many investigators and the existence of diurnal and semi-diurnal components in the daily variation of cosmic ray intensity has been well established. A 22-year variation of the phase and amplitude of the diurnal variation has been reported by Sarabhai and Kane (1953), Thambyahpillai and Elliot (1953), Forbush (1967) and Wada and Kudo (1968). McCracken and Rao (1966) have shown that, on an average, the strength of diurnal anisotropy remained constant during the period 1957 to 1965. However, Duggal et al (1967) have pointed out a decrease of the strength of diurnal anisotropy by about 36% from 1958 to 1965. Willets et al (1969) have pointed out that the average amplitude of the first harmonic increased by $\sim 35\%$ from 1965 to 1966 and remained constant thereafter. On an average the diurnal variation in free space has an amplitude $\sim 6.4\%$ with a time of maximum around 18.00 hours local time (Bercovitch, 1963; McCracken and Rao, 1966; and

Faller and Marsden, 1966). Jacklyn and Humble (1965) have reported that the average diurnal variation is energy independent within the energy range ~ 2 GeV to ~ 100 GeV; and that the upper limit of E varies with the level of solar activity. Sandstrom et al (1962) have suggested that the diurnal amplitude shows a $\cos \lambda$ dependence where λ is the mean asymptotic latitude for the station.

Based on the measurements of the daily variation over a net work of super neutron monitors, Patel et al (1968) have derived the spectrum of variation, the amplitude and the principal direction of maximum and minimum intensity in interplanetary space for each day during 1964-65. They have provided confirmatory evidence to the four suggested processes significantly contributing to the anisotropy in cosmic rays. They are (1) the azimuthal streaming (Parker, 1964; Axford, 1965; and Krymskiy, 1964), (2) streaming due to non-uniform diffusion in a longitudinal sector-structure of the interplanetary magnetic field (Parker, 1964), (3) scattering at irregularities along the interplanetary magnetic field short circuiting latitudinal gradients (Sarabhai and Subramanian, 1966), and (4) latitudinal gradients in a relatively smooth magnetic field (Subramanian and Sarabhai, 1967 and Leitti and Quenby, 1968).

Sarabhai and Bhavsar (1958) have shown, the existence of a 27-day recurrence of the phase of the diurnal variation. Patel et al (1968) have suggested that the diurnal anisotropy caused by latitudinal gradient should reverse as the magnetic field or the gradient reverses. When the cosmic ray gradient is such that solar activity to the north of the equatorial plane is greater than to the south, the latitudinal gradient should

give rise to a diurnal anisotropy with its average direction of maximum along 1500 hours whenever the field is directed away from the sun (+) and along 0300 hours whenever the field is directed towards the sun(-). They have shown that during IMP-1 period, whenever the interplanetary magnetic field was directed away from the sun the amplitude of the diurnal anisotropy was larger compared to what it was when the field was directed towards the sun. Venketesan and Mathews (1968) have reported that enhanced diurnal variation was observed when the average interplanetary magnetic field vector was directed out-wards during IMP-1 period. Sarabhai et al(1965) reported for the first time that on a majority of days there exist a virtual sink of galactic cosmic rays along the garden-hose direction.

The data from super neutron monitors of very high counting rate enables one to examine the daily variation even during a single day, since the statistical uncertainty in a hour's counting rate is as small as $\sim 0.1\%$. Duggal and Pomerantz(1962), Kane (1966), Mathews et al (1969), Hashim and Thambyah Pillai (1969) and Kane (1970) have reported that the day-to-day variability of the diurnal variation of cosmic-ray intensity is very large. The amplitude of the diurnal variation varies from nearly zero to several percent. For certain groups of days there are large increases of ~ 1 to 2% from the 1800 hour direction and large decreases of ~ 1 to 2% from roughly the garden-hose direction. No satisfactory theoretical explanation of these features is available at present.

From a study of the time variation of meson intensity at Ahmedabad during 1957 to 1958, Rao and Sarabhai (1961) have

observed, on many days a difference of about 6 hours in the diurnal time of maximum for east and west directions. However, they have reported that there are many days on which the daily variation has a maximum near noon for both east and west directions. They have attributed this to a modulation by some local source situated within the influence region of the geomagnetic field.

Various theories have been proposed by different investigators to explain the observed diurnal anisotropy (Dattner and Venkatesan, 1958; Ahluwalia and Dessler, 1962; Parker, 1964; Axford, 1965 (a) and Krymskiy, 1966). Ahluwalia and Dessler (1962) have argued that a smooth spiral solar magnetic field which corotates with the sun can produce diurnal anisotropy of cosmic radiation. To an observer on the earth, the cosmic ray particles crossing the stationary frame of reference seems to be subjected to an action of an electric field.

$$\vec{E} = - \frac{1}{c} (\vec{V} \times \vec{B}) \quad \dots (1.24)$$

where \vec{B} is the magnetic field strength at the orbit of the earth. Under the action of this electric field, \vec{E} and the magnetic field, \vec{B} the observer sees the guiding centres of cosmic ray particles, drift in the direction $\vec{E} \times \vec{B}$ with a drift speed of $\vec{V}_D = c \frac{\vec{E} \times \vec{B}}{B^2}$. The cosmic ray particle gains energy as it moves in the direction of the electric field and losses energy when it moves against the field. The anisotropy due to relative motion between the earth and the isotropic cosmic ray flux has been derived using Compton-Getting effect (Compton and Getting, 1935). Their model fits in well with the experimental results on the energy spectrum of variation. But the model suggests that the direction of maximum

of the diurnal anisotropy must always be within the quadrant to the east of the sun-earth line, and never in a direction making an angle more than 90° with the earth-sun line. This is in contradiction with the experimental observations of Bercovitch (1963). Moreover the particle drift has a component directed radially outward from the sun which would make it appear that the sun is a source. Stern (1964) has criticised this model. According to Liouville's theorem, the cosmic ray density in phase space should be preserved in a conservative system (i.e. where $\nabla \times \vec{E} = 0$). Hence, if the cosmic ray intensity is the same in all directions at any given point outside the solar system, it must be the same in all directions at any accessible point inside the solar system. This means that no time independent magnetic field system ($\frac{\partial \vec{B}}{\partial t} = 0$) can produce an anisotropy such as the diurnal variation.

Parker (1964) has proposed a model in which there are two heliocentric, spherically symmetrical regions. The inner region containing the earth has smooth spirial magnetic lines. The outer region, just outside the orbit of the earth as its innerboundary, consists of a large number of magnetic irregularities. In the inner region the smooth spirial magnetic lines of force rotate rigidly with the angular velocity of the sun, $\Omega = 3 \times 10^{-6}$ radians/sec. The conservative electric field $\vec{E} = -\frac{1}{c} (\vec{V} \times \vec{B})$ in the fixed frame of reference (here V is the solar wind velocity and B is the spiral field carried in the wind) deflects the cosmic rays coming into the solar system, producing a density gradient in the direction of E . The resulting cosmic ray gradient produced in the incoming particle is given by

$$\nabla (1/2 NMW^2) + q N \nabla \phi = 0 \quad \dots (1.25)$$

where ϕ is the electrostatic potential ($\vec{E} = -\nabla\phi$), N is the cosmic ray particle density, M and q are the mass and charge per particle and W is the particle velocity perpendicular to the field B . This pressure gradient leads to a streaming U given by

$$\vec{U} = \frac{McB}{B^2 q N} \times \nabla (1/2 N W_{\perp}^2) \quad \dots (1.26)$$

So using equation (1.25) in (1.26)

$$\vec{U} = -c \left(\frac{\vec{E} \times \vec{B}}{B^2} \right) \quad \dots (1.27)$$

If U is added to the electric field drift $= +c \frac{\vec{E} \times \vec{B}}{B^2}$ (which is part of the rigid rotation of the particles with the spiral pattern) there is no net streaming left, hence no anisotropy. But the cosmic ray particles have a "random walk" in the frame of reference moving with the wind. In this frame of reference there is no electric field. This situation leads to diffusion, which reduces the pressure gradient. If there is sufficient diffusion in the small-scale irregularities to reduce the initial $\nabla (1/2 N M W_{\perp}^2)$ to negligible values, then $\vec{U} = 0$ and there would be rigid rotation with the spiral pattern leading to a diurnal amplitude of 0.7% and the direction of the anisotropy would be along the 1800 hour direction. On an average the observed amplitude of the diurnal variation is $\sim 0.4\%$, which suggests that the diffusion wipes out about half the initial pressure gradient (Parker, 1967). Jckipii (1967) has shown that the small-scale magnetic irregularities in the spiral field observed by Mariner-II in 1962 (Coleman, 1966) give $\frac{K_{\perp}}{K_{\parallel}} = 10^{-2}$ for protons. Here K_{\parallel} and K_{\perp} are the diffusion coefficient, parallel and perpendicular to the magnetic lines of force. Parker (1967) has reported that $\frac{K_{\parallel}}{K_{\perp}} = 10^{-2}$ is about the right order of magnitude

to account for the observed amplitude of the diurnal variation. Recently, Subramanian (1971) has suggested that the reduction in amplitude, γ_1 can be explained by the proper choice of E_{max} , the maximum energy in equation (2.21) and by allowing μ in equation (1.30) to have values between 1.5 to 2.5 in the energy range 2 to 15 GeV.

Axford (1965 a and 1965 b) treated the above by considering the spiral magnetic field lines having small scale irregularities which cause scattering of galactic cosmic ray particles. It has been suggested that the main contribution to the diurnal variation of the cosmic ray intensity is due to co-rotation of the cosmic rays with the sun. The streaming velocity U parallel to the earth's orbit is given by

$$U = \frac{R \Omega}{1 + (1/W\tau \sin \theta)^2} \quad \dots (1.28)$$

where W is the gyro-frequency of cosmic ray particle, τ is the collision interval, θ is the garden-hose angle, Ω is the angular velocity of the sun and R is the heliocentric distance.

The streaming produces an anisotropy which is apparent as a diurnal variation of the cosmic ray intensity, with the effective local time of maximum intensity at 1800 hours, and an amplitude of the variation is $\sim 0.6\%$ (Gleeson and Axford 1968). This is calculated from Compton Getting formula

$$\text{Amplitude} = (2 + \mu) u/c \quad \dots (1.29)$$

when the differential energy is of the form

$$D(E) = A.E.^{-\mu} \quad \dots (1.30)$$

and $\mu = 2.5$. This model does not contradict Liouville's theorem,

as they have invoked non-conservative processes associated with irregularities in the magnetic field. Gleeson (1969) has modified this model.

It has been reported by various workers (Sarabhai et al, 1955, Katzman and Venkatesan, 1960; Rao and Sarabhai, 1964; Ables et al , 1966; Patel et al 1968; Hasim et al, 1969; and Rao and Agrawal, 1970) that after correcting for the atmospheric effects there exists a semi-diurnal component of cosmic ray intensity. This anisotropy has an amplitude $\sim 0.1\%$ with a direction of maximum along 0300 hours in space. The semi-diurnal component is approximately proportional to the first power of the rigidity of the particles and seems to vary as $\cos^2 \lambda$, rather than $\cos \lambda$ as in the case of diurnal variation, λ being the mean asymptotic latitude for the station (Subramanian and Sarabhai, 1967; Quenby and Leitti, 1968; Patel et al, 1968; and Rao and Agrawal, 1970).

Subramanian and Sarabhai (1967) have suggested that the semi-diurnal component of the cosmic ray daily variation arises as a result of particle density gradient perpendicular to the ecliptic plane. Viewing in directions parallel and anti-parallel to the interplanetary magnetic field lines, a detector on the earth measures cosmic ray fluxes characteristic of the equatorial plane. Viewing in a direction perpendicular to the interplanetary magnetic field, a detector samples particles arriving from higher heliographic latitudes, corresponding to the gyroradius of the particle under consideration. A detector on the spinning earth measures, in the course of a day, cosmic ray intensity twice along the interplanetary magnetic field and twice perpendicular to it. A positive gradient of cosmic ray

density with increase in heliolatitude can give a semi-diurnal component with a maximum perpendicular to the direction of interplanetary magnetic field. They have considered three different types of cosmic ray density distributions with helio-latitude. They have reported that the amplitude of the semi-diurnal anisotropy

$$r_2 (P) dp = \frac{1}{4} B n P^{-\beta} \frac{P^2 \cos^2 \lambda}{(45H)^2} dp \quad \dots (1.31)$$

B determines the over-all decrease between the pole and the equator, n determines the rapidity of decrease of cosmic-ray intensity with decreasing heliolatitude, H is the interplanetary magnetic field strength, λ the asymptotic latitude of viewing of the detector, P is the rigidity of the particle and β determines the rigidity dependence of the latitudinal variation of cosmic ray intensity. β is usually less than 2, suggesting a positive spectrum of variation. Moreover the anisotropy has $\cos^2 \lambda$ dependence. When the exponent $(2 - \beta)$ is positive, a neutron monitor which responds to lower mean energy can show a smaller semi-diurnal component than a meson detector. The same effect could be seen at a neutron monitor situated at a higher latitude with a lower mean energy of response than a neutron monitor situated at the equator. The latitude effect of semi-diurnal component is further accentuated by its $\cos^2 \lambda$ dependence on asymptotic latitude of viewing of the detector.

Lietti and Quenby (1968) and Quenby and Lietti (1968) have proposed a more or less similar mechanism to explain the semi-diurnal anisotropy. They have considered an interplanetary field model in which particle scattering centres are superimposed

on the quiet time spiral predicted by Parker. Galactic particles arriving over the solar poles experience easy access, since they diffuse along almost straight field lines, but those entering in the solar equatorial plane are constrained to follow many spiral loops. Thus the cosmic ray density should increase on each side of the solar equatorial plane. An anisotropy should be seen, with maximum amplitude, at right angles to the mean spiral field direction for the particles, arriving in those directions, having gyroradii approximately one Larmor radius above or below the equatorial plane. They have shown that the peak to peak amplitude of the semi-diurnal variation.

$$A_2 \approx 0.005 P\% \quad \dots (1.32)$$

where P is the rigidity of the particle.

1.73 Study of cosmic ray daily variation at Trivandrum

A study has been made by the author to gather information concerning the daily variation of μ meson intensity at Trivandrum, which is close to the dip equator, with inclined east-west telescopes and vertical narrow angle and cube telescopes during the period 1964-1966. The experimental set up for the study, the method of analysis of the data and the main results arrived at from the study is reported in Chapter-II

II.

CHAPTER - II

2.1 Experimental technique

2.1.1 Introduction

In April 1963 the author undertook the construction of directional Geiger Counter telescopes pointing to east and west directions at Physical Research Laboratory (outstation) located in the Observatory, Trivandrum (geographic latitude 8.4°N and geographic longitude 76.9°E) which is close to the dip equator. The unit functioned from January 1964 to December 1966. The author also maintained vertical meson telescopes which were already in operation. A description of the experimental set up is presented here.

In an ideal situation the experimental set-up should have a counting rate large enough to enable to study on a statistically significant basis, the daily variation on individual days and also the day-to-day variations. The limitations imposed by the available facilities and difficulty of running Geiger Muller counter telescopes successfully for an extended period of time, may not allow one to realise this sort of ideal set up in practice. Since self-quenched counters have limited life, counter failures are not uncommon and duplicate sets of telescopes not only serve to improve the statistical accuracy of the result but also enable one to standardise and normalise the rates when the counting rate is altered in one of the telescopes due to replacement of a faulty counter by a good one. Satisfactory operation of the unit can be judged by inter-comparison between the independent units of the same geometry in the same direction.

For the study of the behaviour of long term changes of cosmic ray intensity, the long term stability of the unit is essential. This necessitates the regulation of all A.C. and D.C. power supplies. Counter failures can be minimised by using external electronic quenching units. Proper shielding, Where ever necessary, is done to avoid undesirable spurious electrical pick up.

2.12 Geiger Muller Counter

A Geiger Muller counter is a gas-filled diode which operates in a region of the unstable corona discharge. The passage of a single ionizing particle produces a few ion pairs in the sensitive volume of the counter. The free electrons trigger an avalanche and a discharge which rapidly spreads throughout the length of the counter. The discharge lasts only for a few micro-seconds and finally gets quenched due to the development of positive space charge near the central wire. As a result of the discharge and quenching of the counter, a small voltage pulse is developed across the counter, which can be suitably amplified and recorded. The quenching of the discharge is helped by the addition of a polyatomic vapour such as ethyl acetate to the counter gas. The decomposition of the quenching vapour following each discharge sets a limit to the useful life of the counter. The important property of Geiger Muller counter is that the magnitude, duration and general character of the discharge is independent of the specific ionising power of the initial particle.

The important characteristics of a Geiger counter are the threshold voltage, the length and shape of its plateau,

efficiency, stability with use and time, temperature dependence and useful life. All these features cannot be achieved simultaneously to the maximum degree. Montgomery (1940), Wilkinson (1950) and Korff (1955) have studied extensively the theory of counters and their characteristics.

We have used metal counters in the present investigation and all the G. M. counters were prepared at Trivandrum and the author was closely associated with the construction of all the G. M. counters used in the units.

2.13 Geometry of the apparatus

To study the time variations of cosmic ray intensity the author has designed and constructed directional Geiger Muller counter telescopes pointing to east and west directions at 45° to the zenith. Figure 2.01 shows the geometry of the east-west telescope. Each unit consists of three trays of eight G. M. counters with an absorber of 10 cm of lead plates interposed between the middle and bottom trays. To increase the counting rate, long counters of length 91 cm and diameter 3.8 cm are used. The distance between successive trays is 45.5 cm. Four adjacent counters are connected in parallel and their outputs are fed to one quenching unit.

The block diagram of the electronic circuits used in each section (same for both east and west) is shown in figure 2.02. Here the symbols have the following meaning. 'Q' stands for quenching unit, 'M' for mixer circuit 'C' for coincidence and 'S' for scalar unit. C_2 gives a triple coincidence output of Q_1 , Q_1 and Q_1 which is fed to S_2 forming a $10^{\circ} \times 45^{\circ}$

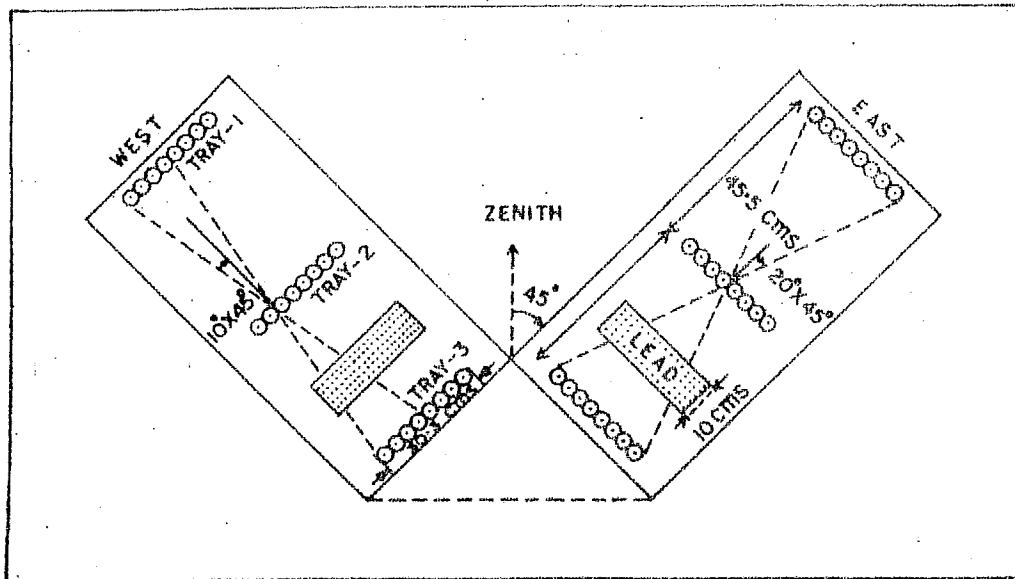
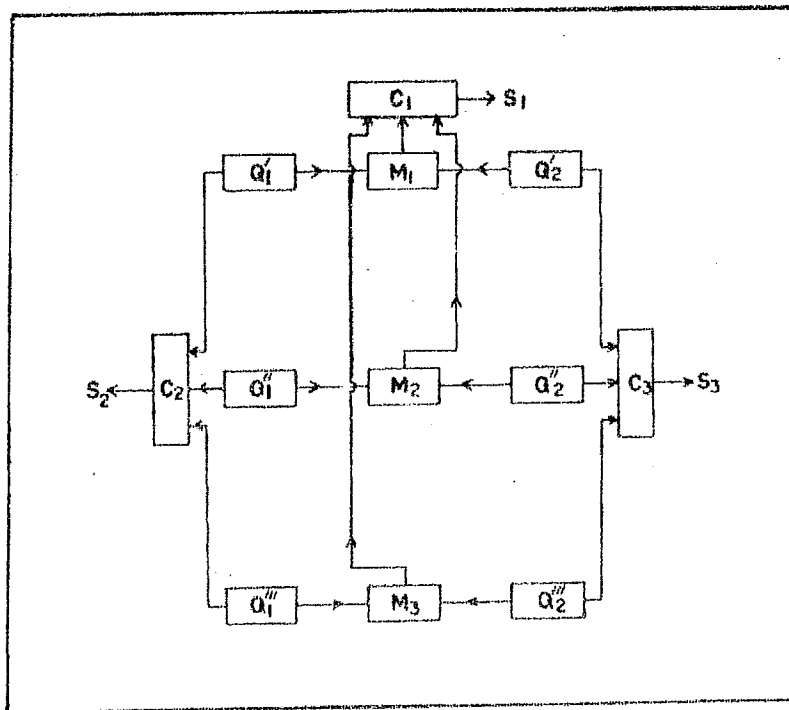


Fig. 2.01 Geometry of east-west telescopes,



M_1 MIXER FOR $Q_1' + Q_2'$, C_1 TRIPLE COINCIDENCE OF M_1 , M_2 & M_3
 M_2 $Q_1' + Q_2'$, C_2 $Q_1' Q_1''$ & Q_1'''
 M_3 $Q_1'' + Q_2''$, C_3 $Q_2' Q_2''$ & Q_2'''
 S_1, S_2 & S_3 ARE SCALARS FOR C_1, C_2 & C_3

Fig. 2.02 Block diagram of electronic circuit for east-west unit.

telescope. Similarly C_3 gives a triple coincidence output of Q_2' , Q_2'' and Q_2''' which is fed to S_3 forming another $10^\circ \times 45^\circ$ telescope. M_1 , M_2 and M_3 are mixer circuits for $(Q_1' + Q_2')$, $(Q_1'' + Q_2'')$ and $(Q_1''' + Q_2''')$ respectively. C_1 gives a triple coincidence output of M_1 , M_2 and M_3 which is fed to S_1 forming a $20^\circ \times 45^\circ$ telescope. The scaling factors of S_1 , S_2 and S_3 are respectively 16, 4 and 4. The set up is identical for east and west telescopes.

The geometry of the cubical meson telescope and the vertical narrow angle telescopes is shown in figure 2.03. The unit consists of 48 Geiger Muller counters each of length 61 cms and diameter 3.8 cm. In each tray there are sixteen such counters arranged with their axis along the geomagnetic north-south direction. There are three such trays as shown in the figure 2.03. The separation between the top and the middle trays is 23 cms and that between middle and the bottom is 61 cms. The entire sensitive area between the middle and the lower most tray is packed with 10 cms of lead to filter out the soft component in the secondary cosmic rays.

The block diagram of the electronic circuits for vertical telescopes of $45^\circ \times 45^\circ$ and $10^\circ \times 36^\circ$ are shown in figure 2.04. Groups of four adjacent counters of the top tray are connected in parallel to quenching units Q_1' , Q_2' , Q_3' and Q_4' . Similarly for middle and bottom trays. Triple coincidence of Q_1' , Q_1'' and Q_1''' corresponds to a telescope of semi-vertical angle 10° in the east-west plane and 36° in the north-south plane. Thus we have four similar independent coincidence outputs of $10^\circ \times 37^\circ$ namely C_1 , C_2 , C_3 and C_4 . The outputs of C_1 and C_2 are mixed in M_1 and is fed to scalar S_2 . Similarly the outputs

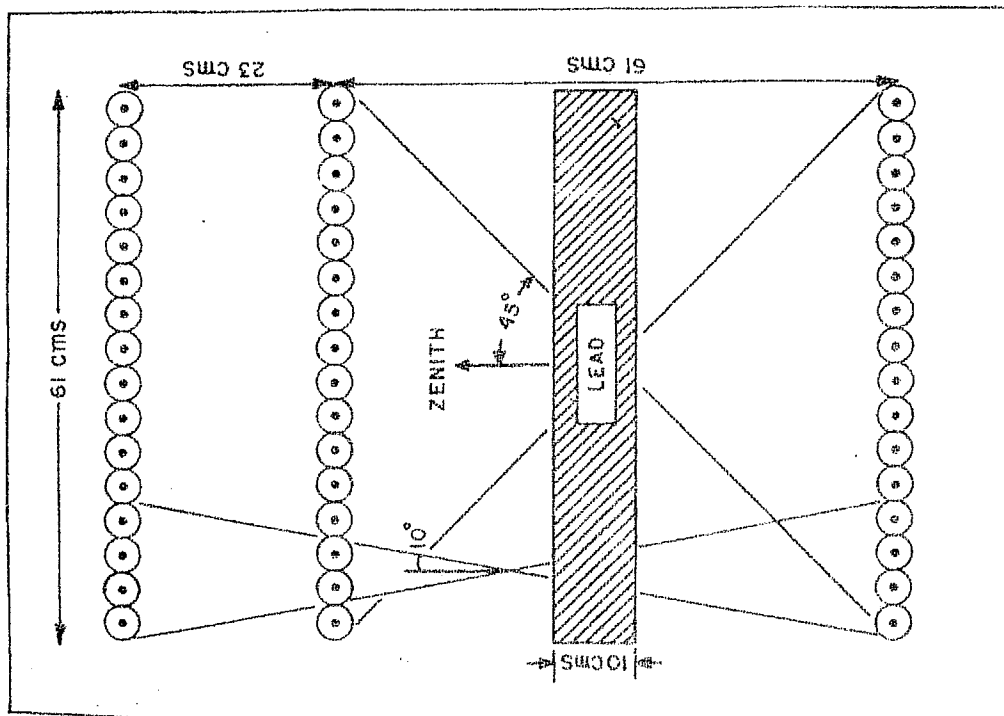
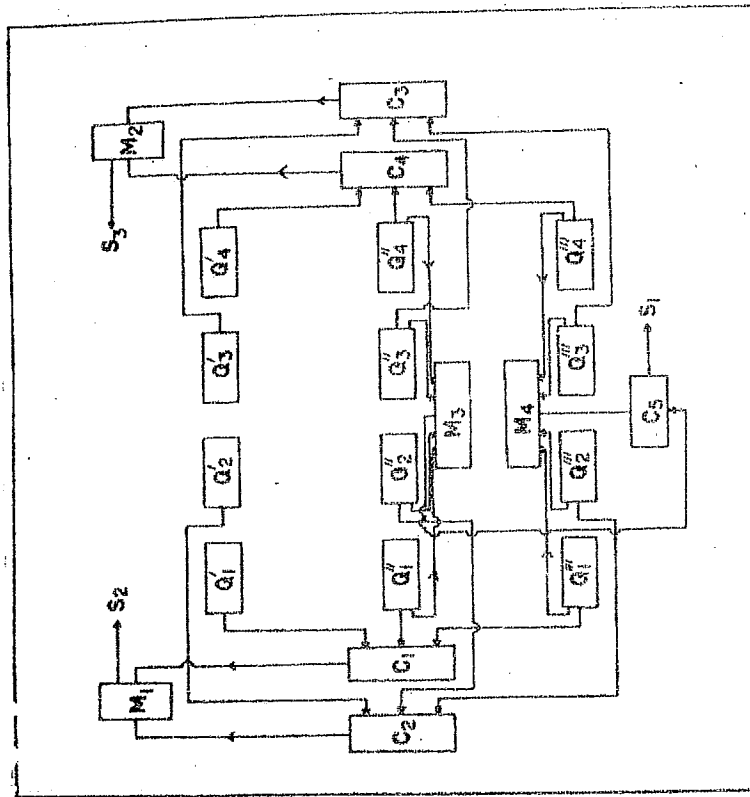


Fig. 2.03 Geometry of vertical narrow angle and cube telescopes.



C_1 TRIPLE COINCIDENCE OF $Q_1, Q'_1 \text{ \& } Q''_1$ M_1 MIXER OF $C_1 \text{ \& } C_2$
 C_2 " $Q_2, Q'_2 \text{ \& } Q''_2$ M_2 " $C_3 \text{ \& } C_4$
 C_3 " $Q_3, Q'_3 \text{ \& } Q''_3$ M_3 MIXER OF $Q_1, Q'_1, Q''_1, Q'_2, Q'_3 \text{ \& } Q''_2, Q''_3$
 C_4 " $Q_4, Q'_4 \text{ \& } Q''_4$ M_4 " $Q'_1, Q'_2, Q'_3 \text{ \& } Q''_1, Q''_2, Q''_3$
 C_5 DOUBLE COINCIDENCE OF $M_3 \text{ \& } M_4$

$S_1, S_2 \text{ \& } S_3$ ARE SCALARS FOR $C_5, M_1 \text{ \& } M_2$

Fig. 2.04 Block diagram of electronic circuits for vertical narrow angle and cube telescopes.

of C_3 and C_4 are mixed in M_2 and is fed to scalar S_3 . The outputs from $Q_1^{///}$, $Q_2^{///}$, $Q_3^{///}$ and $Q_4^{///}$ are fed to mixer M_3 and similarly $Q_1^{////}$, $Q_2^{////}$, $Q_3^{////}$ and $Q_4^{////}$ to M_4 . The double coincidence M_3 and M_4 is achieved through coincidence C_5 and the output is fed to S_1 , forming the cube telescope of $45^\circ \times 45^\circ$ geometry. The scaling factors of S_1 , S_2 and S_3 are respectively 128, 8 and 8. The narrow angle telescopes have independent power supplies.

The outputs from various scalars, both east-west and vertical telescopes, are fed to different electro-mechanical recorders which are kept inside a light proof camera box. An automatic photographic device is used to obtain hourly records of cosmic ray intensity. All the units are designed to work from stabilised D.C. supply voltage of +300 volts and -75 volts. The details of the different telescopes along with the counting rates and probable errors in the amplitude of the daily harmonic σ_r are given in the table (2.01)

TABLE 2.01

Details of different telescopes showing bihourly counting and probable errors in r.

Type of Telescopes	Total bihourly counting rate	Scaling factor	$\sigma_r\%$
$45^\circ \times 45^\circ V$	83200	128	$\pm .14$
$10^\circ \times 45^\circ V$	14400	8	$\pm .34$
$10^\circ \times 45^\circ E$	5200	4	$\pm .57$
$20^\circ \times 45^\circ E$	8800	16	$\pm .43$
$10^\circ \times 45^\circ W$	6200	4	$\pm .52$
$20^\circ \times 45^\circ W$	11200	16	$\pm .38$

2.2 Method of analysis

2.21 Data processing

From the hourly photographs of the mechanical recorder for vertical cube telescope ($45^\circ \times 45^\circ$) reading for 00.00, 01.00, 02.00, , 23.00 hours local time are noted. The difference between successive readings gives the hourly μ meson intensity of cosmic rays centered at $1/2, 1\frac{1}{2}, 2\frac{1}{2}, \dots, 23\frac{1}{2}$ hours. In the case of vertical ($10^\circ \times 36^\circ$), east ($10^\circ \times 45^\circ$), east ($20^\circ \times 45^\circ$), west ($10^\circ \times 45^\circ$) and west ($20^\circ \times 45^\circ$) telescopes readings from recorders for odd hours namely 23.00 (previous day) 01.00, 03.00, , 23.00 are noted. The difference between successive readings gives the bihourly μ meson intensity centered at 00.00, 02.00, , 22.00 hours local time, recorded by the particular telescope.

2.22 Test of self consistency of the data

The data from $10^\circ \times 36^\circ$ vertical, $10^\circ \times 45^\circ$ east and $10^\circ \times 45^\circ$ west telescopes are subjected to the test of self consistency in the following way. Consider the series of bihourly values of two identical but independent telescopes, a_1, a_2, \dots, a_n and b_1, b_2, \dots, b_n . A third series c_1, c_2, \dots, c_n is obtained by subtracting the first series from the second. In the ideal situation $\sum_1^n c_i = 0$. However in practice it is seldom achieved, due to slight differences in geometrical set up and circuitary. The mean values of c_i i.e. $\sum_1^n c_i / n$ may have a value 'd' which is different from zero. The variance, $\overline{G_1^2}$ and $\overline{G_2^2}$ of the two series 'a' and 'b' may not be the same, and $\overline{G_3^2}$ the variance of 'c' series will be equal to $(\overline{G_1^2} + \overline{G_2^2})$. If one assumes a

normal distribution for the 'c' series, then the probability that any c_i value exceeds $d + 2\sigma$ is 4.6%. If there are more than 4.6% c_i values which exceed $d + 2\sigma$, then the individual series 'a' and 'b' are further checked for any systematic error.

2.23 Normalisation of cosmic ray intensity

This is done when a finite number of bihourly values from one series are either not reliable or not available. If the i^{th} value in the 'a' series is missing due to some known cause, then the normalised value a_i can be obtained from the five preceding values of 'a' and 'b' series.

$$a_i = b_i \times \frac{a_{i-5} + a_{i-4} + a_{i-3} + a_{i-2} + a_{i-1}}{b_{i-5} + b_{i-4} + b_{i-3} + b_{i-2} + b_{i-1}} = b_i \times N_1 \quad \dots (2.01)$$

on the other hand if there is a level change in the mean intensity, due to change in sensitive area or efficiency of the detector (this happens when a G.M. counter is replaced in one of the sets) a new normalising factor N_2 is found by using the relation

$$N_2 = \frac{a_{i+5} + a_{i+4} + a_{i+3} + a_{i+2} + a_{i+1}}{b_{i+5} + b_{i+4} + b_{i+3} + b_{i+2} + b_{i+1}} \quad \dots (2.02)$$

The series 'a' after the i^{th} value is normalised by multiplying the values by $\frac{N_1}{N_2}$. This procedure is adopted after every break in the data.

2.24 Pressure correction to cosmic ray intensity

Wada (1960) has calculated theoretically the total barometric coefficient as a function of momentum, zenith angle, latitude and altitude, using momentum spectrum of mesons

For an equatorial sea level station such as Trivandrum, the pressure coefficient is $\sim -0.14\%/m.b.$ for vertical telescopes. Moreover, Pai (1962) has reported a pressure coefficient of $-0.14\%/m.b.$ for mesons of vertical incidence.

To derive the pressure coefficient for μ -meson intensity in inclined directions, two factors have to be considered. Apart from a factor $\sec \theta$, related to mass absorption where θ is the inclination with the vertical, one has a factor related to the difference in the mean energy of radiation incident from inclined directions which alters the survival probability of the secondaries. Rao and Sarabhai (1961) have suggested that the change of barometric coefficient with inclination is expected to be quite small. They have used the same pressure coefficient for east, vertical and west telescopes. Considering these, in the present study a barometric coefficient of $-0.14\%/m.b.$ is used to correct the cosmic ray intensity along vertical and inclined directions.

2.25 Elimination of the long-term trend in cosmic ray intensity

The data corrected for pressure variations are subjected to moving average to separate out the daily variation from changes which have periods of more than a day. For bihourly data the average values of cosmic ray intensity are found out as

$$\bar{C}_{6.5} = \frac{1}{12} \sum_{i=1}^{12} C_i \quad \dots (2.03)$$

where C_i are the bihourly values and bar denotes the average which is centered at 6.5th bihourly or the value corresponding to 13 00 hours. Similarly

$$\bar{C}_{7.5} = \frac{1}{12} \sum_{i=1}^{12} C_i \quad \dots (2.04)$$

which is centered at 15.00 hours and the mean of these two averages is centered at 14.00 hours. As the calculations are continued for other bihourly values, successive means are obtained which are devoid of any periodic variations, with period of a day and harmonics of it. This series therefore represents the long term trend of cosmic ray intensity. This trend is removed in the series, which therefore contains only short term variation with periods of a day or less.

2.26 Harmonic analysis

Every function satisfying certain conditions can be expressed as an infinite series of circular functions.

$$F(t) = a_0 + \sum_{n=1}^{\infty} (a_n \cos(nt) + b_n \sin(nt)) \quad \dots (2.05)$$

where a_n, b_n are the coefficients of the n^{th} harmonic.

The following expressions are used to determine the coefficients.

$$a_0 = \frac{1}{T} \sum_{r=1}^T C_r \quad \dots (2.06)$$

$$a_n = \frac{2}{T} \sum_{r=1}^T C_r \cos(nt_r) \quad \dots (2.07)$$

$$b_n = \frac{2}{T} \sum_{r=1}^T C_r \sin(nt_r) \quad \dots (2.08).$$

The amplitude, r_n and phase ϕ_n of the n^{th} harmonic are found from the relation.

$$r_n \cos(nt - \phi_n) = (a_n \cos nt + b_n \sin nt) \quad \dots (2.09)$$

from which it follows that

$$r_n = \sqrt{a_n^2 + b_n^2} \quad \text{and} \quad \phi_n = \arctan \frac{b_n}{a_n} \quad \dots (2.10)$$

The first two harmonics are sufficient to study the daily variation of cosmic ray intensity. From the harmonic components of first two harmonics namely a_1 , b_1 , a_2 and b_2 a daily built up curve can be derived using the relation

$$V_i = a_1 \cos t_i + b_1 \sin t_i + a_2 \cos 2t_i + b_2 \sin 2t_i \dots (2.11)$$

From the theory of probability it is found that the distribution of a_n and b_n are gaussian if the hourly or bihourly values have also the same distribution. The standard error of the various harmonic coefficients are

$$\sigma_{a_n}^2 = \sigma_{b_n}^2 = \frac{\sigma^2}{6} \quad \text{for bihourly and } \frac{\sigma^2}{12} \quad \text{for hourly (2.12)}$$

where σ is the standard deviation of bihourly or hourly values.

$$\sigma_{r_n} = \sigma_{a_n} \quad \text{and} \quad \sigma_{\phi_n} = \frac{\sigma_{r_n}}{r_n} \dots (2.13)$$

$$\text{The error in built up curve is } \sqrt{2} \sigma_{r_n} \dots (2.14)$$

2.27 Correlation analysis

When variables X and Y are correlated rather than functionally related, one could no longer speak of a 'best' Y-value to correspond to each X-value but only of a most probable Y-value about which observed values may be distributed according to some frequency distribution law. Obviously, the closer the observed values are to the most probable value, the more definite is the relationship between X and Y. This postulate is the basis for the various numerical measures of the degree of correlation. The correlation coefficient is given by

$$r = \frac{n \sum x \cdot y - \sum x \cdot \sum y}{\sqrt{[n \sum x^2 - (\sum x)^2][n \sum y^2 - (\sum y)^2]}} \dots (2.15)$$

The error in correlation coefficient is given by

$$\sigma_{r_m} = \frac{1 - r^2}{\sqrt{n-1}} \quad \dots (2.16)$$

Generally, two regression lines can be calculated for the case of two correlated variables; (1) the regression line of Y on X - the least squares line obtained on the assumption that X values are exact, and (2) the regression line of X on Y - the least squares line obtained on the assumption that Y values are exact. The slopes are

$$m' = \frac{(X - \bar{X})(Y - \bar{Y})}{(X - \bar{X})^2} \quad \dots (2.17)$$

$$m'' = \frac{(X - \bar{X})(Y - \bar{Y})}{(Y - \bar{Y})^2} \quad \dots (2.18)$$

The slope m is then

$$m = \frac{1}{2} \left(m' + \frac{1}{m''} \right) \quad \dots (2.19)$$

2.3 Results and discussions

2.31 Introduction

The daily variation of cosmic ray intensity has been the subject of extensive investigation, mainly because of the information it can give about the anisotropy of the primary radiation and the modulation mechanisms responsible for their production. Continuous monitoring of the intensity, has been made through the recording of secondary radiation at sea-level or mountain altitudes, with the help of neutron monitors, ionization chambers, Geiger-counter telescopes and plastic scintillators. Adequate corrections have to be applied for atmospheric influences and deflection in the geomagnetic field

in order to relate the observed variations to those in the primary variations. This is discussed in sections 1.32, 2.24 and 2.32.

In spite of the difficulties in correcting the μ meson data for temperature variations, counter telescopes possess an advantage over neutron monitors in their ability to record the cosmic ray intensity along different directions.

2.32 Variational coefficient and its application to the daily variation of cosmic ray intensity

Cosmic rays, detected by instruments on the surface of the earth, are subjected to geomagnetic deflections and they come from directions scattered over a large part of the celestial sphere. Dorman (1951) has developed the concept of coupling coefficient to relate the variation measured by a detector to the strength of the anisotropy in space. McCracken et al (1965) have evaluated the variational coefficients for neutron monitors for several stations. The author has used their method to compute the variational coefficients for μ meson intensity along vertical, east and west directions for Trivandrum station.

The energy spectrum of variation of the primary anisotropy can be represented by the relation

$$\frac{\delta D(E)}{D(E)} = aE^\beta \quad \text{for } E_{\text{max}} > E > E_{\text{min}} \quad \dots (2.20)$$

In the present work, for each detector the author has used in equation (2.20) geomagnetic cut off energy as E_{minimum} and 250 BeV as E_{maximum} . The choice of 250 BeV as E_{max} , eventhough arbitrary, has some physical significance. For a

5 ✓ interplanetary magnetic field, charged particles of energy 225 BeV have a gyroradius of 1 A.U. The choice of E_{\max} is still an unsettled problem (Subramanian, 1971). The cut off rigidities for Trivandrum for different zenith and azimuth angles using sixth degree simulation of the geomagnetic field have been calculated following the computer procedure used by Daniel and Stephens (1966). Figure 2.05 shows the variations of cut off rigidity with azimuth, for different zenith angles for Trivandrum. The cut off rigidity for east (zenith angle 45°) is 29.5 B.V., for vertical is 17.4 BV and for west (zenith angle 45°) is 12.7 BV for Trivandrum.

Using sixth degree simulation of the geomagnetic field, the asymptotic directions (ψ, λ) for particles of rigidities, R_k from cut off to 750 BV along vertical and inclined directions for Trivandrum are available (McCracken et al, 1965). Extrapolated values are used in the present work for zenith angles greater than 32° . The errors which could creep in the values of ψ and λ for given rigidities are negligibly small for rigidities above 20 BV. However in this process, very near to cut off rigidity along west, for zenith angle 55° the uncertainty is as high as $\pm 3^{\circ}$. Since the rigidity resolution (IQSY - 10, 1965) at the cut off rigidity range is 2 GV this error is not at all important. To avoid any controversy the longitude resolution for the variational coefficient is restricted to 5° . Figure 2.06 shows the asymptotic directions of approach for the primary cosmic rays with energies from geomagnetic cut off along respective directions to 750 BeV along east (zenith 45°), west (zenith 45°) and vertical at Trivandrum. It can be seen that all the detectors scan the near equatorial regions of the celestial sphere (-6° to $+11^{\circ}$ asymptotic latitudes).

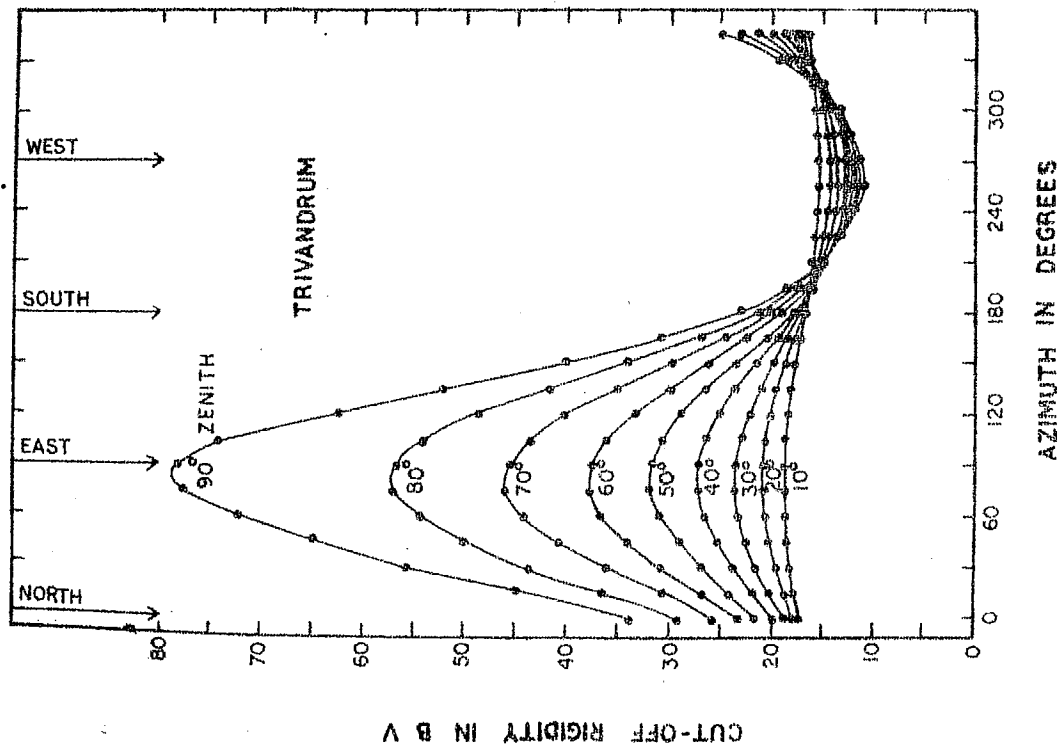


Fig. 2.05 The variation of cut off rigidity with azimuth, for different zenith angles for Trivandrum.

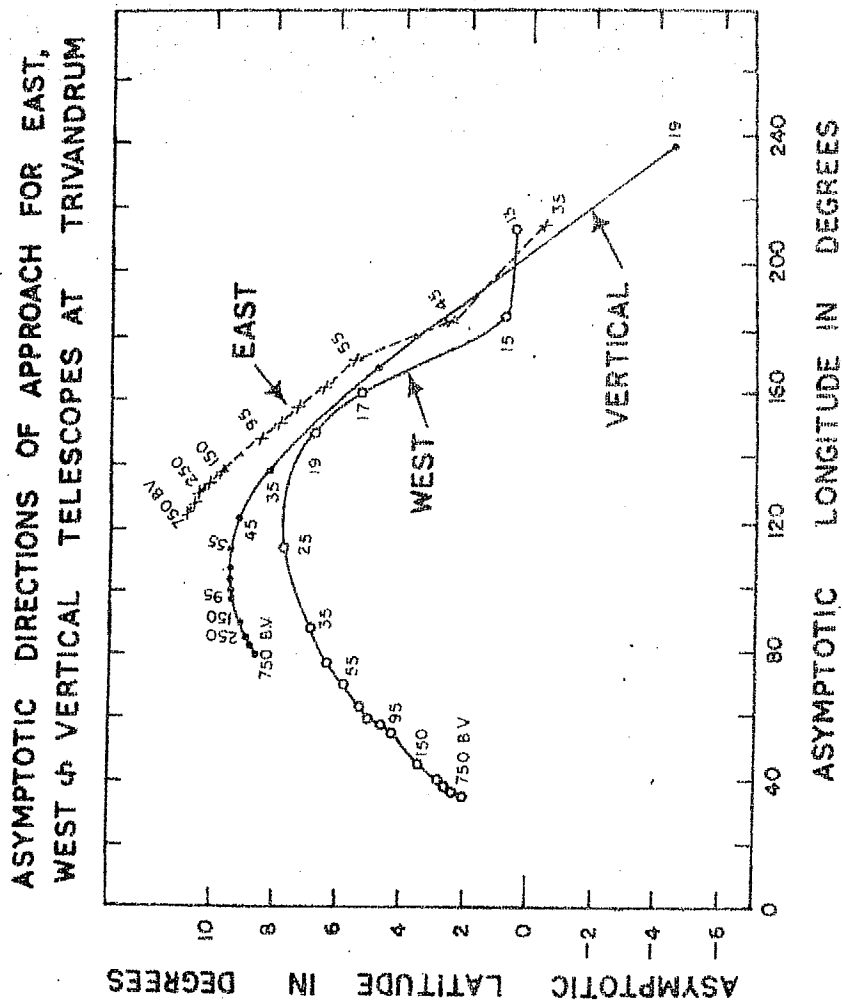


Fig. 2.06 Asymptotic directions of approach for primary cosmic rays along east (45°), vertical and west (45°) for Trivandrum.

The variational coefficient $V(\varphi, \beta)$ which gives the relative contribution to the counting rate from the asymptotic longitude belt between φ and $(\varphi + d\varphi)$ for β , the exponent of the variational part of the energy spectrum of variation of the primary anisotropy, is given by

$$V(\varphi, \beta) = \int_{\text{Cul. alt.}}^{\frac{250.5V}{\cos \lambda} + \frac{1}{2}} \int_{-\pi/2}^{\pi/2} W(R_k) R_k^\beta \frac{Y(\varphi, R_k)}{Y(4\pi, R_k)} \cos \lambda dR_k d\lambda \quad \dots (2.21)$$

Here $W(R_k)$ s are the normalised coupling coefficients, after giving due weightage to the radiation sensitivity of the detector along appropriate directions. Radiation sensitivity of vertical and inclined telescopes have been calculated using the procedure outlined, by Kane and Rao (1958, 1960). The coupling coefficients for vertical direction have been obtained from Webber (1962) and those for inclined directions from Rao and Sarabhai (1961). The function $\frac{Y(\varphi, R_k)}{Y(4\pi, R_k)}$ is evaluated in the following way. The celestial $\frac{Y(\varphi, R_k)}{Y(4\pi, R_k)}$ sphere is divided into 2592 units of Ω_{ij} regions where $i = \lambda$ values from -90° to $+90^\circ$ at intervals of 5° latitude and $j = \varphi$ values from 0° to 360° at intervals of 5° longitude. For a particular value of $R = R_k$, if a particular Ω_{ij} is accessible from the direction (θ, ϕ) where θ is the zenith and ϕ is the azimuth then $\frac{Y(\Omega_{ij}, R_k)}{Y(4\pi, R_k)}$ is counted as one, otherwise it is counted as zero. The $\frac{Y(\Omega_{ij}, R_k)}{Y(4\pi, R_k)}$ sum of all the values namely

$$\sum_{i=1}^{36} \left[\frac{Y(\Omega_{ij}, R_k)}{Y(4\pi, R_k)} \right] = \left[\frac{Y(\varphi, R_k)}{Y(4\pi, R_k)} \right] \quad \dots (2.22)$$

$\cos \lambda$ appears in equation 2.21 is due to the assumption that the anisotropy has a $\cos \lambda$ dependence. The relative amplitude of the j^{th} harmonic, $R_{j\beta}$ is given by

$$R_{j\beta} = A_{j\beta} \cdot B_{j\beta} \quad \dots (2.23)$$

where $A_{j\beta}$ is an arbitrary constant and

$$B_{j\beta} = \sqrt{(X_{j\beta}^2 + Y_{j\beta}^2)} \quad \dots (2.24)$$

$$X_{j\beta} = \int_0^{2\pi} V(\varphi, \beta) \sin(j\varphi) d\varphi \quad \dots (2.25)$$

$$Y_{j\beta} = \int_0^{2\pi} V(\varphi, \beta) \cos(j\varphi) d\varphi \quad \dots (2.26)$$

$$\tan \gamma_{j\beta} = \frac{X_{j\beta}}{Y_{j\beta}} \quad \dots (2.27)$$

The geomagnetic bending for the j^{th} harmonic is $\mathcal{T}_{j\beta}$ where

$$\mathcal{T}_{j\beta} = \frac{\sqrt{j\beta - jL}}{15j} \text{ hours} \quad \dots (2.28)$$

L is the station longitude (76.9° for Trivandrum)

The relative amplitude and geomagnetic bending for $\beta = -1.2$ to $+1.0$ at intervals of 0.2 have been calculated for vertical and east and west pointing telescopes inclined 45° to the zenith at Trivandrum.

Figure 2.07 gives the expected ratios $\frac{R_{1 \text{ West}}}{R_{1 \text{ East}}}$ and $\frac{R_{2 \text{ West}}}{R_{2 \text{ East}}}$ for different values of β . It can be seen that the ratio of $\frac{R_{1W}}{R_{1E}}$ decreases with increase in the value of β . Also in

figure 2.07 is shown the geomagnetic bending for east, vertical and west telescopes. Table 2.02 gives the computed values of $(\phi_{1W} - \phi_{1E})$, the difference in the phase of the 1st harmonic between west and east for β values from -1.2 to $+1.0$. For values of β , from +ve to -ve it can be seen from table 2.02 that $(\phi_{1W} - \phi_{1E})$ decreases.

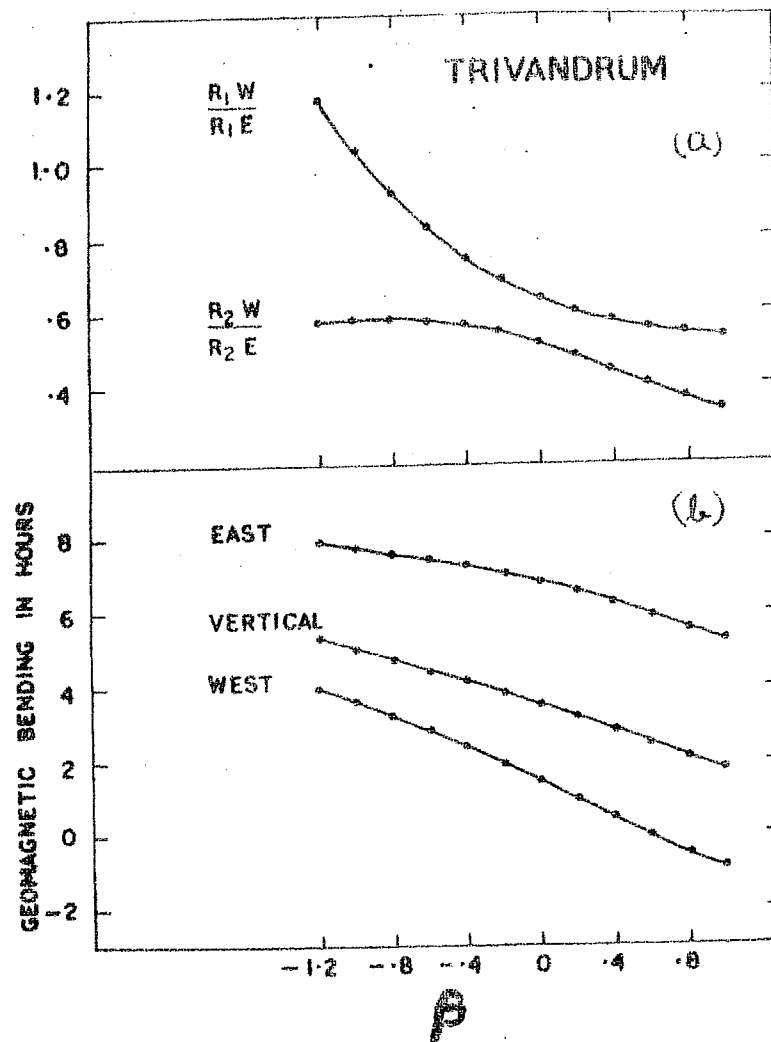


Fig. 2.07 (a) The expected ratios of $\frac{R_{1W}}{R_{1E}}$ and $\frac{R_{2W}}{R_{2E}}$ for

different values of β , (b) Geomagnetic bending for east vertical and west for Trivandrum.

TABLE 2.02

Computed values of the difference in the phase of the first harmonic between west and east for different values of β

β	-1.2	-1.0	-0.8	-0.6	-0.4	-0.2	0.0	0.2	0.4	0.6	0.8	1.0
$(\phi_{1W} - \phi_{1E})$ in hours	4.3	4.5	4.7	4.9	5.2	5.4	5.6	5.8	6.0	6.1	6.3	6.3

2.33 Determination of temperature effect to the daily variation of cosmic ray intensity.

Modulation of μ meson intensity due to temperature variations in the upper atmosphere has long been established. However, the evaluation of its contribution to the daily variation, poses many problems (Sarabhai et al, 1953; Wada and Kudo, 1956; Dorman, 1957; Quenby and Thambyah/Pillai, 1960; Wada, 1961; Bercovitch, 1965; and Bercovitch, 1968). Because of the relatively small amplitude of the diurnal and semi-diurnal variations ($\sim 0.4\%$ for diurnal and $\sim 0.1\%$ for semi-diurnal) in the daily variation of cosmic ray intensity, special care is required to correct for variations which are of atmospheric origin. In the case of a meson component, the diurnal temperature variation in the atmosphere is expected to produce an intensity wave with a time of maximum during early morning hours, more or less opposite in phase to the observed diurnal time of maximum of the primary anisotropy of cosmic rays, which is approximately along 1800 hours local time (Quenby and Thambyah/Pillai, 1960 and Bercovitch, 1968).

Temperature effect for the neutron component is less than $-0.02\%/^{\circ}\text{C}$ change of temperature near the top of the atmosphere and

for all practical purpose, this effect can be neglected (Bercovitch, 1968). Thus it is possible to estimate the anisotropy of cosmic rays in interplanetary space, from the daily variation of the neutron intensity measured at a net work of stations with neutron monitors. The variational coefficient calculated in section 2.32 then provides a means of translating the anisotropy in interplanetary space, to the respective telescopes for Trivandrum. The difference between the observed pressure corrected daily variation of μ -meson intensity and the evaluated daily variation at the telescopes, can be attributed to a temperature effect on the daily variation of μ meson intensity along with any other local source of modulation which may be affecting the cosmic ray intensity.

Patel, 1970 and Patel et al, 1968 have reported the direction and amplitude in space of the diurnal and semi-diurnal anisotropy and β , the exponent of the variational part of the energy spectrum of the primary anisotropy, on a day-to-day basis. To compute the above parameters they analysed the data of neutron monitors from Churchill, Deep River, Sulphur Mountain, Climax, Dallas and Hermanus.

The method employed by them is as follows. In determining the energy spectrum of variation, 36 combinations of β (-1.2 to +1.0 at the interval of 0.2) and E_{\min} (2, 4 and 8 BeV) in equation (2.20) have been considered. For each combination of β and E_{\min} , the attenuation factor α_{ijk} by which the amplitude of the j^{th} harmonic is reduced with respect to its free space value and the effective geomagnetic bending angle \mathcal{I}_{ijk} have been calculated for a station 'i'. From the observed diurnal and semi-diurnal components (a_j , b_j) the free space values (denoted by *) have been estimated following the method of

Sarabhai and Subramanian, 1966

$$a_{ijk}^* = \frac{a_{ij} X_{ijk} + b_{ij} Y_{ijk}}{2 \alpha_{ijk}} \quad \dots\dots(2.29)$$

$$b_{ijk}^* = \frac{a_{ij} Y_{ijk} + b_{ij} X_{ijk}}{2 \alpha_{ijk}} \quad \dots\dots(2.30)$$

$$X_{ijk} = \alpha_{ijk} \cos \tau_{ijk} \quad \dots\dots(2.31)$$

$$Y_{ijk} = \alpha_{ijk} \sin \tau_{ijk} \quad \dots\dots(2.32)$$

A measure of the goodness of the fit of the calculated values for an assumed value of k with the observed values, from different detectors is given by

$$S_k^2 = \sum_{i=1}^N \sum_{j=1}^2 \frac{(a_{ijk}^* - \overline{a_{ijk}^*})^2 + (b_{ijk}^* - \overline{b_{ijk}^*})^2}{\overline{\alpha_{ijk}^2}} \quad \dots\dots(2.33)$$

where the bar denotes values averaged over all stations. The denominator represents the variance of the corresponding terms in the numerator and is given by

$$\overline{\alpha_{ijk}^2} = \frac{(N^2 - 2N) \alpha_{ijk}^2 \overline{\alpha_{ij}^2} + \sum_{i=1}^N \alpha_{ijk}^2 \overline{\alpha_{ij}^2}}{N^2} \quad \dots\dots(2.34)$$

The spectrum which gives the minimum value of S_k^2 is considered to fit the data best.

Even though 36 different spectra have been considered, the inherent resolution that is possible in discriminating between spectra has to be taken into account. The standard error of S_{\min}^2

namely $\chi^2(N)$ is used as a criterion. $\chi^2(N)$ depends on the number of stations, N . In a group of spectra for which S^2 values differ from S_{\min}^2 by more than $\chi^2(N)$, the value of k for which the minimum occurs, is deemed to be the spectrum of choice. On the other hand if the range of S^2 for the different spectra on a particular day does not exceed $\chi^2(N)$, then the determination of the energy spectrum is impossible. By setting up an upper limit of S_{\min}^2 it is possible to isolate days on which major Forbush decreases have occurred or when data from one or more of the stations is erratic. With these as ground rules, a spectrum corresponding to S_{\min}^2 and one or more equivalent spectra are identified for each day. Table 2.03 shows how the days have been classified according to the energy spectra of variation of the primary anisotropy along with the total number of days in each group during 1964 to 1966.

Using the computed values of a_1, b_1, a_2, b_2 and as described above (Patel, 1970 and Patel et al, 1968), the author has computed the expected amplitude and phase of the diurnal and semi-diurnal components due to primary anisotropy at the respective instruments (along east, vertical and west directions) at Trivandrum on a day-to-day basis during the period 1964 to 1966.

TABLE 2.03

Classification of days according to energy spectra of variation
and the total number of days in each group during 1964 to 1966

Classification	No. of days in each group	Exponent of the energy spectrum of variation
$\beta = -ve$	166	$\beta = -0.6$ to -1.2 with $E_{min} = 2, 4$ and 8 BeV $\beta = 0.0$ to -0.4 with $E_{min} = 8$ BeV and $\beta = -0.4$ with $E_{min} = 4$ BeV
$\beta \approx 0$	244	$\beta = +0.4$ to -0.4 with $E_{min} = 2$ BeV $\beta = 0.2$ with $E_{min} = 4$ BeV
$\beta = +ve$	222	$\beta = +1.0$ to 0.8 with $E_{min} = 2, 4$ and 8 BeV
Ambiguous	464	$S^2 < \chi^2 (N)$ and $S_{min}^2 \geq 400$ (in arbitrary unit)

The method employed to compute the expected amplitude and phase of the diurnal and semi-diurnal anisotropy is similar to the method suggested by Sarabhai and Subramanian, 1966.

Let a_{ij}^* and b_{ij}^* are the harmonic components describing the daily variation of cosmic ray intensity in free space and a_j and b_j that expected at the instrument for the j^{th} harmonic of the daily variation. They can be related as

$$a_j = a_{j\beta}^* \alpha_{j\beta} \cos \mathcal{T}_{j\beta} + b_{j\beta}^* \alpha_{j\beta} \sin \mathcal{T}_{j\beta} \quad \dots (2.29)$$

$$b_j = b_{j\beta}^* \alpha_{j\beta} \cos \mathcal{T}_{j\beta} - a_{j\beta}^* \alpha_{j\beta} \sin \mathcal{T}_{j\beta} \quad \dots (2.30)$$

where $a_{j\beta}$ and $J_{j\beta}$ are the attenuation factor and the geomagnetic bending angle of the j^{th} harmonic and β is the exponent of the spectrum of variation.

Table 2.04 shows the availability of good data from cosmic ray detectors at Trivandrum during the period 1964 to 1966. Frequent power failures at Trivandrum not only disturb the continuous operation of the units but also increase the frequency of failures of the G M. Counters. Humidity at Trivandrum is generally high, with the result difficulties were experienced, at times, due to electrical pick up. The plateau characteristics change earlier with 91 Cm counters, which were in operation in east-west units than with 61 Cm counters, which were in operation in vertical units. With the result the continuity of data is more often disturbed in east west telescopes than with vertical telescopes. This can be seen in table 2.04.

A comparison between the observed pressure corrected daily variation and the expected daily variation would represent the modulation of μ meson intensity due to temperature variations in the atmosphere together with modulation due to a local source of non meteorological origin, if there is any. The method adopted here is similar as that reported by Nair and Sarabhai (1967).

In the present analysis, the author has used those days when the primary anisotropy responsible for the diurnal variation is same as primary cosmic ray spectrum ($\beta = 0$) during the period 1964 to 1966. During the period 1964 to 1966 for those days the diurnal anisotropy had an average amplitude of $\sim 0.4\%$ with a time of maximum around 1800 hours in space (Patel et al 1968). The selection of such days is justified for the reason that

TABLE 2.04

Table showing the availability of good data from cosmic ray telescopes at
Trivandrum

Telescope	Year	J	F	M	A	M	J	J	A	S	O	N	D	Total
45x45 ^o	1964	28	28	31	30	26	19	24	24	21	28	27	29	315
Vertical	1965	16	23	31	24	25	13	25	22	28	31	28	27	293
	1966	28	26	25	17	23	17	23	28	28	20	25	31	291
10x36 ^o	1964	27	23	27	27	21	26	29	19	25	26	30	27	307
Vertical	1965	21	24	28	30	11	10	26	26	30	31	28	25	290
	1966	31	28	27	15	18	28	28	29	28	23	23	31	309
10x45 ^o	1964	--	--	--	27	--	12	21	22	21	29	23	27	182
East	1965	28	27	26	27	27	25	25	25	30	31	24	22	317
	1966	18	18	27	19	23	28	26	19	19	13	21	12	243
20x45 ^o	1964	--	--	--	18	--	--	16	19	17	--	13	19	102
East	1965	27	25	19	25	--	18	25	03	30	31	24	20	247
	1966	24	25	27	18	27	26	27	11	24	26	15	06	256
10x45 ^o	1964	26	17	24	28	--	26	20	27	30	29	21	20	268
West	1965	27	25	27	30	28	25	12	26	26	31	24	14	295
	1966	16	28	27	21	22	30	27	25	12	11	17	--	236
20x45 ^o	1964	--	29	19	24	--	21	21	26	30	31	14	20	235
West	1965	24	22	28	25	--	17	19	26	23	29	25	08	246
	1966	13	28	25	19	21	08	17	--	17	11	--	--	159

the physical processes, capable of producing diurnal anisotropy of galactic cosmic rays in interplanetary space are well understood. Theoretically for such days the diurnal anisotropy has been explained on the basis of azimuthal drift of cosmic rays (Parker, 1964, 1967; Axford, 1965). Moreover in the present study, the temperature effect for days when β is either positive or negative cannot be evaluated so accurately as can be done for days when β is zero, due to the following reasons. It can be seen from equation 2.21 that the variational coefficient, $V(f, \beta)$ is a function of the coupling constants, rigidity to the power β and also to the cones of acceptance of the detectors. When $\beta \approx 0$, the computed values of the relative amplitudes are directly comparable. But when β is negative or positive, unless the value of β is extremely accurate, large errors could creep in while translating the anisotropy in free space to the respective telescopes at the station. Another error which is more important is that, for the determination of the energy spectrum of variation as explained earlier, Patel et al (1968) have used either 2, 4 or 8 BeV as E_{\min} . Where as for Trivandrum Station E_{\min} for west (45°) = 12.7 BeV, for vertical = 17.4 BeV and for east (45°) = 29.5 BeV. This will introduce further uncertainties while translating values from space to instrument for days when β is -ve or +ve (but not so when $\beta = 0$).

It can be seen from table 2.01 that the standard errors in the daily harmonics ranges from 0.14% to 0.57% (0.14% for vertical cube and 0.57% for east $10^\circ \times 45^\circ$) and so the data analysed over a number of days alone are meaningful.

Figure 2.08 (a) shows the harmonic dials for the average (observed-computed) diurnal variations along east, vertical and the west telescopes at Trivandrum for 202 days during

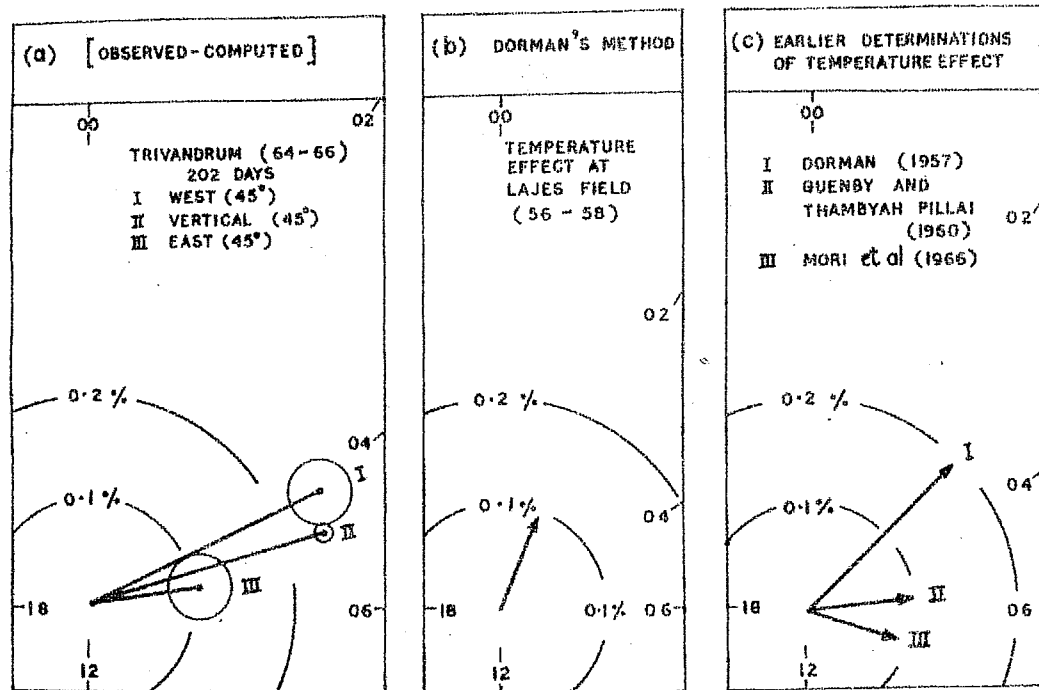


Fig. 2.08 Harmonic dials showing

(a) Present estimate of the (observed — computed) vectors along east, vertical and west for Trivandrum.

(b) Present estimate of temperature correction vector for Lajes Field using Dorman's method.

(c) Earlier determinations of the temperature correction vectors by (1) Dorman (1957), (2) Quenby and Thambyahpillai (1960) and (3) Mori et al (1966).

the period January 1964 to December 1966, when $\beta = 0$. If this residual effect can be attributed only to temperature variations in the upper atmosphere, the diurnal time of maximum of the residual effect along east, vertical and west directions should remain practically constant within statistical errors. It is observed that the residual effect has a time of maximum almost same along east, vertical and west directions as is expected and is around 0500 hours local time.

However the diurnal amplitude γ_i of the residual curve obtained from the present study shows different values along east, vertical and west directions (γ_i (east) = $-0.11 \pm 0.03\%$, γ_i (vertical) = $0.24 \pm 0.01\%$ and γ_i (west) = $0.25 \pm 0.03\%$). The mean energies of response of the detectors at Trivandrum along east (45°), vertical and west (45°) are respectively 64.0, 53.5 and 37.5 BeV. This shows that the mean energy of mesons arriving from east is higher than the mean energy of mesons arriving from west. The relativistic life time for μ mesons arriving from east is consequently longer than that arriving from west. With increase in the atmospheric temperature the path length for μ mesons, from their production level to the ground, increases. So the low energy μ mesons arriving from west decay more compared to the higher energy μ mesons arriving from east. Thus it is expected that the amplitude of the temperature effect should be maximum along west and minimum along east. Assuming the residual effect to be entirely due to temperature effect on meson intensity, it can be seen that the present estimate is consistent with what is expected.

In principle the temperature effect on the daily variation of μ meson intensity could be removed if sufficiently frequent and accurate atmospheric temperature sounding data were

available. Unfortunately even though meteorological radiosonde observations are available for Trivandrum very close to where the meson monitors were housed, they are only twice per day, which is insufficient to determine the diurnal wave. Moreover data up to 50 mb are available only for few days, and their accuracy is doubtful due to radiation errors.

At present there are only a few reliable studies about the daily variation of temperature at various altitudes, ranging from ground to say 50 mb height. Harris et al (1962) have computed the diurnal variation of temperature at Lajes Field, Terceira, Azores for 30 isobaric levels between the surface and 10 mb. Rawinsonde observations spaced at intervals of six hours during the period 1956 to 1958 have been used by them to determine the annual mean values of the diurnal variation of temperature which is shown in table 2.05. The relation between the phase and the time of maximum is given by $t_{\max} = \frac{450 - \alpha}{15}$ hours. It can be seen that the amplitude of the diurnal temperature variation in the atmosphere decreases from surface level to 500 mb but increases from 500 mb to 10 mb. The diurnal temperature variation has a time of maximum around 1400 hours local time at all levels. Their observations enable one to calculate the temperature effect for Lajes Field. The computed value of $\frac{\delta N_{\mu}}{N_{\mu}}$ for Lajes Field during 1956-58, using Dorman's method as described below, is $\approx 0.1\%$ with a time of maximum around 0020 hours local time. This is shown in figure 2.08(b).

Comparison of figure 2.08(a) with figure 2.08(b) shows that the diurnal amplitude and the time of maximum of the temperature effect determined by the (observed - computed) method and by Dorman's method are not in agreement. The probable reasons for the inconsistency may be due to (1) that

TABLE 2.05

Table showing the diurnal amplitude and phase of the atmospheric temperature, the temperature coefficient, and the temperature effect on meson intensity at Lajes Field using Dorman's method

Height in mb (Pressure scale)	Diurnal amplitude of tempe- rature in degree C	Diurnal phase of tempera- ture in degrees	Temperature coefficient K_1 in % per per degree C	Temperature effect on meson intensity in %
Surface	1.12	260	-0.020	-0.022
900	0.16	221	-0.021	-0.003
800	0.16	205	-0.022	-0.004
700	0.14	245	-0.024	-0.003
600	0.18	239	-0.025	-0.005
500	0.19	239	-0.025	-0.005
400	0.20	247	-0.028	-0.006
300	0.27	264	-0.033	-0.009
200	0.29	265	-0.038	-0.011
100	0.40	276	-0.031	-0.012
50	0.68	269	-0.023	-0.016
			Total	-0.096

the diurnal variation of the temperature at different altitudes at Trivandrum (geographic latitude 8.4°N) is more than that at Lajes Field (geographic latitude $38^{\circ}-44^{\circ}\text{N}$) and the studies are related to two different periods namely 1956 to 1958 and 1964 to 1966, (2) that a local source of modulation of meson intensity having time of maximum around 1200 hours local time as suggested by Rao and Sarabhai (1961) is operative at Trivandrum during the period, besides the temperature effect.

For the purpose of comparison, the results obtained by other authors are shown in figure 2.08 (c). Dorman and Feinberg (1958) and Dorman (1957) have proposed an elegant method for correcting cosmic ray intensity for temperature variations in the upper atmosphere. They have calculated the temperature coefficients, K_i for various isobaric levels, which are shown in table 2.05. The total temperature correction to μ meson intensity is given by

$$\frac{\delta N_\mu}{N_\mu} = \sum_{i=1}^n K_i \delta T_i \quad \dots (2.31)$$

where $\frac{\delta N_\mu}{N_\mu}$ is the relative variation in the μ meson intensity due to variations in temperature at various layers, and K_i and δT_i are respectively the partial temperature coefficient and amplitude of the temperature variation for the i^{th} layer. Figure 2.08(c)-I shows the temperature correction vector to μ meson intensity as derived by Dorman (1957), using the above method. The temperature effect has an amplitude 0.2% with a time of maximum 0300 hours local time.

Under the assumption that the response of the neutron monitor and the ion-chamber to primary variations is likely to be similar, Quenby and Thambyahpillai (1960) have determined the atmospheric temperature contribution to μ meson intensity at Huancayo by taking the difference between the pressure corrected neutron and meson data. This has an amplitude of 0.11% and a time of maximum around 0550 hour local time, which is shown in figure 2.08(c)-II.

The atmospheric temperature effect on the diurnal variation of μ meson intensity has been derived by Mori et al (1966) by comparing the expected intensity variations, to the

observed pressure corrected intensity variations for days when $\beta = 0$, during 1957-1958. It is interesting to note that for Kodaikanal, Huancayo, Makerere, Lae and Churchill, the residual effect has an amplitude $\sim 0.2\%$ with time of maximum around 0600 hours, which is consistent with the present estimate (Figure 2.08 a). Figure 2.08(c)-III shows the vector average of 17 stations during the period. The mean vector has an amplitude of $0.095 \pm 0.018\%$ and the time of maximum is at 7.1 ± 0.7 hours local time. Mori et al (1966) have pointed out that "irrespective of the magnitude, the phases of the temperature vectors deduced from cosmic rays are concentrated around 0600 hours local time and are considerably later than those obtained from meteorological data". The results obtained from the present study are consistent with the observations of Mori et al (1966).

Measurements of temperature at higher altitudes (say above 30 kms) have been carried out by Rocket-sonde and at still higher heights (say about 200 kms) through satellite drag observations. It is interesting to note that the diurnal variation of temperature above 50 mb height also shows a time of maximum between 1400 hours to 1600 hours local time with a significant amplitude. The meteorological Rocket Net Work (MRN) has made possible the examination of the gross atmospheric circulation patterns on a global scale. From extensive analysis of MRN data, Webb(1966) has reported that the diurnal temperature in the upper stratosphere (~ 50 kms) has an amplitude of 15° to 20°C , with a time of maximum between 1400 to 1600 local time. Beyers et al (1966) have reported the diurnal variation of temperature between 40 to 60 kms. Data data, from Rocket Soundings at 6 hour interval, equipped with 4.6 m. parachute wind sensors and Arcasond-1A temperature measuring system, over White-Sand Missile Range, has been

used in the analysis. Table 2.06 shows the amplitude and time of maximum of diurnal temperature variations at various heights between 40 to 60 km.

TABLE 2.06

Amplitude and time of maximum of the daily variation of temperature over White Sand Missile Range during 30th June to 2nd July 1965.

Height in Kms	Amplitude in °C	Time of maximum in hours local time
40	1.4	14.4
44	3.6	17.3
48	5.5	15.3
52	8.2	13.6
56	7.4	12.3
60	9.8	12.1

From satellite drag observations Jacchia (1966) has reported different types of variations in temperature at about 350 kms. They are (1) the 11-year variation, (2) the semi-annual variation, (3) the latitude dependent seasonal variations, (4) the variations associated with geomagnetic activity and (5) the diurnal variations. The diurnal variation is the most regular of all these variations. There is a pronounced diurnal variation with time of maximum around 1400 hours and time of minimum around 0500 hours, and amplitude $\sim 250^{\circ}\text{C}$ during high solar activity and $\sim 90^{\circ}\text{C}$ during low solar activity - Both extreme ultra violet rays and corpuscular radiation from the sun are important in the heating process.

2.4 Conclusions

In spite of the low counting rate of the cosmic ray detectors at Trivandrum and disruption of data due to frequent power failures and limited life of G. M. Counters, the present study has enabled us to estimate the residual modulation of μ meson intensity. This residual modulation appears to be mainly due to modulation of μ meson intensity by temperature variations in the atmosphere and to a certain extent to the modulation due to a local source of non-meteorological origin

The station was discontinued from January 1967. Studies which are being conducted with data from high counting rate directional east, west, north, south and vertical scintillation telescopes operating at Physical Research Laboratory, Ahmedabad would give better insight to this problem (Sarabhai and Kargathra, 1971). The hourly counting rate of these detectors are ~ 1.8 million for vertical telescopes and ~ 0.2 million for inclined telescopes.

CHAPTER - III

3.1 Introduction:

A number of types of geomagnetic indices, like K_p , A_p , D_{st} and A_E , have for long been known to be influenced by the particle radiation from the sun. These indices however, are not strictly related to physical models of the magnetosphere. The present study is devoted to an exploration of a possible relationship between the electromagnetic state of the interplanetary medium and ΔH , the daily range of the horizontal component of the geomagnetic field at a low latitude station, away from the effects of the equatorial electrojet.

From the global study of the daily variation of the geomagnetic field, Schuster (1889) estimated the electric current systems which could be responsible for geomagnetic field variations. He suggested that the location of these current systems would be mainly external to the surface of the earth. The ionospheric dynamo current system has for long been established to ^{be} the only source of quiet day daily variation of H . However, the development of magnetospheric physics in the last decade has shown that there are atleast four other current systems which are external to the earth's surface, which exist even during very quiet conditions. They are (1) the surface currents at the magnetopause (Beard and Jenkins, 1962; Mead, 1964; Olson, 1969 and Alfven and Falthammar, 1971) (2) the tail currents (Williams and Mead, 1965; Axford et al, 1965; Siscoe and Cummings, 1969; Alfven and Falthammar, 1971) (3) the symmetric ring current (Singer, 1957; Akasofu and Chapman, 1963; Hirshberg, 1963; Frank, 1967; Van Allen, 1959; Schield, 1969 a,b), the eccentric

ring current (Kavanagh et al, 1968; Reorderer, 1969 and Olson, 1970) and (4) the partial ring current (Fejer, 1961; Cummings, 1966; Freeman and Maguire, 1967; Kavanagh et al 1968; Schield et al, 1969; Chen, 1970).

In order to test the above theoretical models and hypothesis and also to study the solar wind effects on ΔH , the author has analysed the geomagnetic field data from Alibag (Geomagnetic latitude 9.5°N) Honolulu (geomagnetic latitude 21.3°N) Guam (geomagnetic latitude 4.0°N) and Trivandrum (geomagnetic latitude 1.1°S) along with solar wind plasma data from IMP-1 satellite and interplanetary magnetic field data from the satellite IMP-1, IMP-3 and Explorer-33. These studies are reported in Chapter IV.

3.2 Magnetosphere

The first stage of the interaction of the solar wind with the geomagnetic field is the formation of a bow shock. The shock is formed for the reason that the solar wind speed exceeds the two principal wave propagation speeds namely the velocity of sound in the medium and the Alfvén velocity. The properties of the solar wind get modified while passing through the shock, increasing the plasma temperature and density and reducing the bulk streaming velocity to zero in the vicinity of the magnetopause. The second stage is the overall confinement of the geomagnetic field. This is due to the effective high electrical conductivity of the solar wind and the dynamic balance between the pressure of the geomagnetic field and the total pressure of the impacting solar wind and the interplanetary

magnetic field. The third effect is the stretching of the high latitude geomagnetic field lines over the polar cap behind the earth to form an extended magnetospheric tail. The field in the northern half of the tail is directed towards the sun and the field in the southern half is directed away from the sun, leading to a fairly well defined neutral sheet between the two halves and running length-wise to the tail (O'Brien, 1967). The present day view of the geomagnetic field and the tail as distorted by the solar wind in the noon-midnight magnetic meridian plane is shown in figure 3.01.

3.21 Models of the magnetosphere

Roederer (1969) has stressed the importance of a reliable quantitative model of the magnetosphere in understanding the motion of charged particles and the nature of spatial and temporal field changes in the outer magnetosphere. Due to the azimuthal asymmetry of the magnetic field in the outer magnetosphere, say at 7 earth's radii, for trapped particles McIlwain's L parameter (McIlwain, 1961) ceases to be a measure of the radial distance to the equatorial point of a field line, shell splitting becomes prominent, and the pitch angle distribution of particles gets modified. Moreover for the studies connected with particles mapping in the outer magnetosphere, trapped-particle time variations, plasma convection, high latitude conjugate point phenomena and low energy cosmic ray propagation it is necessary to have a very accurate model of the magnetosphere. In studies related to magnetosphere, the following three models are used very often.

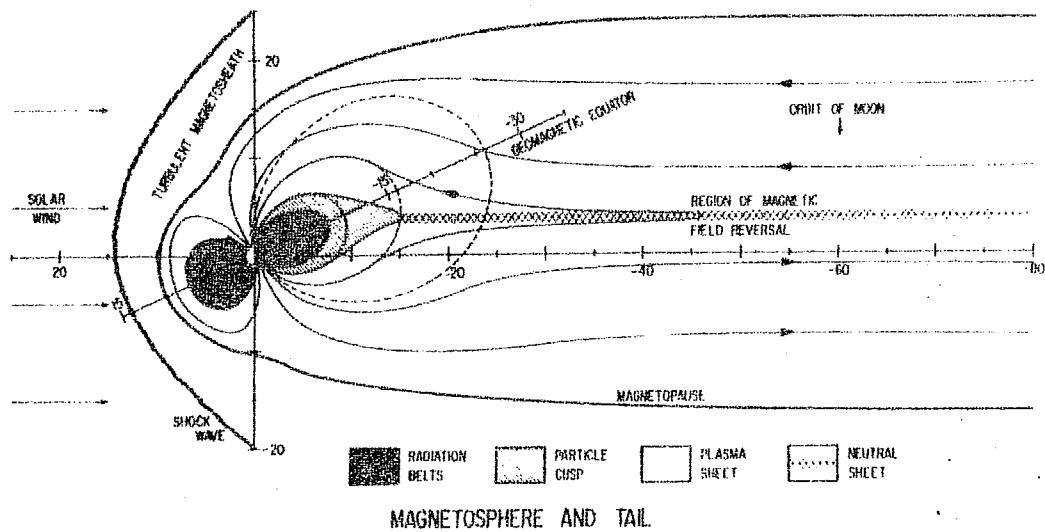


Fig. 3.01 The present day view in noon-midnight magnetic meridian plane of the geomagnetic field and tail as distorted by the solar wind. (Ness, 1967).

3.211 Mead - Beard Model

The surface boundary between the solar wind and the geomagnetic field has been computed by Mead and Beard (1964). With the assumption of zero-temperature, field free solar wind plasma incident perpendicular to the geomagnetic dipole and undergoing specular reflection, the boundary shape has been determined by them, by equating the stream pressure of the ions on one side of the boundary, to the magnetic field pressure on the other side.

The contribution to the daily variation of H due to deformation of the geomagnetic field ^{and} due to the surface currents at the magnetopause has been worked out by Mead (1964). An approximate analytical expression for the daily variation of H namely $\delta H_{CF}(\lambda, \phi)$ produced by this process for a given local time ϕ and for a given latitude λ is given by the relation.

$$\delta H_{CF}(\lambda, \phi) = \sqrt{X^2(\lambda, \phi) + Y^2(\lambda, \phi)} \text{ gammas} \dots (3.01)$$

where $X(\lambda, \phi) = -\frac{21500}{r_b^4} \cos 2\lambda \cos \phi \text{ gammas} \dots (3.02)$

$$Y(\lambda, \phi) = \frac{21500}{r_b^4} \sin \lambda \sin \phi \text{ gammas} \dots (3.03)$$

The stand-off distance of the magnetopause from the centre of the earth, in earth's radii, is given by

$$r_b = 1.068 \left[\frac{B_o^2}{4\pi n m v^2} \right]^{1/6} \dots (3.04)$$

Here B_0 is the field strength at the earth's surface and ' n ' is the ion density, ' m ' is the ion mass, ' v ' the stream velocity of the solar wind.

Olson (1969) has developed a model, which is an improvement of the Mead and Beard's (1964) and Mead's (1964) models, which represents the shape of the magnetopause for different angles of incidence of the solar wind on the earth's dipole. In this model, the equatorial cross sections are almost independent of the tilt angle, whereas the meridional cross sections are highly dependent upon the tilt angle. This model can be used to calculate quantitatively, the spatial distribution and temporal variations in the magnetic field produced by the magnetopause current system.

3.212 Mead-Williams model

This model (Williams and Mead, 1965) uses the boundary surface derived by Beard (1964) and places currents on that surface in such a way that they cancel the total field (earth's dipole field plus the field due to boundary currents) outside the magnetosphere. The earth's dipole is taken as stationary, and perpendicular to the ecliptic plane. A current sheet, in the geomagnetic equatorial plane, is added in the night side to simulate the neutral sheet of the tail. The magnetic field configuration in the noon midnight plane due to the addition of such a current sheet has been calculated by them as

$$\vec{B} = \vec{B}_d + \vec{B}_s + \vec{B}_{cs} \quad \dots (3.05)$$

Here B_d is the contribution due to internal sources, B_s due to currents at the magnetopause and B_{cs} due to currents in the neutral sheet within the magnetospheric tail.

$$\vec{B}_d = - \left(\frac{0.62 \cos \theta}{r^3} \right) \vec{e}_r - \left(\frac{0.31 \sin \theta}{r^3} \right) \vec{e}_\theta \quad \dots (3.06)$$

$$\begin{aligned} \vec{B}_s = & \left(-g_1^0 \cos \theta + 2\sqrt{3} g_2^0 r \sin \theta \cos \theta \cos \phi \right) \vec{e}_r \\ & + \left(g_1^0 \sin \theta - \sqrt{3} g_2^0 r (2 \cos^2 \theta - 1) \cos \phi \right) \vec{e}_\theta \\ & + \left(\sqrt{3} g_2^0 r \cos \theta \sin \phi \right) \vec{e}_\phi \end{aligned} \quad \dots (3.07)$$

where $g_1^0 = -\frac{0.2515}{r_b^3}$ gauss and $g_2^0 = \frac{0.1215}{r_b^4}$ gauss. r_b is the stand off distance of the sub-solar point of the magnetopause as defined in equation (3.04)

$$\begin{aligned} \vec{B}_{cs} = & (B_x \sin \theta \cos \phi - B_y \cos \theta) \vec{e}_r \\ & + (B_x \cos \theta \cos \phi + B_y \sin \theta) \vec{e}_\theta \\ & + (-B_x \sin \phi) \vec{e}_\phi \end{aligned} \quad \dots (3.08)$$

$$\text{where } B_x = -2j \left(\frac{R_2}{r_1} - \frac{R_1}{r_2} \right) \quad \dots (3.09)$$

$$\text{and } B_y = 2j \log \frac{r_2}{r_1} \quad \dots (3.10)$$

here j is the current per unit length in the sheet. The X axis points away from the sun and the Y axis points south. R_2 and R_1 are the near and far off distances to the edges of the tail current sheet respectively.

3.213 Taylor-Hones Model

In the image-dipole model due to Hones (1963), the effect of the magnetopause current is simulated by a large image dipole

moment to the earth's dipole moment and the distance 'S' between the two. For a stand off distance of the magnetopause of 11 earth's radii the values of r and S are respectively 28 and 40.

Taylor and Hones (1965) and Taylor (1966) have modified Hone's model by incorporating the effects due to neutral sheet at the anti-solar side and the electric field in the magnetosphere, over and above the effects of the solar wind pressure on the sunward side of the earth.

Antonova and Shabansky (1968) have proposed the two-dipole model by synthesising Mead-Beard's and Hone's models, incorporating the effect due to the temperature of the solar wind plasma.

3.22 Electric fields in the magnetosphere

3.221 Electric field in the outer magnetosphere

The generally accepted mechanisms about the origin of large-scale electric fields in the outer magnetosphere are due to Axford-Hines (1961), Dungey (1961), Alfven (1964), and further improvements to it by various authors (Axford, 1962; Dungey, 1963; Axford et al, 1965; Levy et al, 1964; Dungey, 1967; Brice, 1967; and Alfven and Falthammar, 1971).

In Axford and Hine's (1961) model the magnetosphere is assumed to be electrically shielded from the interplanetary space, and the bulk motion of plasma across the magnetopause is prohibited. They have assumed that the geomagnetic field is enclosed in a limited volume (the magnetosphere) with no field

line going to infinity. The electric conductivity along the field line is high, as a consequence, the potential difference between any two points at the magnetopause will be eliminated by the current flow. Thus the magnetosphere is electrically insulated from the interplanetary medium. They have postulated the existence of viscous-like interaction between solar wind and magnetosphere by means of which a small part of the momentum of the solar wind is transferred to the magnetosphere. Due to this viscous interaction, charge separation occurs and polarisation charge is accumulated at the inner edge of the boundary region. The magnetospheric plasma is dragged by the solar wind, with a velocity \vec{U} , which is related to the electric field \vec{E} , caused by polarisation, through the relation

$$\vec{E} + \frac{1}{c} (\vec{U} \times \vec{B}) = 0 \quad \dots (3.11)$$

The equatorial view of the flow pattern within the magnetosphere to be expected in the presence of rotation of the earth and a viscous-like interaction between the solar wind and the surface of the magnetosphere is as shown in figure 3.02.

Dungey (1961) has pointed out that the southward component of the interplanetary magnetic field could merge with the earth's magnetic field as shown in figure 3.03. The earth's merged field lines would then be pulled over the polar caps by the solar wind and become reconnected in the antisolar side of the earth. The interplanetary electric field \vec{E} , which is associated with the solar wind velocity \vec{V} across the interplanetary magnetic field \vec{B} by the relation

$$\vec{E} = - \frac{1}{c} (\vec{V} \times \vec{B}) \quad \dots (3.12)$$

is thought to enter the magnetosphere (Obayashi and Nishida, 1968).

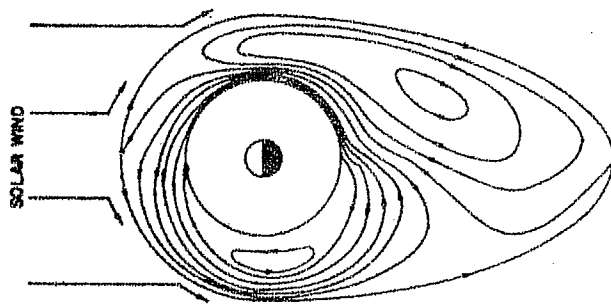


Fig. 3.02 Motion of charged particles in the magnetosphere in the equatorial plane to be expected in the presence of rotation of the earth and a viscous-like interaction between the solar wind and the surface of the magnetosphere (Axford and Hines, 1961)

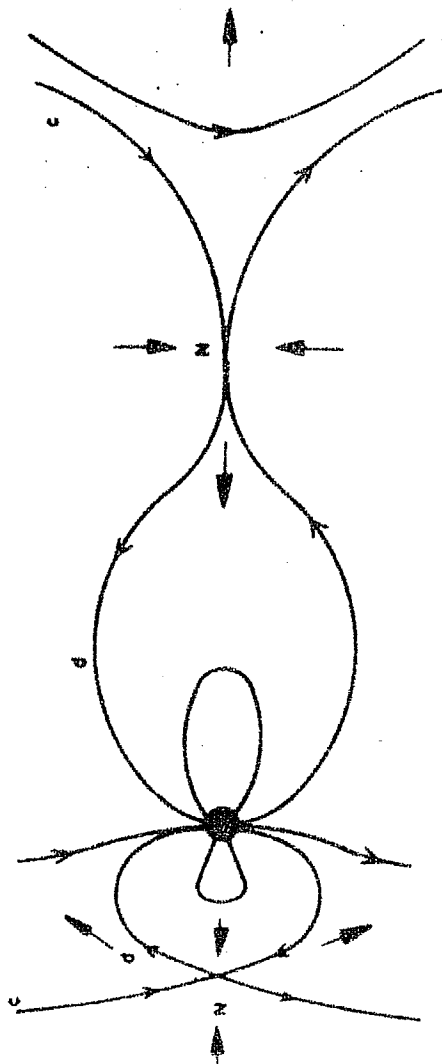


Fig. 3.03 Steady convection in the noon-midnight geomagnetic meridian when the interplanetary magnetic field has a southward component (Dungey, 1961)

The direction of the drift of particles from the tail towards the earth is opposite to the direction of the solar wind. This happens for the reason that the geomagnetic field component is perpendicular to the equatorial plane of the earth and is opposite to the direction of the magnetic field in the interplanetary space. The electric field is directed from the morning to evening side, so that the associated electrostatic potential is larger on the morning side than on the evening side.

3.222 Radial electric field

The role the earth's rotation plays in determining the characteristics of the electric and magnetic fields in the magnetosphere is not fully understood. Axford and Hines (1961) in their model have included a circulatory pattern of plasma convection driven by the rotation of the earth. Davis (1947, 1948) has shown that plasma surrounding a rotating magnetised conducting sphere, should rotate with the sphere if the plasma particles are constrained to move along the magnetic lines of force. Under these conditions, charge will flow in the plasma until the electric field

$$\vec{E} = -\frac{1}{c} (\vec{\omega} \times \vec{r}) \times \vec{B} \quad \dots (3.13)$$

(as seen in a nonrotating reference frame) is established in the plasma. Here $\vec{\omega}$ is the angular velocity of the sphere, \vec{r} is the radial position vector, and \vec{B} is the magnetic field vector. The potential of this electric field for a dipole whose magnetic moment is anti-parallel to the axis of rotation, just as in the case of earth, is given by

$$\phi_{\text{corotation}} = -\frac{1}{c} \Omega M_E \frac{\sin^2 \theta}{R} \quad \dots (3.14)$$

where Ω is the angular velocity of rotation, M_E is the magnetic moment and θ is the co-latitude of the earth. R is the radial distance from the centre of the earth (Taylor and Hones, 1965).

3.23 Plasmapause

From Whistler data, Carpenter (1963) deduced that in the equatorial plane the electron number density drops abruptly at a radial distance of several earth radii, and he used the word 'knee' to designate this abrupt density decrease. It was later found that the knee represents an essentially field - aligned structure, and the term 'plasma pause' was introduced to emphasise the three-dimensional qualities of the phenomenon (Carpenter, 1966; Angerami and Carpenter, 1966). A persistent feature of the plasma sphere is the bulge in the dusk sector. Nishida (1966), Brice (1967), and Dungey (1967) have treated the bulge in terms of an interaction between the convection of plasma from the tail of the magnetosphere and the flow associated with the rotation of the earth. On the assumption that the outer limit of the bulge includes a stagnation point in the combined flow, the plasmapause radius in the dusk sector has been considered as a possible measure of the intensity of the convective electric field (Vasyliunas, 1968). Carpenter (1970) has reported that the intensity of the convective electric field, E_{YSM} within the plasmapause, inferred from the stagnation distance and from the motions of the bulge is $\sim 1-4$ mv/m during substorms, and ~ 0.1 mv/m during prolonged quiet periods.

3.24 Geomagnetically trapped particles

Stormer (1936) from trajectory calculations has shown that there are possible orbits for trapped particles in the earth's magnetic field. Singer (1957) has proposed the formation

of a ring current due to the motion of trapped particles. In early 1958 Van Allen (1959) discovered the existence of the radiation belts through instruments carried by satellites, Explorer-1 and Explorer-2.

3.241 Motion of a charged particle trapped in the geomagnetic field

A charged particle in an undistorted static magnetic field B in the absence of an electric field, has a circular motion in a disk perpendicular to B , a motion in latitude parallel to B , and a drift in longitude.

A charged particle, of charge ' Ze ' and rest mass ' m_0 ' moving with velocity ' \vec{v} ' at an angle α with \vec{B} , gyrates about the direction of \vec{B} with a radius of curvature ' ρ ' given by

$$\rho = \frac{\gamma m v_{\perp} c}{BZe} \quad \dots (3.15)$$

where v_{\perp} is the component of ' v ' perpendicular to B and

$$\gamma = \left(1 - \frac{v^2}{c^2}\right)^{-1/2} \quad \dots (3.16)$$

Due to the gyratory motion the particle will have a magnetic moment μ given by

$$\mu = \frac{1}{2} \gamma m v^2 \frac{\sin^2 \alpha}{B} \quad \dots (3.17)$$

In a steady magnetic field, μ is constant with the result $\frac{\sin^2 \alpha}{B}$ is constant. As the particle's guiding center moves along the line of force towards higher latitudes the value of α and B increase and at a point m , α will have a value $\pi/2$ and B will

have a value B_m . The particle cannot go beyond the point m because its direction of motion reverses and it begins to come back. This reversal occurs at m' also on the other hemisphere. m and m' are known as mirror points. The particles should thus oscillate between m and m' .

In addition to the above two motions, the trapped particles should drift in longitude, toward east if they are negatively charged and towards west if they are positively charged. As the guiding center follows a curved line of force, there is a net centrifugal force acting away from the earth. This gives a drift to the particles and the drift velocity v_{d1} due to this is given by

$$\vec{v}_{d1} = \frac{\gamma m v_{11}^2}{Z e B^3} \cdot \vec{B} \times (\nabla_{\perp} B) \quad \dots (3.18)$$

where $\nabla_{\perp} B$ is the component of ∇B which is perpendicular to B . The magnetic field is weaker as we go away from the earth. This gradient in the field gives rise to a drift, the drift velocity v_{d2} is given by

$$\vec{v}_{d2} = \frac{1}{2} \gamma m v^2 \frac{\vec{B} \times \nabla_{\perp} B}{Z e B^3} \quad \dots (3.19)$$

Thus both the effects work in the same direction and the total drift velocity of the particle, v_d is given by

$$\vec{v}_d = \vec{v}_{d1} + \vec{v}_{d2} = \frac{\vec{B} \times \nabla_{\perp} B}{Z e B^3} \left(\gamma m v_{11}^2 + \frac{1}{2} \gamma m v_{\perp}^2 \right) \quad \dots (3.20)$$

The total current including the current produced by gyration and drift is given by

$$= \frac{c}{8 \pi P_m} \vec{B} \times \left[\nabla P_n + \frac{P_s - P_n}{P_m} (\vec{B} \cdot \nabla) \frac{\vec{B}}{8 \pi} \right] \quad \dots (3.21)$$

where P_s and P_n are the plasma pressure along and perpendicular to \vec{B} , and P_m is the magnetic pressure (Hoffman and Brachen, 1967)

The motion of geomagnetically trapped particles are governed by three invariants.

- 1) Magnetic moment invariant

$$\mu = \frac{1/2 \gamma m v_{\perp}^2}{B} \text{ is constant} \quad \dots (3.22)$$

The cyclotron rotation of the particle about \vec{B} has a cyclotron frequency

$$W_c = \frac{Z e B}{\gamma m c} = \frac{1}{T_1} \quad \dots (3.23)$$

The instantaneous center of cyclotron motion is called the guiding center.

- 2) Integral or longitudinal invariant.

$$J = \oint v_{11} dl \quad \dots (3.24)$$

If a particle drifts in the geomagnetic field so that μ and J are constant the particle must drift in such a way that it returns to the same field line from which it started. The latitudinal motion of the guiding center along \vec{B} has a period.

$$T_2 = \int_{m'}^m \frac{dl}{v_{11}} \quad \dots (3.25)$$

- 3) The flux invariant

$$\Phi = \int_S \vec{B} \cdot d\vec{s} \quad \dots (3.26)$$

where ds is the element of area. The constancy of Φ requires that if the geomagnetic field were slowly to contract or expand, the integral invariant surface must change its size accordingly so that Φ is conserved. The longitudinal drift has a period

$$T_3 = \frac{2.7 \times 10^9 \times g(\theta_m)}{L \times V} \text{ seconds} \quad \dots (3.27)$$

where L is the magnetic shell radius measured in earth radii, V is the volt-equivalent of the particle energy. The numerical factor $g(\theta_m)$ varies monotonically with the mirror colatitude θ_m .

3.242 Diffusion and acceleration of charged particles in the earth's radiation belts.

Diffusion and acceleration of magnetically trapped particles require that one or more of the adiabatic invariants be violated. The electromagnetic waves with frequencies in the gyro-frequency range can change the magnetic moment, and waves in the bounce frequency range can violate the second adiabatic invariant. The third adiabatic invariant is violated by field variations of the time scale of the azimuthal drift period. This happens due to (1) compressions and expansions of the magnetosphere due to changes in the solar wind pressure, (2) internal magnetic field deformations associated with variable ring currents and tail currents and (3) time dependent electric potential fields associated with magnetospheric plasma convection (Falthammar, 1968).

Radial diffusion is now believed to be the main process by which charged particles, probably from the solar wind, are transported inwards from the outer regions of the magnetosphere populating the Van Allen radiation belts. This process of radial diffusion may be accompanied by, or directly related to, acceleration mechanisms. If the first two adiabatic invariants are conserved during the radial diffusion process, the acceleration is of the betatron type (Kellogg, 1959 and Roederer, 1968 a).

Nakada and Mead (1965) have shown that the changes in the kinetic energy density of the solar wind, in time short compared to the longitudinal drift period of the particles, result in an inward displacement of the particles, violating the flux invariant leading to particle acceleration.

The electric potential field variations, associated with fluctuating plasma convection with or without deforming the magnetic field, has been proposed as a dominant contributor to the diffusion process (Dungey, 1965; Falthammar, 1965, 1966; and Birmingham, 1969).

Radial diffusion can also result as a consequence of pitch-angle scattering (Herlofson, 1960). Although in a symmetric field this contribution is small. The asymmetry of the magnetosphere would enhance it very much by shell splitting (Roederer 1967, 1968 a, b). This has been experimentally verified by Pfizter et al (1969). Quantitative analysis of the radial diffusion has been carried out by Roederer and Schultz (1969) and Falthammar and Walt (1969) and Walt (1971).

Roederer (1968 a, b) has pointed out that particles would experience repeated accelerations by first travelling inward conserving μ and J , then outward conserving energy, then again inward conserving μ and J and so on, thereby finally reaching very high energies. This process is known as "bimodel diffusion". This multi-step acceleration process has a basic similarity with the "magnetic pumping" process introduced by Alfven (1958).

The energy supply needed for the radiation belts including the ring current is only a fraction of the power carried by the

solar wind over an area such as the magnetospheric cross-section. Falthammar (1970) while reviewing diffusion and acceleration of particles in the radiation belts have stressed the importance of the interplanetary electric field and its fluctuations, as sources of energy input to the magnetospheric plasma.

3.243 Plasma flow in the magnetosphere

Many authors have discussed trajectories of charged particles in the magnetosphere under the influence of assumed electric fields and geomagnetic field gradients. (Alfven, 1939; 1950; Axford and Hines, 1961; Taylor and Hones, 1965; Block, 1967; and Brice, 1967).

The drift paths of charged particles, in the equatorial plane of the earth's dipole field with convective electric field and corotational electric field superimposed, have been computed by Kavanagh et al (1968), Chen (1970) and Wolf (1970). The drift velocity of charged particles, \vec{V}_d would be the same as a pure $\vec{E} \times B$ drift in an equivalent electric field, where

$$\vec{E}_{eq} = -\nabla \phi \quad \dots (3.28)$$

and

$$\phi = -\frac{1}{c} \Omega M_E \frac{1}{R} - E_o R \sin \varphi + \frac{\mu M_E}{qR^3} \quad \dots (3.29)$$

In equation 3.29 the first term $(\frac{1}{c} \Omega M_E \frac{1}{R})$ represents the potential due to corotation of the plasma with the geomagnetic field, the second term $(E_o R \sin \varphi)$ is the potential due to convective electric field and the third term $\frac{\mu M_E}{qR^3}$ is the potential

due to geomagnetic field gradient. M_E and Ω are the magnetic moment and angular velocity of the earth, R is the radial distance defining the position of the particle, φ is the azimuthal angle measured counter-clock wise from the solar direction, μ and q are the magnetic moment and charge of the particle and \vec{V}_d , the drift velocity of the particle

$$\vec{V}_d = c \frac{\vec{B} \times \nabla \phi}{B^2} \quad \dots (3.30)$$

3.25 Particles and fields in the magnetosphere

The earliest study of the spatial and temporal variations of the energetic electrons in the outer radiation zones was conducted with low altitude satellites (Van Allen and Lin, 1960; Forbush et al, 1961; Pizzella et al, 1962 and Forbush et al, 1962). The significant aspect of this study is that the intensity of energetic electrons in the outer radiation zone is well, but negatively correlated with the Kertz geomagnetic 'ring current' measure, the 'U' parameter and with the geomagnetic index a_p (Forbush et al, 1961).

ATS-1 geostationary satellite observations (Freeman, 1968) have confirmed that there is flow of plasma from the tail of the magnetosphere, in the equatorial plane as shown in figure 3.04. The flow velocity is approximately 30 km/sec and the observed direction and magnitude are consistent with present theories of the motion of charged particles in the magnetosphere. The electric field required to account for the observed flow velocity is 5 millivolts/meter and the electric field direction is across the magnetosphere from the dawn to dusk side.

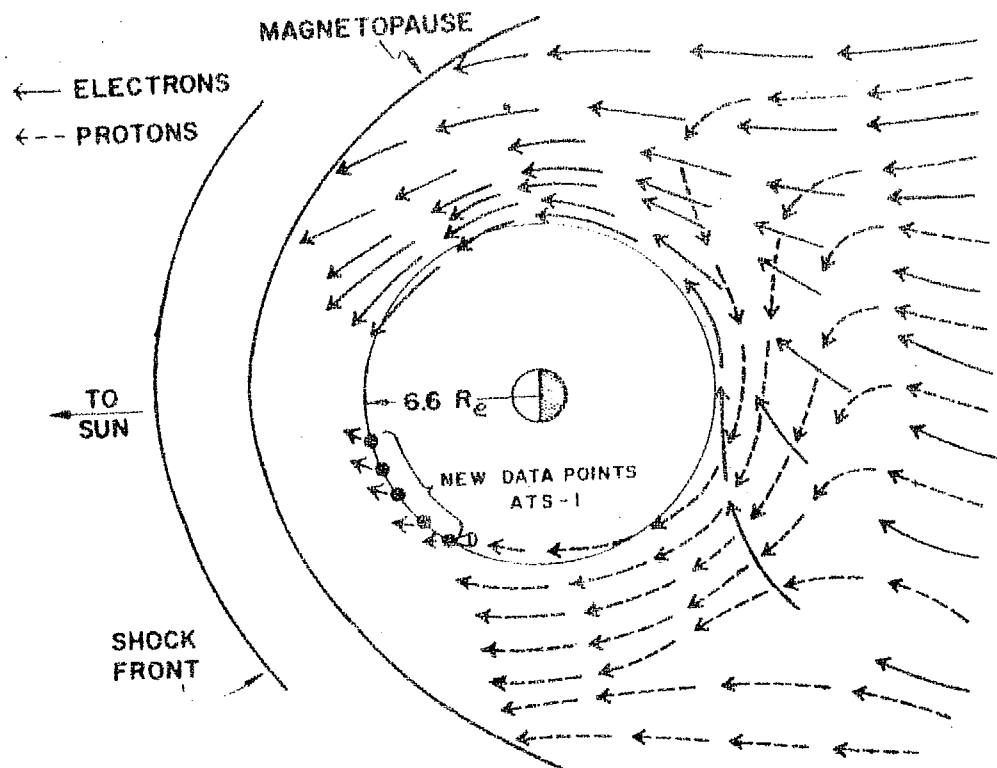


Fig. 3.04 A diagrammatic representation of the flow of energetic plasma through the magnetosphere in the equatorial plane (Freeman, 1968).

From observations of a number of Soviet space probes Gringauz and Khokhlov (1965) have inferred the presence of low-energy electrons in the outer radiation belt. Vasyliunas (1968) has suggested in a sketch of the average low-energy electron distribution in the equatorial region of the magnetosphere, on the basis of the OGO and Vela surveys as shown in figure 3.05. The view is from north pole. The density of dots is intended to convey a rough qualitative idea of the flux of electrons with energies from 100 eV to several KeV.

Van Allen (1969), Vernov et al (1969) and Gringauz (1969) have reviewed different aspects of the particle distribution in the magnetosphere.

The first magnetic field measurements of the outer regions of the magnetosphere were made in 1958 on Pioneer-1 space probe by Sonett (1960). A comprehensive survey of the geomagnetic boundary and the first magnetic measurements of the collisionless shock wave were performed by IMP-1 satellite in late 1963 (Ness et al, 1964).

Magnetometers on board ATS-1 satellite have measured with high accuracy the true diurnal variation of the geomagnetic field at the equator at an altitude of 6.6 earth's radii. The amplitude of the diurnal variation of H for quiet days is nearly 35 to 45 γ (Cummings et al, 1971 and Coleman, 1970). This space craft orbits with the same velocity with which the geomagnetic field is corotating and so the asymmetries in the internal field are not important and radial motion of the space-craft through spatially varying field is not a complicating factor. Figure 3.06 illustrates the diurnal variation of H (in the DHV system)

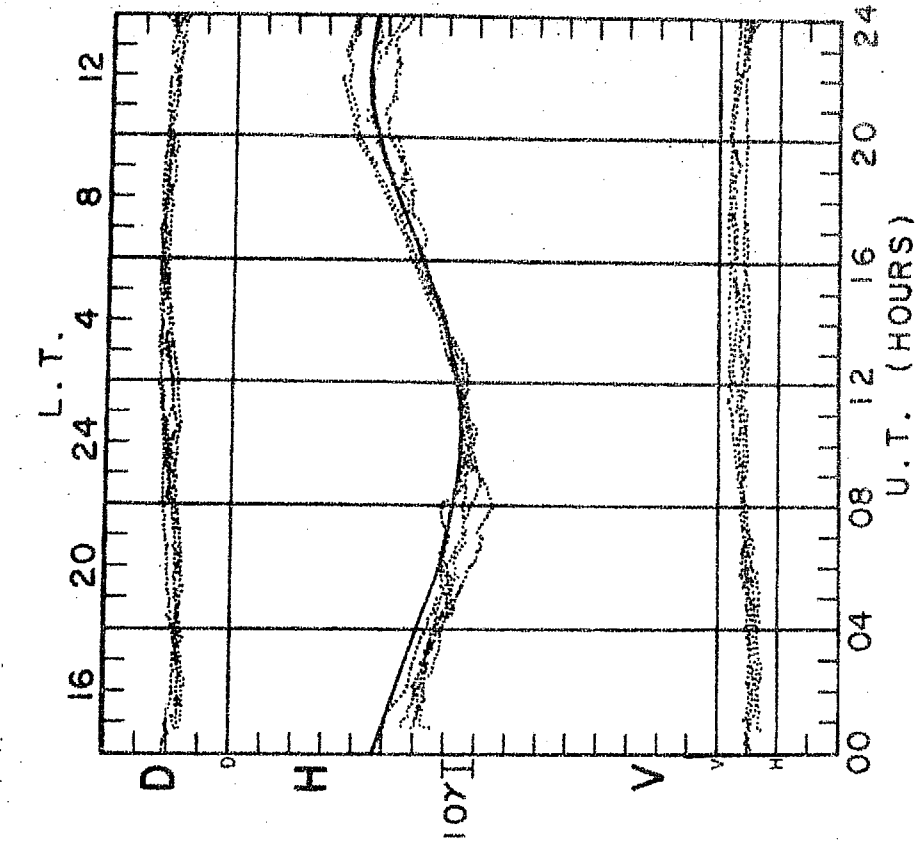


Fig. 3.06 A superposition of the magnetograms from ATS-1 for quiet days on January 4, 5, 24, 30 and 31, 1967. (Cummings et al, 1968).

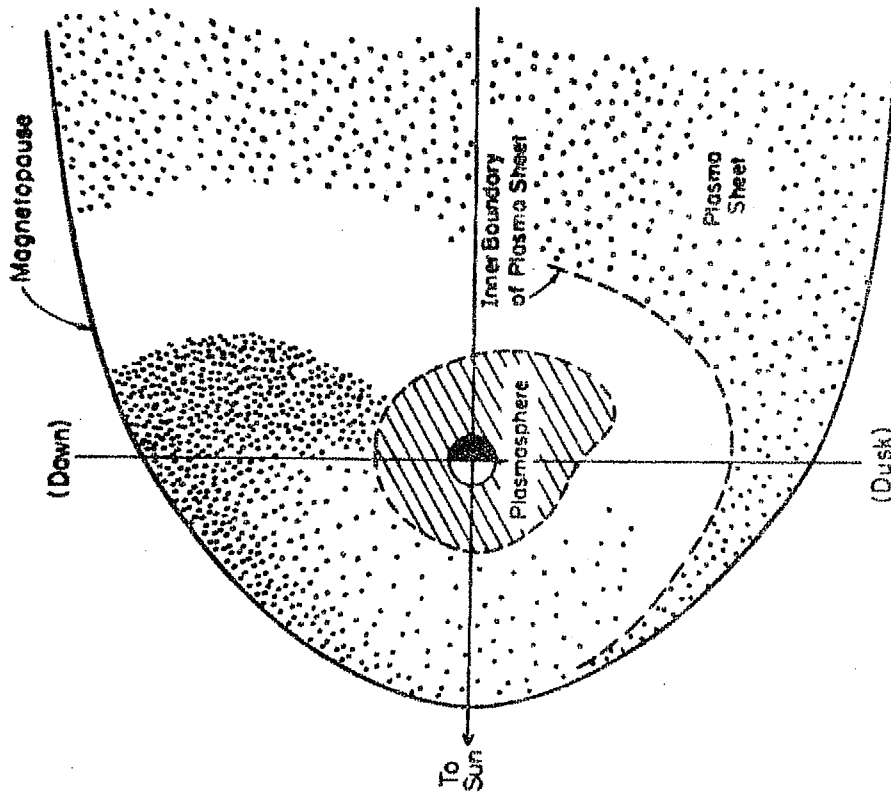


Fig. 3.05 A sketch of the average low energy electron distribution in the equatorial region of the magnetosphere, on the basis of the OGO and Vela surveys. (Vasyliunas, 1968).

on five quiet days at ATS-1 altitude as reported by Cumming et al (1968). Sugiura et al (1969) using data from OGO satellites 1, 2 and 3 have computed contours of ΔB , the constant deviation of the measured field magnitude from the reference field. It can be seen that even during geomagnetically quiet periods, at an altitude of 6 earth's radii in the equatorial plane, there is a field depression of about 30γ during night side compared to day side.

A numerical description of the geomagnetic field intensity at the equator, reasonably good in the region $1.5R_e < r < 7R_e$ is given by (Roederer, 1970)

$$B = \frac{K_0}{r^3} + K_1 - K_2 r \cos \varphi \quad \dots (3.31)$$

where $K_0 = 31100$ gammas. R_e^3 , $K_1 = 12 \left(\frac{10}{R_b} \right)^3$ gammas and $K_2 = 2.77 \left(\frac{10}{R_b} \right)^4$ gammas/ R_e . Here φ is the longitude east of midnight and R_b is the distance from the center of the earth to the subsolar point of the magnetopause in earth's radii and R_e is the earth's average radius. The values of K_1 and K_2 are based on ATS-1 magnetometer surveys (Cumming et al, 1968). According to relation 3.31, for a stand off distance of $10 R_e$, currents outside $6.6 R_e$ could produce a day-night difference in B , of $\sim 8.3\gamma$ in the form of a night decrease at $1.5 R_e$.

The contours of constant field magnitude in the equatorial plane have been constructed by Fairfield (1968), using the data from the satellites IMP-1, 2 and 3. It can be seen from figure 3.07 that contours of constant B , with $B < 150\gamma$ are not symmetrical in the equatorial plane and they are nearer to the earth on the anti-solar direction compared to the subsolar direction. This is due to compression of the magnetic field by the solar wind

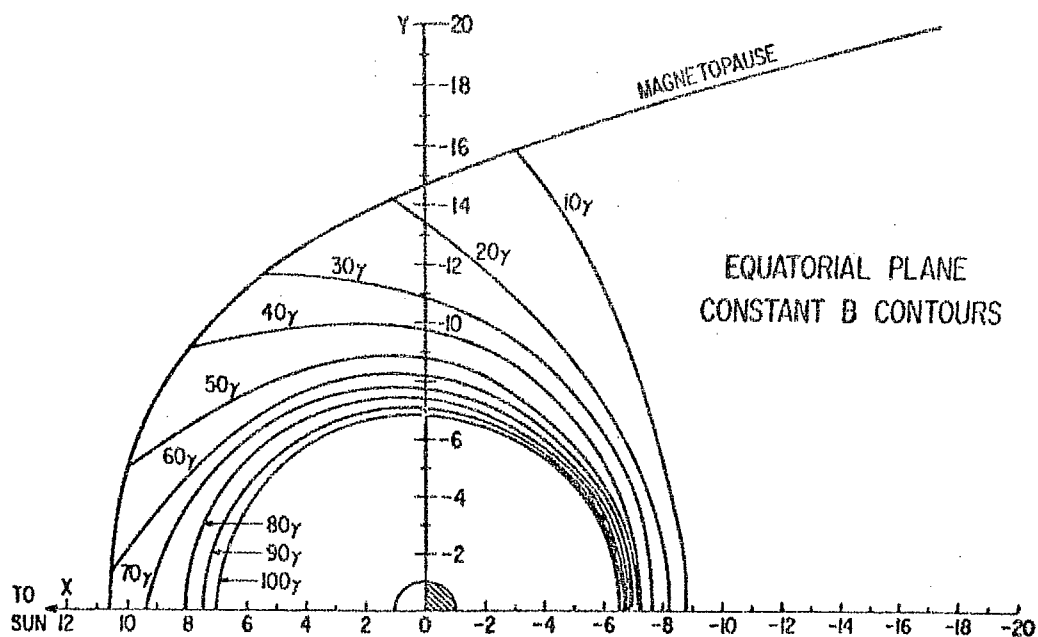


Fig. 3.07 Contours of constant magnetic field intensity in the equatorial plane. Curves based on experimental observations (Fairfield, 1968).

on the dayside. The eccentricity of the constant B contours is enhanced when the solar wind pressure is high.

3.3 Earth's magnetic field

3.31 Sources of the magnetic field at the surface of the earth

The major contribution to the surface magnetic field of the earth comes from its main field. The main field is probably produced in the earth's fluid core where the magnetic field and the convective motions of thermal origin are coupled to constitute a self maintaining-dynamo. There are variations due to crustal anomalies and due to sources external to the earth. The external contributions are mainly from (a) ionospheric currents (b) ring currents in the magnetosphere (c) solar wind induced currents at the magnetopause and the geomagnetic tail (d) the electric field in the interplanetary medium and its coupling with the magnetosphere.

3.32 Geomagnetic co-ordinate system

The geomagnetic field vector is described by three orthogonal components, by magnitude and two angles specifying the direction. X, Y and Z are the three components measured positively north-ward, east-ward and vertically down-ward respectively. The magnitude of the field vector

$$F = (X^2 + Y^2 + Z^2)^{1/2} \quad \dots (3.32)$$

The horizontal component

$$H = (X^2 + Y^2)^{1/2} \quad \dots (3.33)$$

The angles, specifying the direction of the field vector, are D the declination and I the inclination. Here D is the angular deviation of the horizontal projection of the field vector from geographic north, taken positive when eastward and is given by

$$D = \tan^{-1} \frac{X}{Y} \quad \dots (3.34)$$

I is the inclination, or dip angle which is defined as the field vector from the horizontal plane, taken positive when down-ward and is given by

$$I = \tan^{-1} \frac{Z}{H} \quad \dots (3.35)$$

3.4 Ionospheric effects

3.41 Electric conductivity in the ionosphere

The E-region extends from about 90 km to 140 km height. The ions there, are mainly NO^+ and O_2^+ , with N_2^+ ions as secondary constituent. The steep increase in the electron density in the lower part of the E-region is due to the ionization by X-rays. Hydrogen Lyman at 1025.6 \AA and C-III at 976 \AA are also important ionizing agencies. The maximum electron density in the E-region is of the order of $10^5 \text{ electrons/cm}^3$.

If the ionized gas in the ionospheric heights is set in motion an electric current is induced because of the presence of the earth's permanent magnetic field. However, the manner in which the current is produced is complex, because, in an ionized gas permeated by a magnetic field, the electric current produced by an electric field does not flow in the direction of the electric field.

In the absence of magnetic field, the current density, j , can be written as

$$\vec{j} = \sigma_0 \vec{E} \quad \dots (3.36)$$

$$\text{where } \sigma_0 = N_e^2 \left\{ \left(\frac{1}{m_i \nu_i} \right) + \left(\frac{1}{m_e \nu_e} \right) \right\} \quad \dots (3.37)$$

'N' is the number density, 'e' the charge, ' ν ' the collision frequency and 'm' the mass. The subscripts 'i' and 'e' refer to the ions and electrons respectively. σ_0 is often referred to as the direct conductivity.

A charged particle moving in the direction parallel to the magnetic field, the particle does not experience any force. But if the particle moves in a plane perpendicular to the magnetic field, the magnetic field exerts a force on the particle in the direction perpendicular to both the velocity of the particle and the magnetic field. When the motion of a charge particle has components both parallel and perpendicular to the uniform magnetic field, the particle spirals about the magnetic field along a helical path, with the component of its velocity parallel to the magnetic field unaffected by the presence of the field. When the electric field and the magnetic field are mutually orthogonal, the component of motion along the x-axis (parallel to E) produces a Lorentz force in the y-direction (perpendicular to both E and B) which, in equilibrium, must be balanced by the frictional force. Parallel to the x-axis, the frictional force is balanced by the combination of the electric force and the Lorentz force due to the motion parallel to the y-axis. These relations give the mean velocities in the x and y-directions and hence enable one to derive expressions for the components of the electric current densities j_x and j_y .

$$j_x = \sigma_1 E \quad \dots (3.38)$$

$$j_y = \sigma_2 E \quad \dots (3.39)$$

where

$$\sigma_1 = Ne^2 \left[\frac{1}{m_i \omega_i} \cdot \frac{\omega_i^2}{(\omega_i^2 + \omega_c^2)} + \frac{1}{m_e \omega_e} \cdot \frac{\omega_e^2}{(\omega_e^2 + \omega_c^2)} \right] \quad (3.40)$$

$$\sigma_2 = Ne^2 \left[-\frac{1}{m_i \omega_i} \cdot \frac{\omega_i \omega_c}{(\omega_i^2 + \omega_c^2)} + \frac{1}{m_e \omega_e} \cdot \frac{\omega_e \omega_c}{(\omega_e^2 + \omega_c^2)} \right] \quad (3.41)$$

ω_i and ω_e are the cyclotron frequency (in angular measure) for ions and electrons respectively. σ_1 and σ_2 are respectively the Pedersen and Hall conductivities. Electrons and ions both move in the same direction of the negative y-axis. Due to the difference in the mean velocities for electrons and ions, the boundaries of the ionized layer cannot remain electrically neutral and the two sides of the layer will be oppositely charged. The electric field due to this charge separation is such as to oppose the Hall current. This polarization electric field E_p produces the Pedersen current $\sigma_1 E_p$ and this current and the Hall current $\sigma_2 E$ are equal in magnitude and opposite in direction. Thus in equilibrium, the polarization field is $\frac{\sigma_2}{\sigma_1}$ times the original electric field E . Due to polarization electric field, E_p there will be a second Hall current driven in the direction of the x-axis, which is $\sigma_2 E_p$ or $\frac{\sigma_2^2}{\sigma_1} E$. Hence in the x-direction the total current is the sum of the direct Pedersen current due to E and the Hall current due to the polarization field, thus

$$j_x = \left(\sigma_1 + \frac{\sigma_2^2}{\sigma_1} \right) E = \sigma_3 E \quad \dots (2.42)$$

σ_3 is called the Cowling conductivity. Between 90 to 130 kms $\sigma_0 > \sigma_1$ and $\sigma_2 > \sigma_1$ with the result σ_3 is important at these heights. Above 160 kms σ_0 is large and σ_2 and σ_1 are much smaller.

3.42 Sq. variation

All the components in geomagnetic records occasionally show very smooth traces that indicate clear patterns of daily variations with respect to solar local time. This sort of variation is called solar quiet daily variation or Sq. variation. Chapman and Bartels (1940) have suggested that five quiet days per month having low international character figure are to be considered as quiet days. One difficulty with their definition is that depending on season and phase of the solar cycle, five quiet days per month are not always similarly quiet. It has long been a difficult problem to determine a datum line for each component from which to measure the amplitude of Sq. variation. Some workers use daily mean value as the datum line, while others prefer to use night time mean value. There should be at all times and even during quiet periods a field reduction due to symmetric west ward ring current which is mainly at 3.5 earth radii, (Shield 1969 a, b). The variations in the current strength lead to a variation in the level of the geomagnetic field at the ground. Thus unfortunately it is difficult to fix a proper datum line.

3.43 Ionospheric current system for Sq.

Large scale motions of air at high altitude (~ 100 kms) are probably mainly horizontal. Such ionised gas motions in the

presence of the earth's magnetic field induce an electric field, which is perpendicular to both the ionised gas velocity and magnetic field. This electric field is called the dynamo electric field. The horizontal current generated in the ionosphere in this way accumulates charges over some parts of the globe, creating an electrostatic field which, in turn, drives an additional current. From the magnetic observations from a net work of stations distributed over the earth one can draw equivalent current system in the ionosphere that could produce the observed magnetic variations, if such magnetic variations are caused only due to ionospheric E-region currents (Sugiura and Heppner, 1965; Chapman and Bartels, 1940 and Matsushita and Campbell, 1967).

Rocket-borne magnetometers have observed the magnetic field discontinuity at E-region heights in the equatorial electrojet region. But at low and middle latitudes the results are not consistent. The explanation given for the ill defined detection was attributed to high values of the dip, I at these regions. The rocket instruments measure the scalar magnetic field B which is equal to $2 \times 0.6 \times H \times \cos I$. So

$$\Delta B = 2 \times 0.6 \times \Delta H \times \cos I \quad \dots (3.43)$$

and in consequence ΔH is small for large values of I and hence below detection limits for high latitudes.

3.44 Short comings of dynamo theory

The dynamo theory was first suggested by Stewart (1882) to account for the daily variation of the geomagnetic field and quantitatively developed by Schuster (1908). Chapman (1919)

extended the work to account for solar and lunar daily variations.

The basic steps are as follows. The sun and moon produce tidal forces in the atmosphere, the periods being fractions of the solar or lunar day (24 and 24.8 hours respectively). These forces set up standing waves in the atmosphere below 100 kms, which result in (primarily horizontal) air motions. There is evidence to believe a natural resonance of the atmosphere of about 12 hour period, which selectively amplifies the solar semi-diurnal component. The motion of ionized gas across the geomagnetic field induces electromotive forces, which drive currents at levels where the electrical conductivity is appreciable (principally in the E-region), thus causing the solar quiet and lunar magnetic variations. Because of the vertical and horizontal variations of the conductivity, currents cannot flow freely in all directions; and polarization charges are thereby set up, modifying the flow of currents. The electrostatic fields associated with these charges are transmitted to the F-region, through the highly conducting geomagnetic field lines, where they produce electromagnetic drifts (Sugiura and Heppner, 1965).

Thus it can be seen that the development of the dynamo theory has been based on the assumption that ionospheric currents, induced by atmospheric motions, flow horizontally in a relatively thin conducting, layer in the E-region. It is wrong to assume that the thin shell be bounded by an upper as well as a lower insulating medium, so that the currents can flow horizontally. In the actual physical situation only the lower medium is an insulator so that at the lower boundary surface the current flows horizontally. But to fix an upper boundary is not

meaningful, hence a three dimensional approach to dynamo theory is necessary (Prince, 1968).

3.5 Geomagnetic variations in relation to interplanetary conditions

The present day knowledge, of the interplanetary space from theoretical studies and informations gathered from experimental studies of data obtained from satellites and space probes is dealt with in section 1.6. In this section the present status, of the interaction of solar wind plasma with the geomagnetic field and the part the interplanetary magnetic field plays in geomagnetic variations, is reported.

3.51 Solar wind plasma and geomagnetic effects

Chapman and Ferraro (1931, 1932) have suggested that a cloud of ionized gas emitted from the sun at the time of a solar flare would exert a pressure on the geomagnetic dipole field resulting in the sudden commencement of a geomagnetic storm. As described in section 1.62, Biermann's (1951, 1952) comet tail observations, Parker's (1958, 1960) theoretical prediction and satellite observations (Gringauz, 1961, Bridge et al, 1962 and Snyder et al, 1963) have proved beyond doubt the continuous bombardment of the corpuscular stream from the sun (the solar wind) on the geomagnetic field.

Pai and Sarabhai (1964) have pointed out that the recurring variations of the geomagnetic field during a storm with a typical period of 40 minutes, can be attributed to large scale inhomogenities in the solar wind plasma impinging on the

magnetosphere with scale lengths of the inhomogeneities in the solar wind ~ 0.02 A. U.

Snyder et al (1963) have shown, on the basis of Mariner-2 data, that a positive relationship exists between solar wind velocity, V_s and the daily sum of the geomagnetic index, $\sum K_p$. Meer and Dessler (1964) have reported a power-law relationship between V_s and the geomagnetic A_p index.

Verzariu et al (1969) from the comparison of the solar wind data obtained from Vela 2-A satellite with the positive D_{st} values have shown that even during magnetically quiet days, the square root of the solar wind pressure is found to be linearly correlated with the positive D_{st} values. From the study of the magnetic field data obtained from Explorer-12, Nishida and Cahill (1964) have shown that a positive sudden impulse on the ground is accompanied by an increase in the field strength everywhere within the magnetosphere and that a negative sudden impulse on the ground is associated with a decrease in the field strength in the magnetosphere. They have also shown that the magnetospheric boundary moved outward at the time of a negative sudden impulse.

Theoretical studies relating to the interaction of the solar wind plasma with the geomagnetic field have been carried out by various investigators (Beard, 1960; Kellogg, 1962; Spreiter and Briggs, 1962; Axford, 1962; Dessler and Parker, 1959; Fejer, 1964; Parker and Ferraro, 1969; Spreiter and Jones, 1963; Mead and Beard, 1964; Mead, 1964; Williams and Mead, 1965 and Olson, 1969).

Geomagnetic disturbances show a tendency of recurrence at regular intervals of 27 days, which is the rotational period of the sun as seen from the earth. It is generally assumed that from certain regions on the rotating sun and enhanced corpuscular radiation is emitted continually during certain period of time. These regions on the sun have been called the M-regions. Sarabhai (1963) and Dessler and Fejer (1963) have examined the situation, when a fast solar wind overtakes a slow solar wind. This process should lead to a turbulence and or a shock wave towards the leading edge of each sector. Dessler and Fejer (1963) have argued that the leading portions of the sectors would be responsible for the recurring geomagnetic storms with out solar outbursts.

Axford and Hines (1961) have postulated the existence of a viscous-like interaction between solar wind and the magnetosphere by means of which a small part of the momentum of the solar wind is transferred to the magnetosphere. Through this process the plasma, in the boundary layer of the magnetosphere, convects to the rear part of it and the return flow takes place through the interior of the magnetosphere.

3.52 Interplanetary magnetic field and geomagnetic effects

Fairfield and Cahill (1966), Wilcox et al (1967) and Rostoker and Falthammar (1967), using satellite data, have shown that K_p is higher when the interplanetary magnetic field has a southward component. Nishida (1968), from the comparison of the worldwide geomagnetic field data with the interplanetary magnetic field data obtained from IMP-1 satellite, has reported the coherence between the geomagnetic field oscillations with

the oscillations in the north south component of the interplanetary magnetic field. Ballief et al (1967, 1969) have analysed the data of the interplanetary magnetic field obtained from Mariners-2, 4 and 5 and have reported that there exists a good correlation between geomagnetic variability and the fluctuations of the interplanetary magnetic field in the plane normal to the sun-earth line. Wilcox and Ness (1965) have shown the effect of the sectoring of the interplanetary magnetic field on K_p .

A positive correlation between K_p and the strength of the interplanetary magnetic field has been obtained by various workers (Coleman et al, 1961; Greenstadt, 1961; and Wilcox et al 1967). Behannon and Ness (1966) have reported a positive correlation between B_T , the tail field magnitude and K_p . However Mihalev et al (1968) from the data of Explorer-33 have reported that the relation connecting K_p and B_T is nonlinear and a more linear relationship exists between B_T and a_p . The most direct evidence for inter-connection of the geomagnetic and interplanetary magnetic fields is from the observations of solar energetic particles (Lin and Anderson, 1966; Lin, 1968 and Van Allen and Ness 1968).

Theoretical studies of Alfven (1958, 1963, 1967 and 1968) and Dungey (1961) have shown that the interplanetary magnetic field plays an important role in the studies related with the interactions of the solar wind with the geomagnetic field. Dungey (1961) has suggested that the merging of magnetic field lines across the neutral sheet in the geomagnetic tail causes flow of plasma toward the earth. Recently Alfven and Falthammar (1971) have proposed a new approach to the theory of the solar wind-magnetosphere interaction. They have considered a

simple model which can explain the transfer of solar wind energy to the magnetosphere. They have suggested that "the southward interplanetary magnetic field favours release of energy that may drive geomagnetic activity".

Several reviews on the solar wind-geomagnetic field interactions are available (Ness, 1967, 1969; Heppner, 1967; Sugiura, 1969; Spreiter and Alksne, 1969; Williams and Mead, 1964, Fairfield, 1970; and Wolf and Intriligator, 1970).

3.6 ΔH in relation to changes in solar wind conditions

Recent experimental observations and theoretical studies as reported in this chapter have shown that there are currents at the magnetopause and in the magnetosphere which are related to the interaction of the solar wind with the geomagnetic field. In the next chapter the author has investigated the extent to which the features of ΔH , the daily variation of H at a low latitude station can be related to the characteristics of the solar wind plasma impinging on the magnetosphere and the interplanetary magnetic field.

CHAPTER -IV

4.1 Nature of ΔH , the daily variation of H for low latitude stations

A study has been made using the magnetograms from the observatories at Alibag (geomagnetic latitude 9.5°N), Honolulu (geomagnetic latitude 21.1°N), Guam (geomagnetic latitude 4.0°N) and Trivandrum (geomagnetic latitude 1.1°S) to understand the nature of the daily variation of the horizontal component of the geomagnetic field, H for low latitude stations. Figure 4.01 shows a magnetogram at Alibag on a typical day. Here H_{max} , H_{min} , and ΔH are respectively the maximum value of H, the minimum value of H and the range of H defined by $(H_{\text{max}} - H_{\text{min}})$. T_{max} and T_{min} are the time of maximum and time of minimum of H during a period of 24 hours from local mid-night to mid-night. Figure 4.02 shows for the individual years 1961, 1962, 1963 and 1964 the histograms of the frequency of occurrence of T_{max} and T_{min} of H for Alibag. It can be seen that there is no qualitative change in the histogram from year to year. Figure 4.03 indicates the normalised polar histograms of T_{max} and T_{min} of H for Alibag for the period 1961-1964 separately for (a) all days combined, (b) quiet days, (c) days with sudden commencement storms (d) days with gradual commencement storms (e) disturbed days and (f) internationally disturbed days but during which sudden commencement and gradual commencement storms did not occur. T_{max} histograms are relatively unaffected by the degree of geomagnetic disturbances and is around 1100 hours local time. However, T_{min} occurs at 0500 hours significantly more often on geomagnetically quiet days than on all other groups of days.

ALIBAG MAGNETOGRAM
6-7-1966

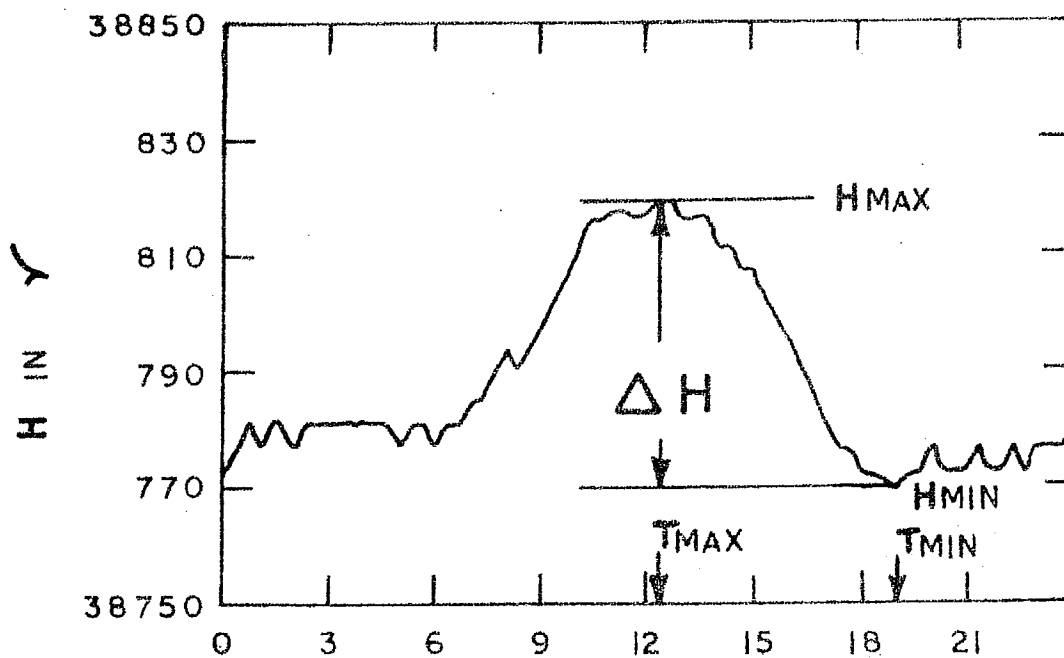


Fig. 4.01 A typical magnetogram at Alibag.

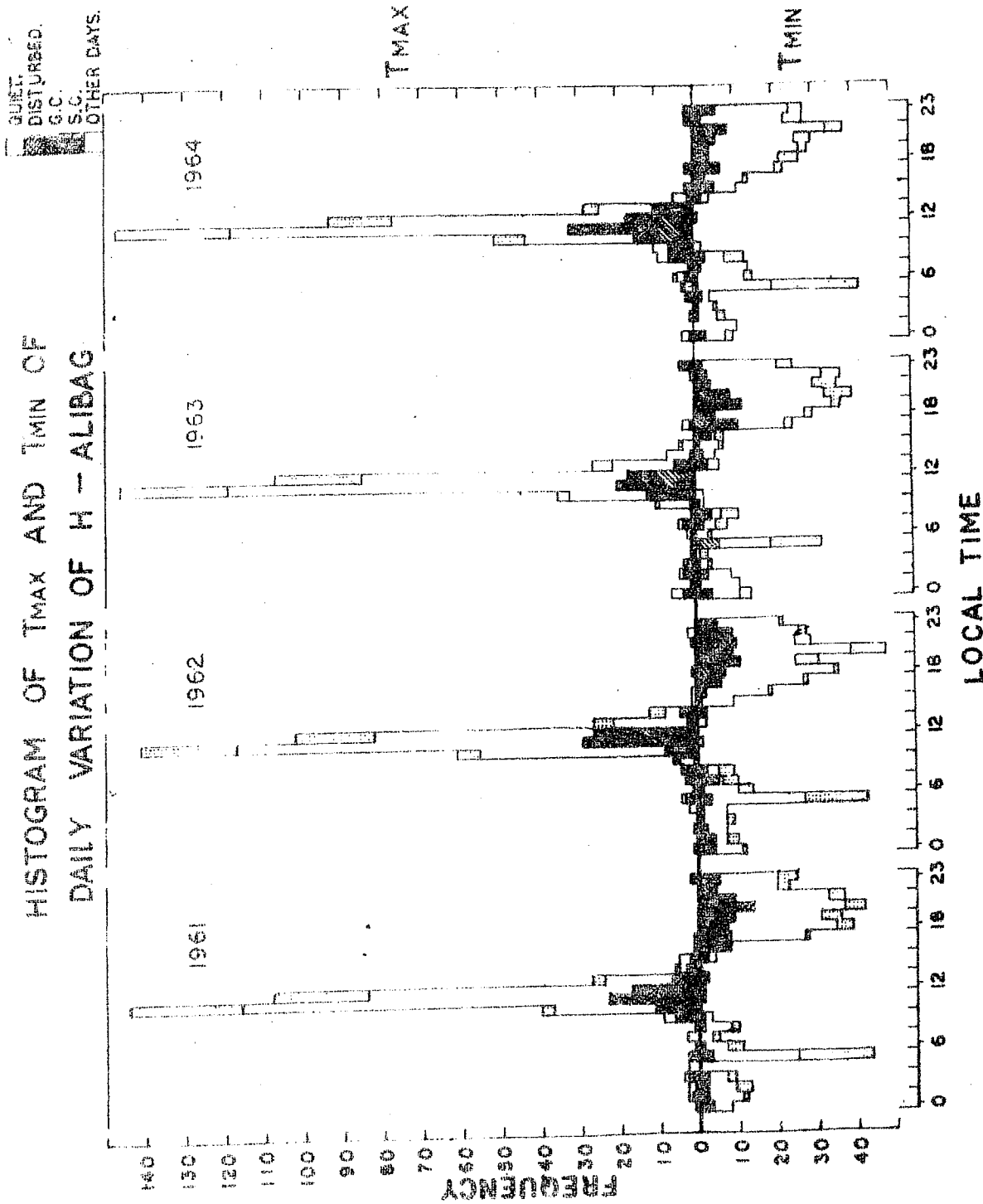


Fig. 4.02 Histograms of the time of occurrence of maximum and minimum of the daily variation of H at Alibag for the year 1961, 1962, 1963 and 1964

NORMALISED POLAR HISTOGRAM OF TMAX & TMIN
OF H. ALIBAG 1961-1964

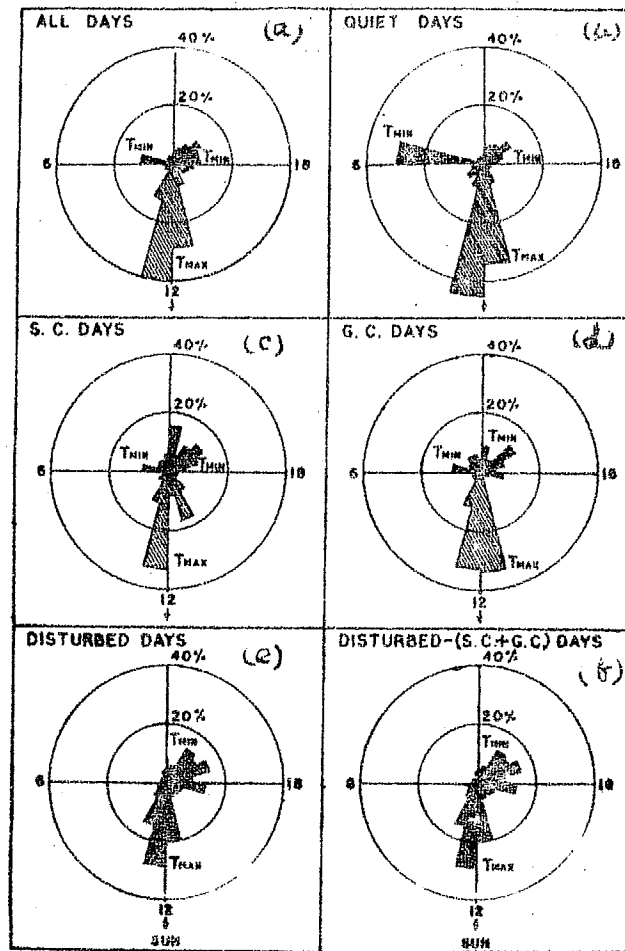


Fig. 4.03 Normalised polar histograms of local times of maximum and minimum of H at Alibag from year 1961 to year 1964, showing separately. (a) all days combined, (b) quiet days, (c) days with sudden commencement storms, (d) days with gradual commencement storms, (e) disturbed days and (f) internationally disturbed days but during which sudden commencement and gradual commencement storms did not occur.

The almost absence of T_{\min} of H between 0200 to 0600 hours on disturbed days is also noteworthy. In section 5.134 a theoretical interpretation is proposed to explain the occurrences of T_{\min} of H in the morning quadrant for quiet days and evening quadrant for disturbed days.

4.2 ΔH as a consequence of lowering of H_{\min} , the minimum value of H during night time

It is important to investigate whether at a low latitude station, outside the influence of the equatorial electrojet, ΔH represents an increase on the day side over a base level at H_{\min} , or alternatively it is a decrease on the night side from a base level at H_{\max} . In the former case, one should have a positive correlation between ΔH and H_{\max} , with poor correlation between ΔH and H_{\min} . On the other hand, in the latter case, one should get a negative correlation between ΔH and H_{\min} and a poor correlation between ΔH and H_{\max} .

Figure 4.04 shows the scatter plot of H_{\min} against ΔH for the year 1961. Here all the days in the year have been considered for the analysis. X and \odot respectively indicate days on which sudden commencement and gradual commencement storms occurred. The correlation between the two is negative and quiet significant. The corresponding scatter diagram for ΔH and H_{\max} is shown in figure 4.05, where the correlation between the two is only $+0.315 \pm 0.047$. The characteristics described here are seen at Alibag not only in 1961 but in all years of the solar cycle 1954 to 1964 (Sarabhai and Nair, 1963 a). In order to confirm the experimental results from the analysis of data from Alibag, the author has examined data from the

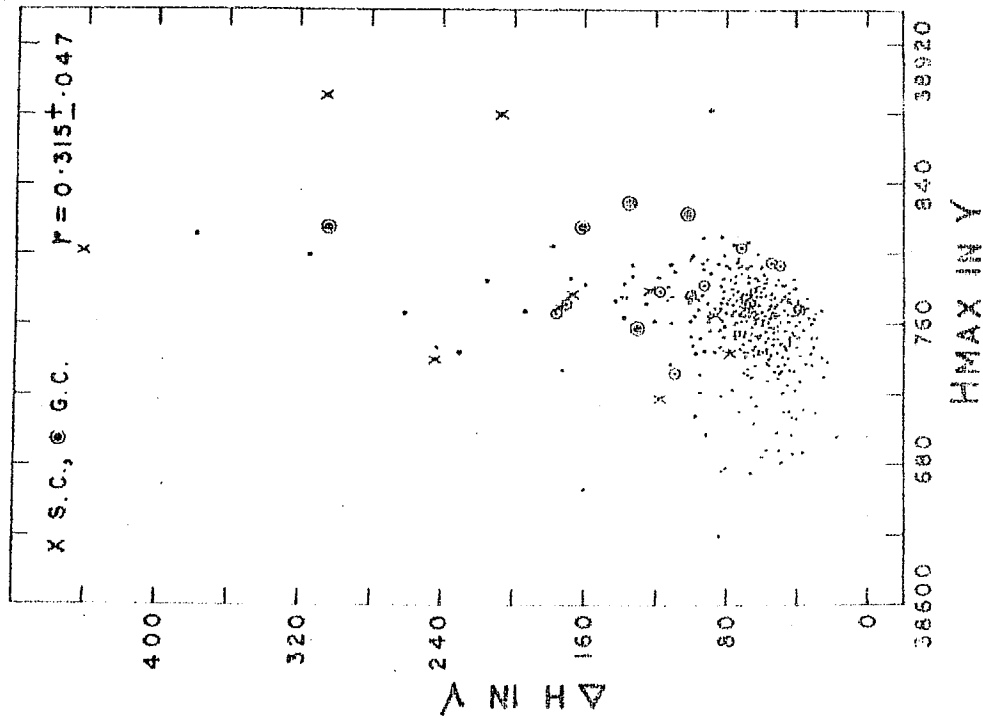


Fig. 4.05 Scatter plot of H_{\max} against H_{\min} for the year 1961 for Alibag. 'x' and 'o' respectively indicate days on which sudden commencement and gradual commencement storms occurred.

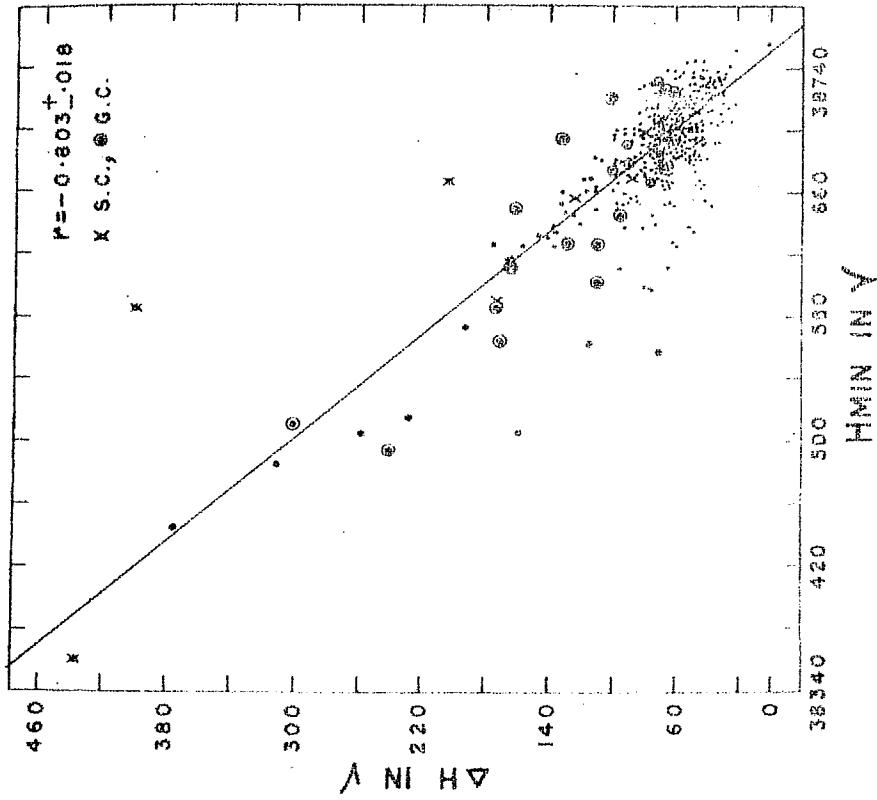


Fig. 4.04 Scatter diagram of H_{\min} against H_{\max} for the year 1961 for Alibag. 'x' and 'o' respectively indicate days on which sudden commencement and gradual commencement storms occurred.

magnetic observatories at Honolulu and Guam which like Alibag, are low latitude stations outside the effect of the equatorial electrojet. Figure 4.06 shows the scatter diagrams of ΔH against H_{\max} and ΔH against H_{\min} for Alibag and Honolulu for the year 1954 and figure 4.07 that for Alibag and Guam for the year 1961. Here H_{\max} and H_{\min} are respectively the maximum and minimum hourly values during the day and ΔH is the difference between them. It can be seen that ΔH is negatively correlated with H_{\min} with a high correlation and not well correlated with H_{\max} , even though, the correlation between ΔH and H_{\max} is positive.

The successive annual mean values of the magnetic elements at an observatory show that the earth's magnetic field undergoes secular changes, though not necessarily or usually at a constant rate. Bhargava and Yacob (1969) have determined the secular variation of the horizontal force at Alibag by the application of digital filters. They have evaluated the secular trend in the annual mean values of H at Alibag for the years 1860 to 1954 and for Honolulu for the years 1915-54. It is seen that the rate of increase of H at Alibag is about 40 γ per year between 1924 to 1964 while for Honolulu the rate of decrease is about 23 γ per year. The secular variation varies from place to place and from time to time. To eliminate the influence of secular changes in H , the author has derived H_{\min}^* and ΔH^* by taking 27-day moving average of the daily values from the corresponding values on the 14 day falling in the middle of the interval. Since ΔH^* is defined as $(\Delta H - \overline{\Delta H})$, there are negative values of ΔH^* which can be seen in figure 4.08.

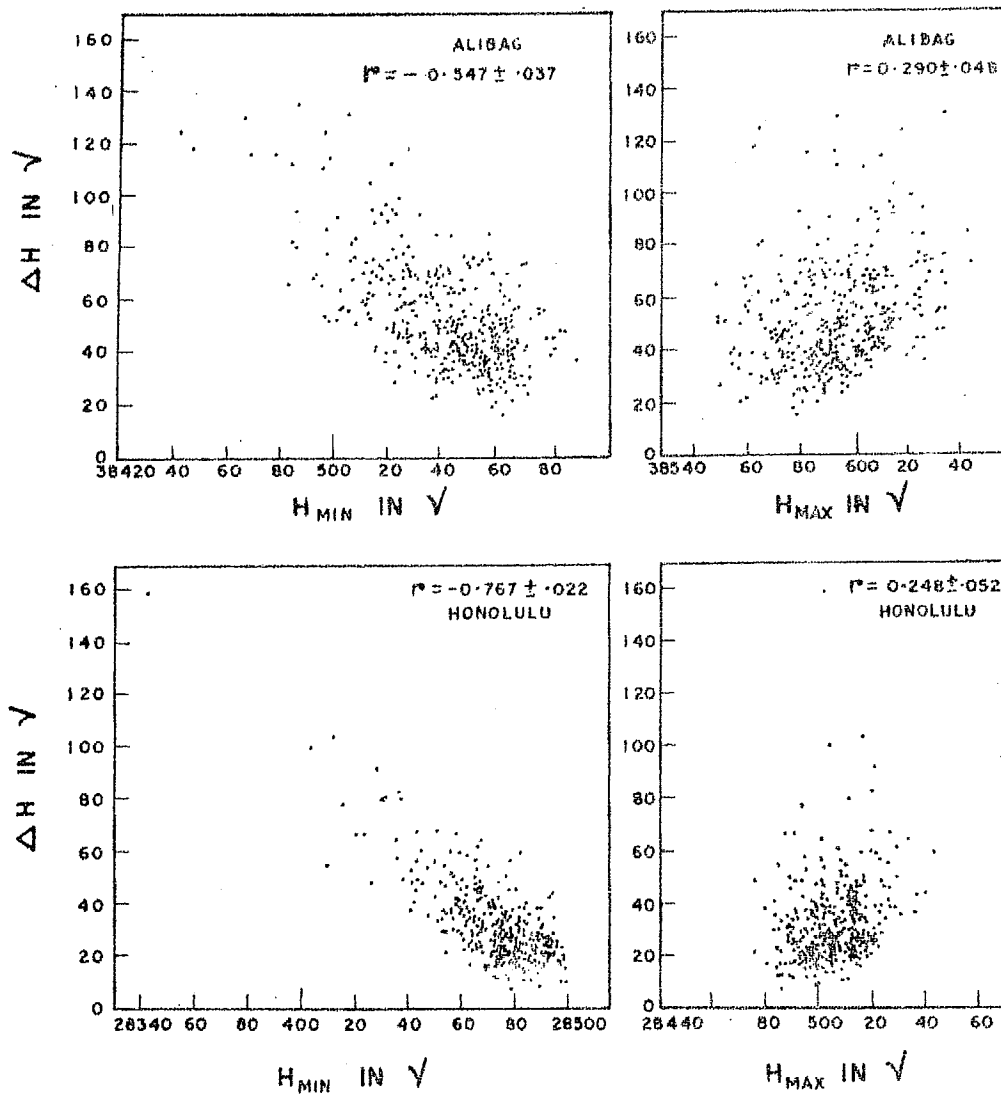


Fig. 4.06 Scatter diagrams of ΔH against H_{max} and ΔH against H_{min} for Alibag and Honolulu for the year 1954.

SCATTER PLOTS OF H_{\min} , ΔH & H_{\max} , ΔH FOR
ALIBAG AND GUAM 1961

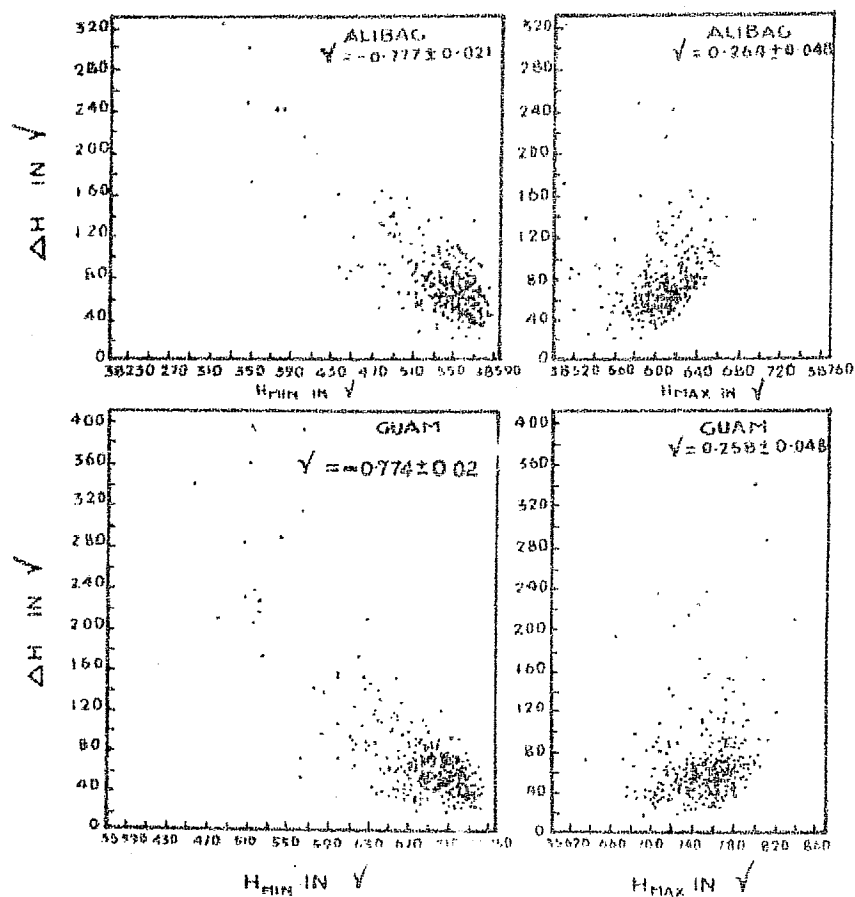


Fig. 4.07 Scatter diagram of ΔH against H_{\max} and ΔH against H_{\min} for Alibag and Guam for the year 1961.

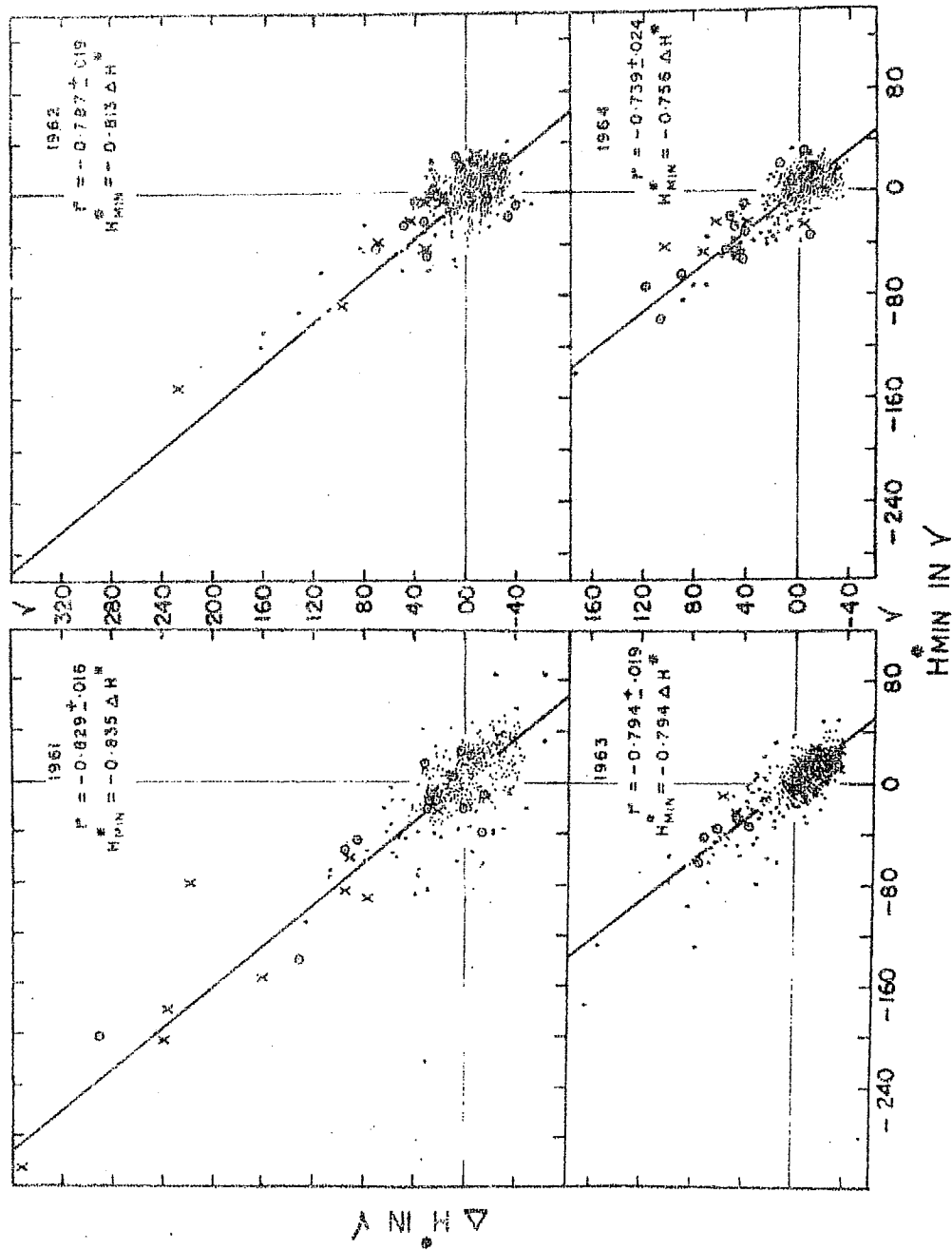


Fig. 4.08 Scatter plots of H^* against ΔH^* for individual years 1961 to 1964. 'x' and 'o' respectively indicate days on which sudden commencement and gradual commencement storms occurred.

The relationship of H_{\min}^* and ΔH^* during each of the four years for Alibag can be seen, in figure 4.08, from the scatter diagrams and statistically best fit lines derived by correlation analysis. During each year, ΔH^* and H_{\min}^* are negatively correlated with a coefficient of about -0.8 ± 0.02 . The points in the diagram indicated by 'X' and 'O' correspond to days when sudden commencement and gradual commencement storms occurred. It would be observed that by and large there is no qualitative difference in the relationship of ΔH^* and H_{\min}^* with increasing degree of geomagnetic disturbances. The fundamental character of ΔH^* and H_{\min}^* during the period of a solar cycle is best brought out in table 4.01.

TABLE 4.01

Correlation coefficient and slope between H_{\min}^* and ΔH^* at Alibag

Year	Correlation coefficient	Slope
1954	$-0.61 \pm .03$	-0.620
1955	$-0.60 \pm .03$	-0.630
1956	$-0.72 \pm .03$	-0.730
1957	$-0.88 \pm .01$	-0.880
1958	$-0.80 \pm .02$	-0.797
1959	$-0.79 \pm .02$	-0.800
1960	$-0.83 \pm .02$	-0.850
1961	$-0.83 \pm .02$	-0.835
1962	$-0.79 \pm .02$	-0.813
1963	$-0.79 \pm .02$	-0.794
1964	$-0.74 \pm .02$	-0.756

Disregarding for the time being the small but systematic difference in the slope of the regression line (Table 4.01) during the years from 1957 to 1962 compared to the years of low solar activity 1954 to 1956 and 1963 to 1964, it can be seen that ΔH^* , H_{\min}^* relationship is relatively constant

The overall relationship between H_{\min}^* and ΔH^* is best brought out in figure 4.09, where data for ΔH^* and H_{\min}^* for each individual day for all the eleven years from 1954 to 1964 have been included. The area of each circle is proportional to the number of days having appropriate pair of values of ΔH^* and H_{\min}^* . Figure 4.10 shows such a plot for Honolulu for the period 1963 to 1967. By all standards the relationship between ΔH^* and H_{\min}^* is remarkable. Since the correlation is negative that with increasing ΔH^* , H_{\min}^* decreases, we can conclude that H_{\min} is, predominantly produced by the removal of the field on the night side (Sarabhai and Nair, 1969 a, 1971).

In deriving ΔH^* we have subtracted the 27 day moving average of ΔH namely $\overline{\Delta H}$ from the value of ΔH on each day. The eleven year variation of $\overline{\Delta H}$ for Alibag is shown in figure 4.11, where the normalised yearly histograms of $\overline{\Delta H}$ are plotted for individual years 1954 to 1964 and also for all the eleven years combined. $\overline{\Delta H}$ has a minimum value of 40 γ even during years of low solar activity. On the other hand during years of low solar activity there are days when ΔH is as low as 20 γ . The observation of Nair et al (1970), that the ionospheric contribution is about 17 γ at Alibag is consistent with the present evidence. A note worthy feature seen in figure 4.11 is that during the years of high solar activity, not only is the mean $\overline{\Delta H}$ about double of what it is at low sunspot activity, but the spread of $\overline{\Delta H}$ during a

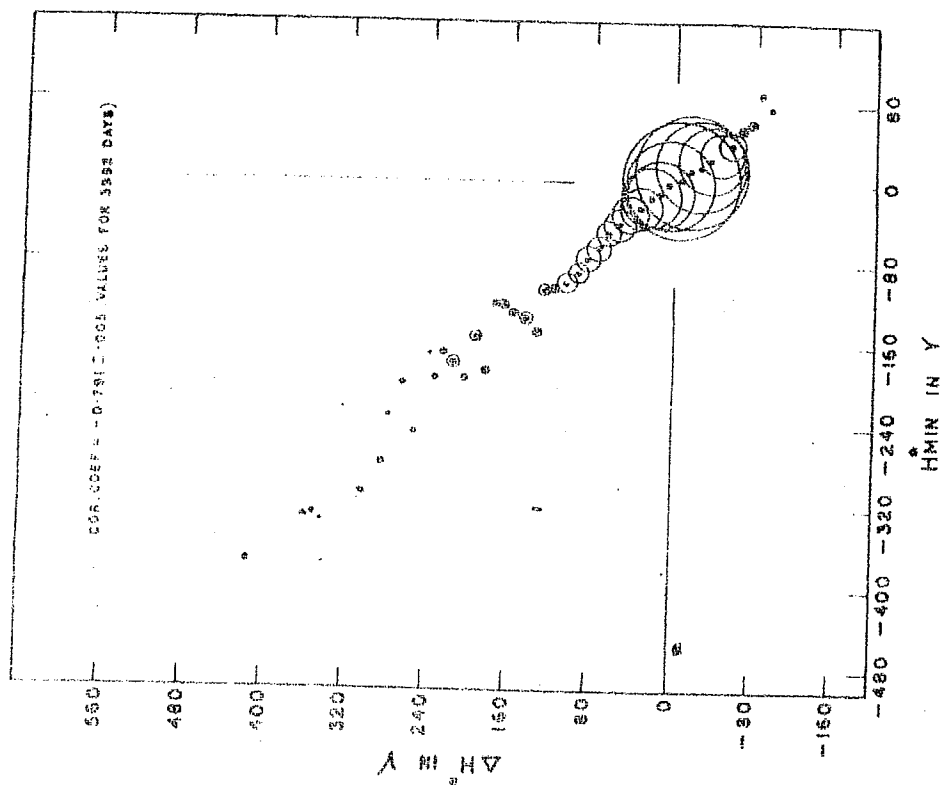


Fig 4.09 H^*_{min} , ΔH^* relationship combining values for the years 1954 to 1964 for Alibag.

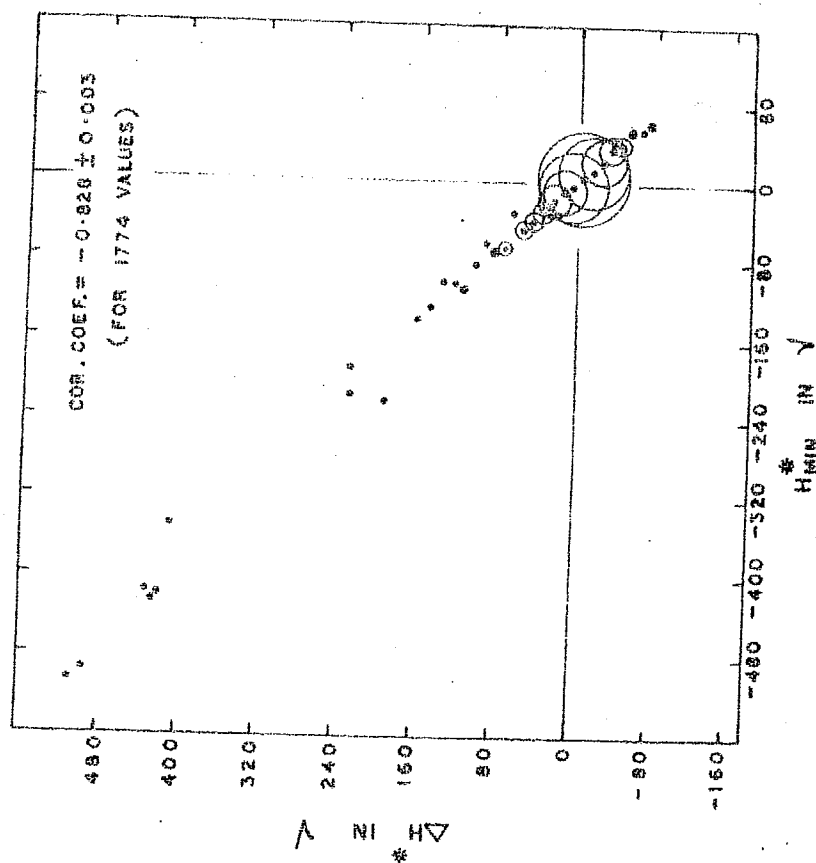


Fig. 4.10 H^*_{min} , ΔH^* relationship combining values for the years 1963 to 1967 for Honolulu.

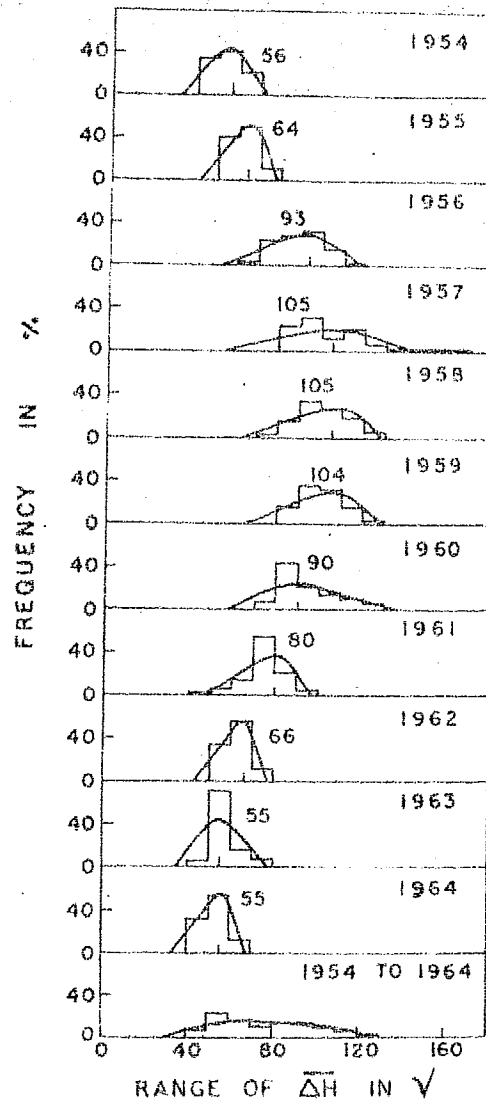


Fig. 4.11 The eleven year variation of $\overline{\Delta H}$ for Alibag showing the normalised histograms of $\overline{\Delta H}$ for individual years 1954 to 1964 and also for all the eleven year combined.

particular year is also larger (Sarabhai and Nair, 1971).

4.3 Magnetospheric and ionospheric contribution to ΔH

At Trivandrum, which at the dip equator, the magnetic effect of the electrojet current has been experimentally verified in rocket flights (Maynard and Cahill, 1965; Sastry, 1968). On the average at Trivandrum the daily variation has an amplitude, about 1.8 times the daily variation at Alibag. Since magnetospheric currents would be located at distances exceeding about 30000 kms. above the surface of the earth, their effect must be almost identical at Alibag and Trivandrum, 1100 kms south of Alibag but situated at the dip equator; neglecting differences in the induced field arising from local ground conditions. On the other hand the well-known enhancement of ΔH at the dip equator is caused by the influence of the equatorial electrojet. A conformation can be sought, about the proposition regarding the interpretation of ΔH at Alibag being largely due to magnetospheric currents, by taking the scatter diagram of $(\Delta H_{\text{Trivandrum}} - \Delta H_{\text{Alibag}})$ against H_{Alibag} . Figure 4.12 shows the plot of ΔH_A against $(\Delta H_T - \Delta H_A)$ for the year 1961. The correlation between the two is negligible and insignificant, clearly confirming that the basic process operative at Alibag is not directly related to the known ionospheric effect which is more important at Trivandrum. In consequence $(\Delta H_T - \Delta H_A)$ must be related to purely ionospheric currents. Here it is worthwhile to examine the validity of these assumptions particularly because they are at variance with the dynamo theory, according to which the contribution of ionospheric currents should predominate at both stations on days which are not geomagnetically disturbed. Moreover the author has derived an estimate of the relative

contributions due to ionospheric and magnetospheric currents at Trivandrum and at Alibag.

Fig. 4.13 shows the normalised histogram of $(\Delta H_T - \Delta H_A)$ for different ranges of ΔH_A for the years 1962, 1963, 1964 and for all the three years combined. It is observed that on a day-to-day basis ΔH_A is more or less independent of the purely ionospheric contribution namely $(\Delta H_T - \Delta H_A)$. Similarly as shown in table 4.02, ΔH_A is independent of the changes of F region ionospheric electron density related to the midday mean value of $f_o F_2$ over Kodaikanal, also close to the dip equator. These facts suggest that ΔH_A does not track the changes in the ionosphere.

TABLE 4.02

$(\Delta H_T - \Delta H_A)$ and $f_o F_2$ at Kodaikanal for different ranges of ΔH_A

ΔH_A (range)	Mean $(\Delta H_T - \Delta H_A)$ in γ	Mean midday $f_o F_2$ in MHz	Number of days
31 to 50 γ	50	7.3	319
51 to 70 γ	51	7.6	314
71 γ and above	49	7.7	292
31 γ and above	50	7.6	925

From these studies it is possible to estimate the relative contributions due to magnetospheric and ionospheric processes at Trivandrum and Alibag. According to the dynamo theory, the mean current density $J = (\sum \cdot E)$ where \sum is the height

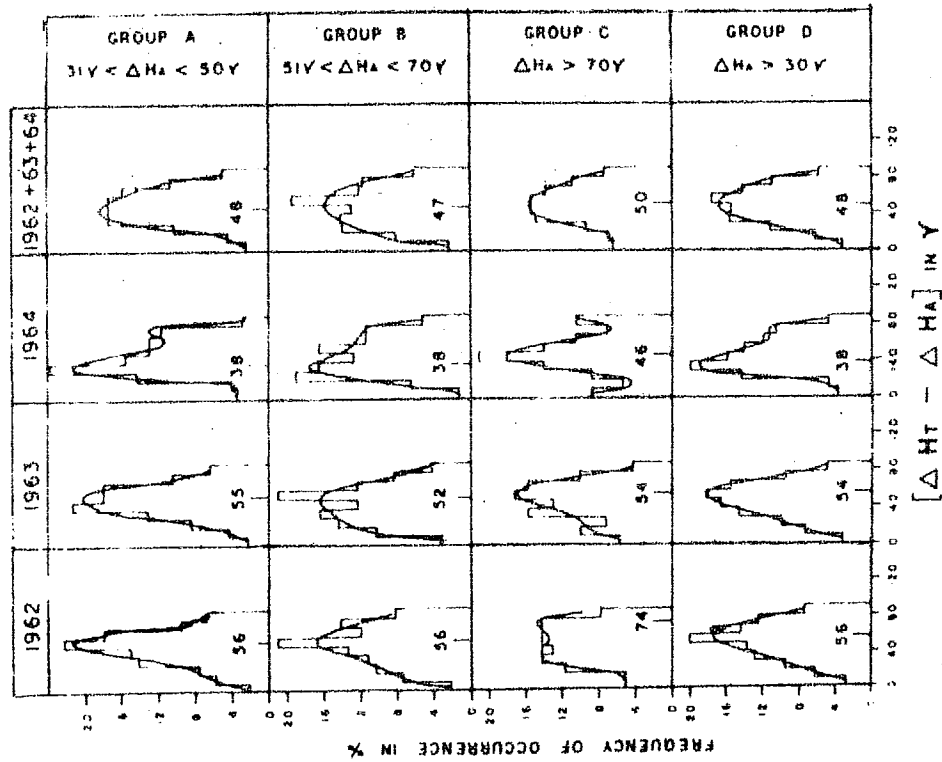


Fig. 4.13 Normalised histograms of $(\Delta H_T - \Delta H_A)$ for different ranges of ΔH_A for the years 1962, 1963 and 1964 and for all the three years combined.

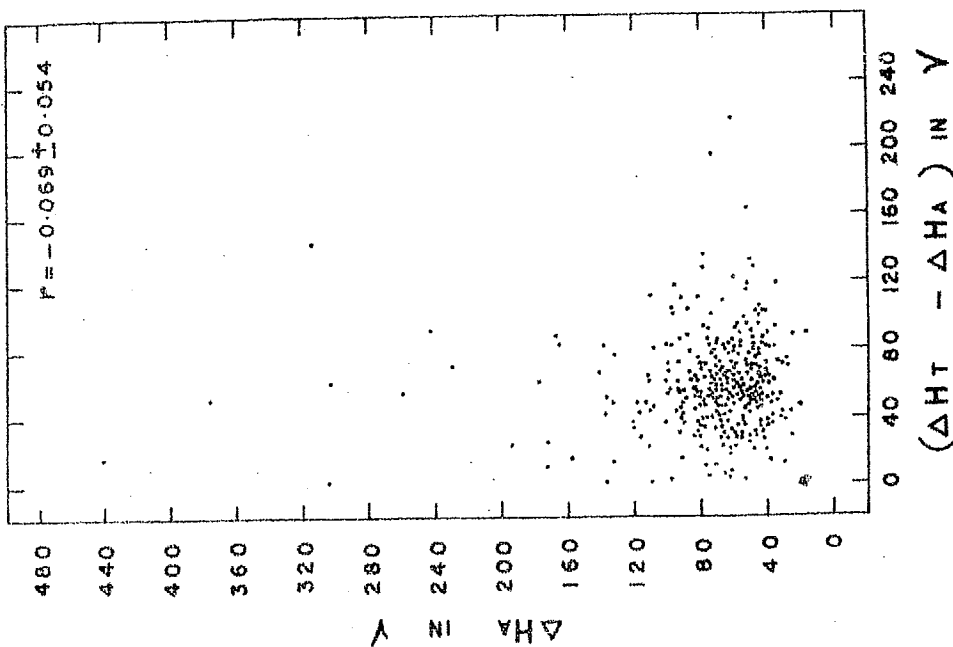


Fig. 4.12 Scatter diagram of $(\Delta H_T - \Delta H_A)$ against ΔH_A for the year 1961.

integrated conductivity and E is the primary electric field. The derived values of $\overline{\Sigma}$ for E-region at 0° , 30° , 60° and 90° dip latitudes (Maeda, 1953) enable a smooth curve to be drawn to express the variation of conductivity with latitudes. For this, the ratio of conductivities at Trivandrum and Alibag derived as $\frac{7.58 \times 10^{-8}}{2.61 \times 10^{-8}} = 2.9$. It is seen from Table 4.02 that on the average the ionospheric contribution at Trivandrum is about 50%.

Consequently, the average ionospheric contribution to ΔH_A would be $\frac{50}{2.9} \approx 17\%$ (Nair et al, 1970).

4.4 Relation between $(\Delta H_T - \Delta H_A)$ and the electron drift speed at E-region at Thumba.

Since January 1964, regular measurements of the drift speeds of the ionospheric irregularities in the E and F regions have been made at Thumba, near Trivandrum, by recording the fading of radio reflections at three spaced aeriels. The drift was always towards west during the day time hours. The mean drift speed during the midday hours (1100-1300 hours) correlates well with $(\Delta H_T - \Delta H_A)$ as shown in Fig. 4.14. Rocket borne magnetometers have measured the magnetic field of the electrojet current in the E-region (Maynard and Cahill, 1965; Sastry, 1968). R. Raghaya Rao (private communication) has shown, taking current density derived from similar measurements and simultaneously observed electron density, that the average electron velocity is comparable with the drift velocities measured with the spaced aerial technique. A linear relationship between the drift speed in the E-region and $(\Delta H_T - \Delta H_A)$ is therefore consistent with the interpretation that the drift velocity measured by the spaced aerial technique is proportional to the electron drift velocity in the

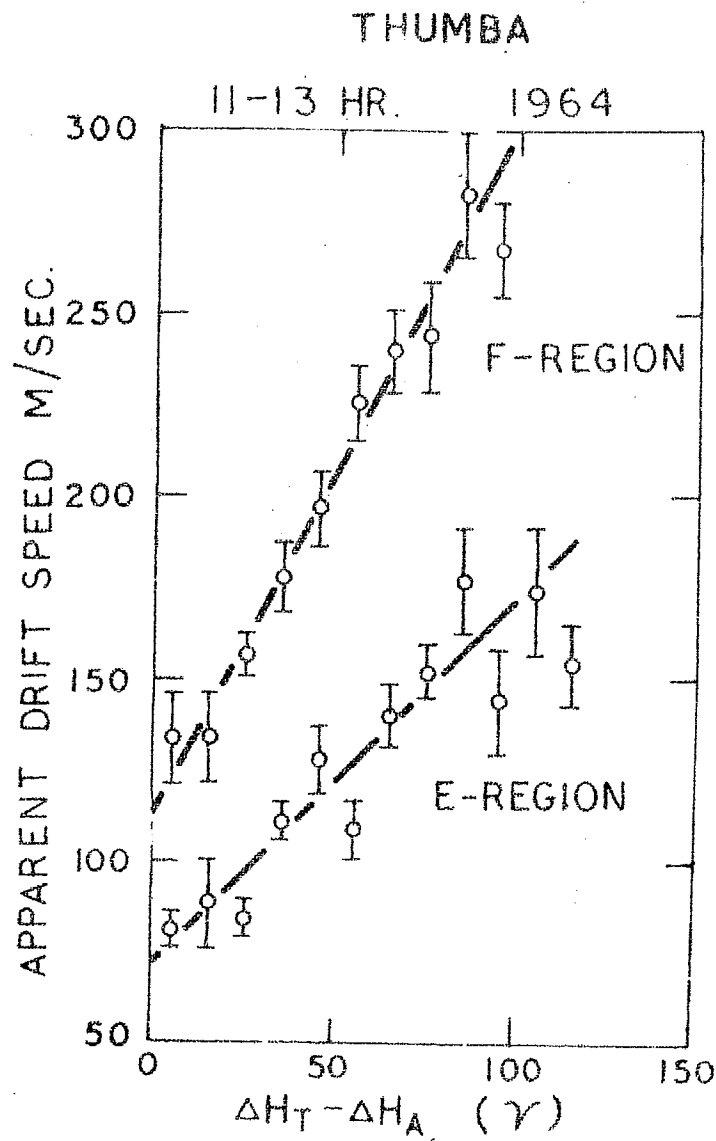


Fig. 4.14 The relations showing the mean westward apparent drift speed during midday hours (1100 - 1300 h) for different ranges of $(\Delta H_T - \Delta H_A)$.

electrojet and that moreover the latter at noon can be deduced from $(\Delta H_T - \Delta H_A)$, derived exclusively from ground measurements. In the F region, the currents due to electrons and ions would produce equal and oppositely directed magnetic effects, and therefore the correlation of $(\Delta H_T - \Delta H_A)$ with F region drifts indicates that the latter are themselves correlated with the E region drifts. On comparing the magnetograms from Tamale (dip $1^\circ-14'$) and Legon (dip $10^\circ-11'$), Osborne (1963) has earlier argued that the electrojet cannot be a simple enhancement of the normal current in a belt of high conductivity. Moreover Osborne and Skinner (1963) have shown a correlation similar to one presented here between the electrojet strength and the F region drifts. The conclusions of these authors are therefore consistent with the present study. Moreover the present study lend support to the view that drift velocities measured by the technique of spaced aeriels is related to the drift velocity of electrons in the electrojet.

4.5 Variability of H at different hours related to day-to-day changes of the daily variation

In section 5.1 the author has identified the ionosphere, the magnetopause and the magnetosphere as three regions from where currents or drifts can contribute to the observed daily variation of H at a low latitude station. The contribution from magnetopause currents is small compared to the contributions from the other two and in consequence one can confine attention to ionospheric and magnetospheric current systems. For a station like Trivandrum, which is at the dip equator, ΔH is controlled mainly by dynamo electrojet currents and in consequence the variability of the currents would exhibit itself

through a large variance of hourly H from one day to another during day time hours only. But at a low latitude station outside the effect of the equatorial electrojet the situation would be quite different if ΔH is controlled largely by the magnetospheric currents systems which are effective during day as well as night hours, contributing a variance from day-to-day which is insensitive to local time.

In order to confirm the view that there are two independent processes contributing to ΔH even during quiet days, the author has studied variations with local time of the variance of H_T^r and H_A^r , the r^{th} hour values of H for Trivandrum and Alibag for internationally quiet days during high and low solar active periods. Figure 4.15 shows the local time dependence of the variances $(\overline{H_T^r})^2$ and $(\overline{H_A^r})^2$ for the years 1958 to 1960 and for 1962 to 1964. We observe that (1) the variance at Alibag is insensitive to local time while at Trivandrum it is much larger during day time than at night, as expected; (2) the variance at night at each station is of the same magnitude indicating a common source for both stations during night; (3) the variance due to both factors is larger during years of high solar activity than when the sun is quiet.

4.6 Equinoxial maxima in equatorial electrojet strength

The monthly mean values of $(\Delta H_T - \Delta H_A)$ and ΔH_A are shown in figure 4.16 separately for the years 1958 to 1966 and for all the nine years combined. $(\Delta H_T - \Delta H_A)$ which is purely due to ionospheric currents, shows clear equinoxial maxima. It is satisfactory to note that drift speed as measured by spaced aerial technique, at Thumba very near to Trivandrum also exhibit equinoxial maximum (Chandra and Rastogi, 1969).

DAILY VARIATIONS OF $[\overline{\sigma_{H_T^r}}]^2$ AND $[\overline{\sigma_{H_A^r}}]^2$
FOR QUIET DAYS DURING HIGH AND LOW
SOLAR ACTIVITY PERIODS

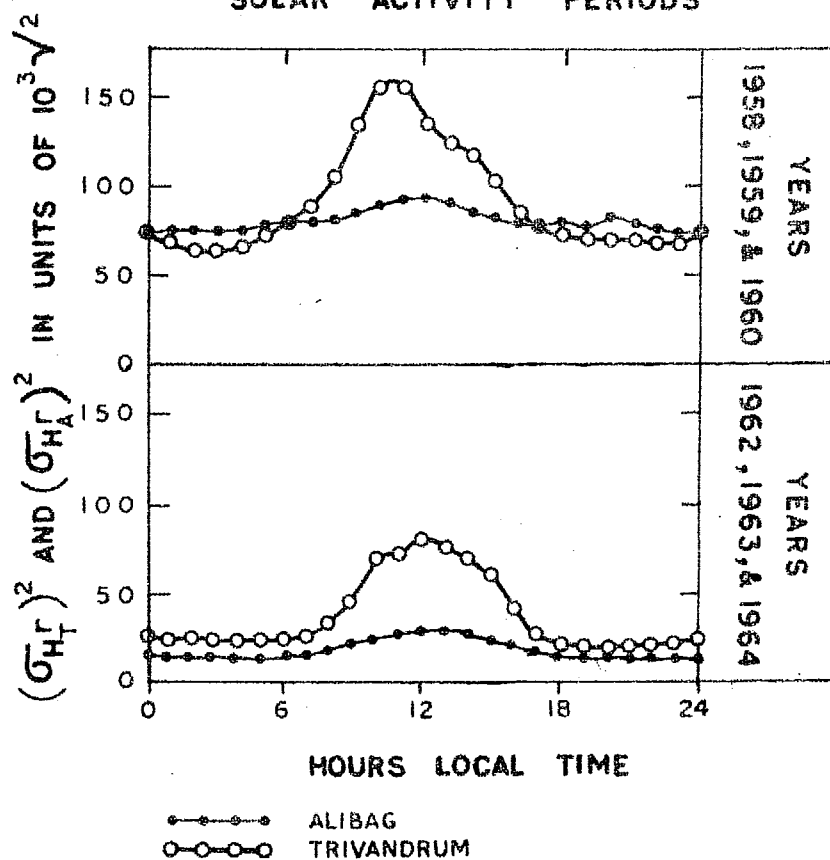


Fig. 4.15 Daily variations of $(\overline{\sigma_{H_T^r}})^2$ and $(\overline{\sigma_{H_A^r}})^2$ for quiet days during 1958, 1959 and 1960 combined and 1962, 1963 and 1964 combined.

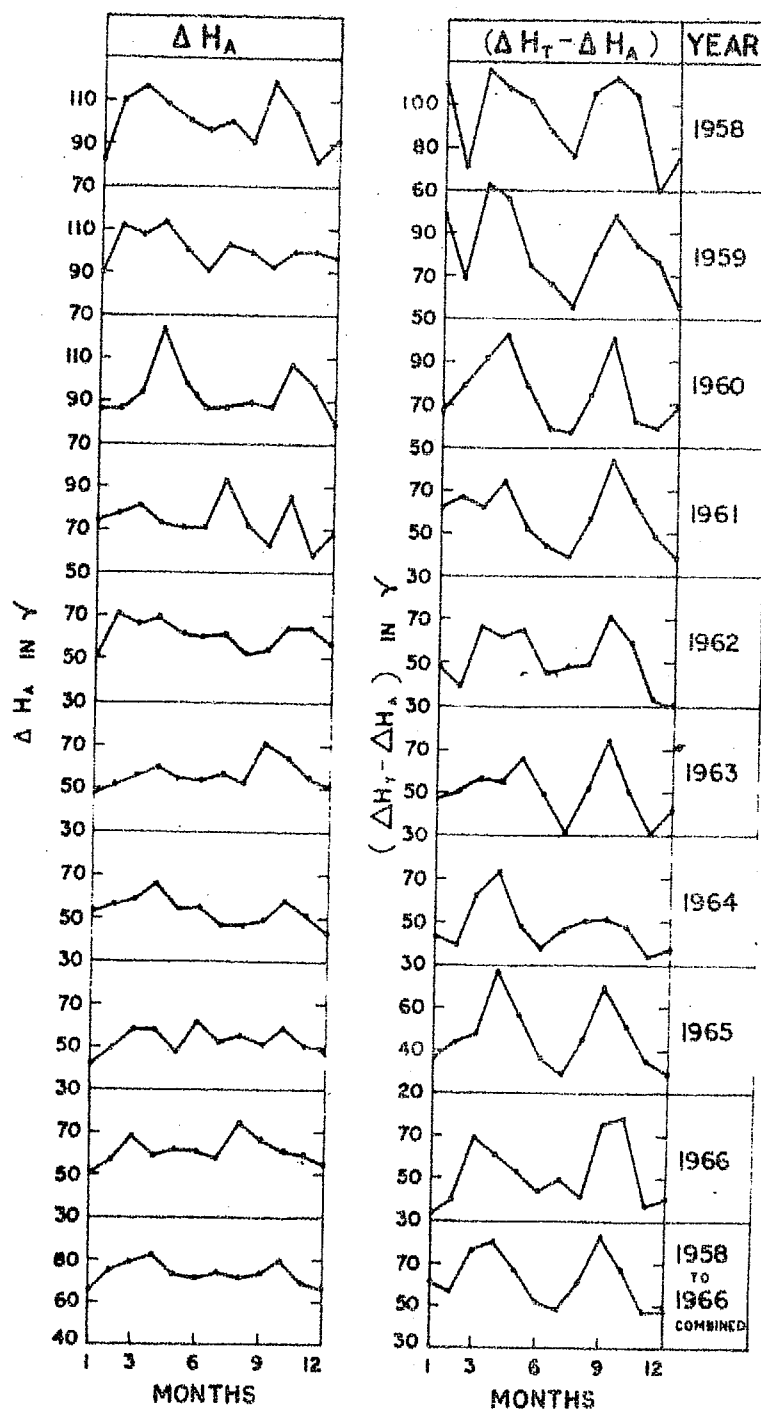


Fig. 4.16 Monthly mean values of $(\Delta H_T - \Delta H_A)$ and ΔH_A for the years 1958 to 1966 and for all the nine years combined.

In contrast with the purely ionospheric effect, ΔH_A has no consistent seasonal variation. The absence of equinoxial maxima in ΔH_A is surprising and is not well understood.

According to Hones and Bergeson (1965) a radial electric field generated by the wobbling of the earth's magnetic axis in the magnetosphere, distorted by the solar wind, should cause charged particles to experience net energy changes over a number of revolutions around the earth. From this theory, an explanation for the enhancement of the strength of the equatorial electrojet at equinoxes can be visualised as follows. If one assumes that the kinetic energy density of the solar wind, which compresses the magnetosphere in the sub-solar direction is constant over a period of one year then, since the earth's magnetic axis is more nearly perpendicular to the solar wind flow at equinoxes than at solstices, the compression of the magnetosphere and the radial electric field produced in the ionosphere would be maximum during equinoxial months. This effect should be more pronounced at the equator than at higher latitudes. This also supports the contention that there are two independent processes which are operative, and that at Trivandrum the ionospheric contribution is similar in magnitude to the magnetospheric contributions on a normal day, while at Alibag the ionospheric contribution is only about a third of ΔH_A .

4.7 ΔH_A in relation to changes in K. E. density of solar wind and $\overline{B_z}$ of the interplanetary magnetic field.

By means of spacecrafts it is now possible to obtain direct information regarding the electro-magnetic state of the

interplanetary medium. Different types of plasma probes have been used in space vehicles. One is a plasma cup which is used essentially as an integral analyser for the energy, with a wide angle of acceptance for the arriving particles. Such instruments have been developed by the group at MIT (Bonetti et al, 1963). Similar devices, called ion traps, have been used in Russian Space-crafts (Gringauz et al, 1961). Another type is an electrostatic differential energy analyser with a narrow angle of acceptance (Neugebauer and Snyder, 1963).

There are different types of magnetometers which have been developed and used in space measurements. They are (1) Induction or search coil (2) Fluxgate or saturable core (3) Proton precession (4) Alkali vapour self - oscillating and (5) Helium vapour low-field.

Ness et al (1964) have discussed in detail the magnetic instrumentation used by them on satellites IMP-1 and IMP-3. They have used two types of magnetic instruments, namely rubidium-87 vapour magnetometer to measure the absolute scalar intensity of the magnetic field and two mono-axial flux-gate magnetometers to delineate the vector characteristics of the field. The Ames magnetometers used on Explorer-33 are of the flux gate type, specially designed. A detailed report of the instrumentation used by the Ames group is available (Mihalov et al 1968).

The solar wind plasma data from IMP-1, used in the present analysis, have been experimentally measured by the MIT plasma probe on board IMP-1 satellite. Pai et al (1967)

have reported the three hourly averages of the velocity, V_s ; density, n_s ; flux, ϕ_s and kinetic energy density of solar wind plasma. The primary interplanetary magnetic field data, in the solar magnetospheric co-ordinate system, used in the present analysis, is obtained by N.F. Ness from magnetometers on board IMP-1 and IMP-3. In the solar magnetospheric coordinate system the positive X axis points towards the sun, while the Z axis lies in the plane formed by the X axis and the geomagnetic dipole axis; Z is positive in the northern hemisphere. The Y axis of the right-handed coordinate system is always orthogonal both to the sun-earth line and to the geomagnetic dipole axis (Ness, 1965). The primary interplanetary magnetic field data used in the present analysis consists of hourly averages of B, the magnitude of the interplanetary magnetic field and $\overline{B_x}$, $\overline{B_y}$ and $\overline{B_z}$, the standard deviations of B_x , B_y and B_z the field components along X, Y and Z directions, derived from 5.46 minute values. From these, daily values have been computed for each parameter.

During IMP-1 period (27-11-1963 to 15-2-1964) a fairly well established sector structure has been observed (Wilcox and Ness, 1964) in the interplanetary plasma indicating the stability of the regions of activity. In order to improve the statistical accuracy of these parameters the author has derived, by super-position of successive 27-day values, the average B, B_x , B_y and B_z for each heliographic longitude at the central meridian passage (CMP). Similarly the values of V_s , the solar wind velocity; kinetic energy density of the solar wind (K.E. density); ΔH_A , the daily range of H at Alibag and $\sum K_p$ the daily sum of K_p have been computed. Figure 4.17 shows the average 27-day pattern of these

27 DAY AVERAGE VARIATION OF THE
INTERPLANETARY AND GEOMAGNETIC FIELD
PARAMETERS DURING IMP-1 PERIOD

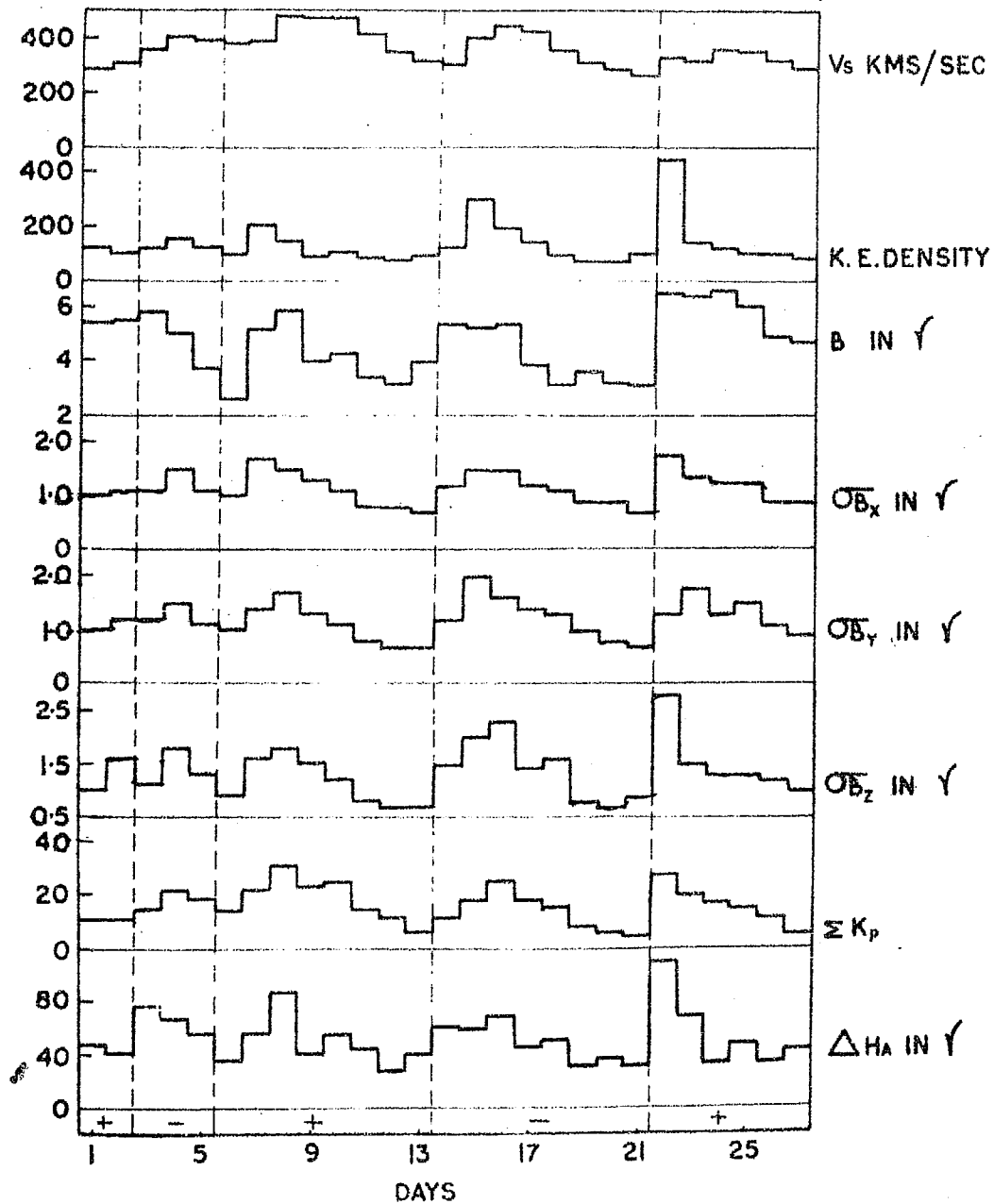


Fig. 4.17 The 27 day recurrence during IMP-1 period of V_s , K.E. density, B , \overline{B}_x , \overline{B}_y , \overline{B}_z , ΣK_p and ΔH_A

parameters. Here V_s is in Kms/sec, K.E. density in units of 8.8×10^{-11} ergs/cm³, B , $\overline{B_x}$, $\overline{B_y}$, $\overline{B_z}$ and ΔH_A are in gammas. Table 4.03 shows the correlation coefficients between the geomagnetic and interplanetary parameters during IMP-1 period.

TABLE 4.03

Correlations between interplanetary parameters and geomagnetic field parameters during IMP-1 period (for 27-day average pattern)

	V_s	n_s	K. E. density	B	$\overline{B_x}$	$\overline{B_y}$	$\overline{B_z}$
ΔH_A	$\frac{0.29}{0.18}^+$	$\frac{0.60}{0.13}^+$	$\frac{0.73}{0.09}^+$	$\frac{0.60}{0.13}^+$	$\frac{0.56}{0.13}^+$	$\frac{0.57}{0.13}^+$	$\frac{0.77}{2.08}^+$
$\sum K_p$	$\frac{0.79}{0.07}^+$	$\frac{0.23}{0.17}^+$	$\frac{0.56}{0.14}^+$	$\frac{0.42}{0.14}^+$	$\frac{0.67}{0.11}^+$	$\frac{0.69}{0.10}^+$	$\frac{0.74}{0.09}^+$

The correlation coefficient of $\sum K_p$ is best with V_s , in agreement with the observations of Snyder et al, 1963. In Chapter V the relationship of V_s and $\overline{B_z}$ with $\sum K_p$ is explained in the light of the interaction of the solar wind with the magnetosphere.

It is observed that ΔH_A is well correlated with K.E. density and $\overline{B_z}$ and insignificantly so with V_s . ΔH_A has the dimensions $M^{1/2} L^{-1/2} T^{-1}$ and therefore a meaningful physical relationship can be expressed by considering $(\Delta H_A)^2$ and observed kinetic energy density of the solar wind plasma, both having the same dimensions.

The correlation between the two is 0.78 ± 0.08 for the 27-day superposed values during IMP-1 period. The scatter diagram of K. E. density against $(\Delta H_A)^2$ is shown in figure 4.18. The expression connecting the two quantities during IMP-1 period is

$$\text{K. E. density} = (20 \pm 11) \cdot 10^{-10} + (3.65 \pm 0.45) 10^{-12} (\Delta H_A)^2 \text{ ergs/cm}^3 \quad \dots (4.02)$$

Figure 4.19 shows the scatter plot of the 27-day values of the K. E. density of the observed solar wind with $(\overline{B_z})^2$ during IMP-1 period. The correlation between K. E. density and $(\overline{B_z})^2$ is 0.30 ± 0.07 . This is not surprising since an increase in K. E. density due to enhancement of solar wind velocity must simultaneously result in a compression of the plasma in interplanetary space and a change in the interplanetary magnetic field. In this connection Sarabhai (1963) and Dessler and Fejer (1963) have earlier examined the situation when a fast solar wind overtakes a slow solar wind.

Figure 4.20 shows the scatter diagram of the average 27-day values of ΔH_A and $\overline{B_z}$ during IMP-1 and IMP-3 periods combined. The correlation between ΔH_A and $\overline{B_z}$ is 0.75 ± 0.06 suggesting that there is a statistically significant relation between the two. It can be seen that the relation holds good in the same way for two different periods (27-11-1963 to 15-2-64 and 15-6-1965 to 26-1-1966).

In order to confirm the relation between $\overline{B_z}$ and ΔH_A the author has conducted the analysis for the years 1967 and 1968. The interplanetary magnetic field data, from Ames

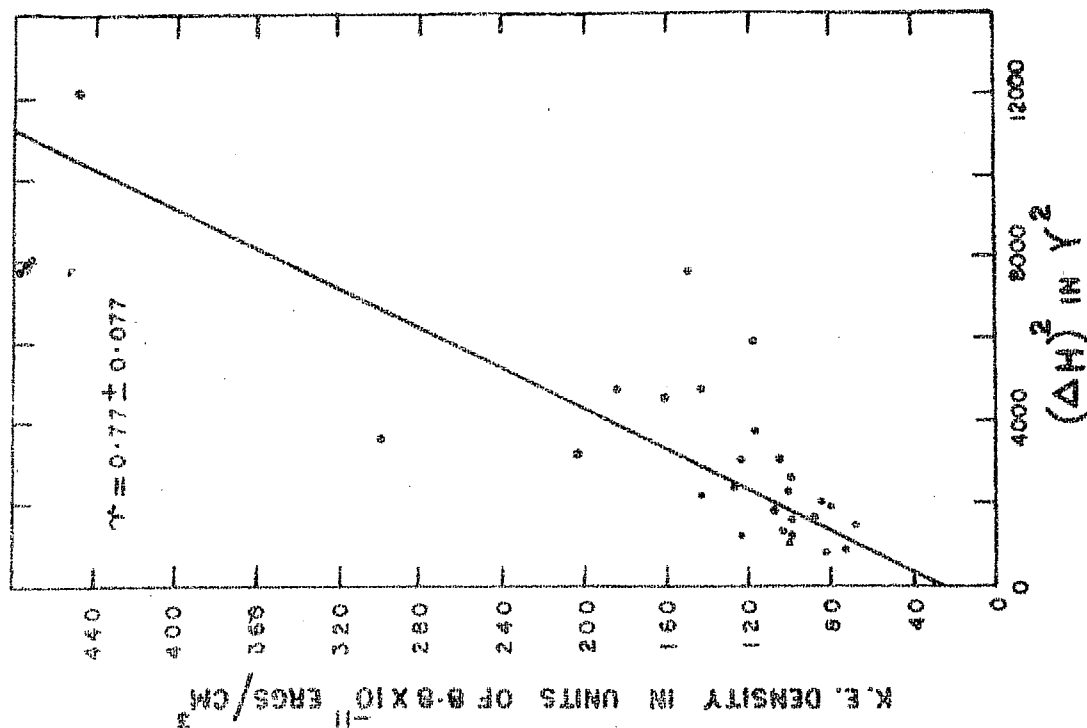


Fig. 4.18 Scatter plot of the average 27 day values of K.E. density of the solar wind and $(\Delta H)^2$ of Alibag, during IMP-1 period.

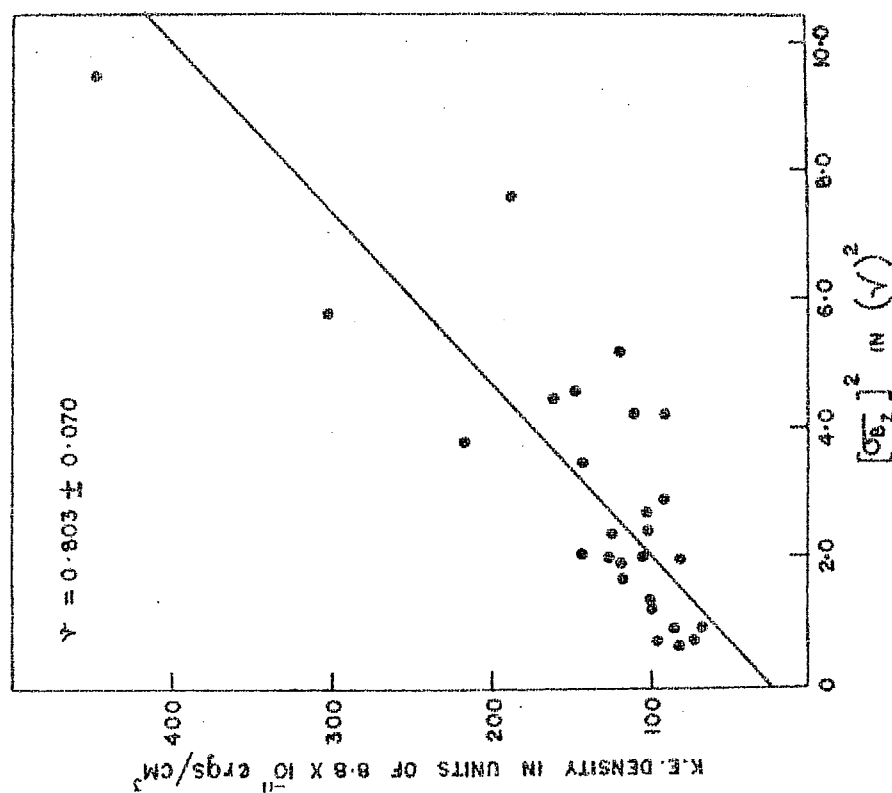


Fig. 4.19 Scatter plot of the average 27 day values of the K.E. density with $(\overline{G_B})^2$ during IMP-1 period.

magnetometers on Explorer-33 in the solar magnetospheric coordinate system, used in the present work have been obtained by C. P. Sonnet.

The primary data consists of hourly averages of B , B_x , B_y and B_z . The daily values of $\overline{B_z}$ for days when there is no break in the data have been computed using the relation

$$\overline{B_z}' \text{ (daily)} = \sqrt{\frac{1}{24} \sum_{i=0}^{23} (B_{zi} - \overline{B_z})^2} \quad \dots (4.08)$$

It has been noted that during 1967 and 1968 the 27-day recurrence of the interplanetary magnetic field strength was poor. Consequently averaging data according to synodic rotation, suppresses detailed informations. However, since data are available for 382 days during 1967 and 1968, it is meaningful to group the days into different sets according to ΔH_A values at intervals of 10γ. Figure 4.21 shows the scatter plot of the mean values of ΔH_A and $\overline{B_z}'$ for different sets. The area of each circle is proportional to the number of days having appropriate pair of values of ΔH_A and $\overline{B_z}'$. The solid line in figure 4.21 corresponds to the regression between ΔH_A and $\overline{B_z}'$ for IMP-1 and IMP-3 periods (figure 4.20). It is remarkable that the relationship between ΔH_A and $\overline{B_z}'$ remains relatively unaltered during the solar cycle from 1963-64 (IMP-1) through 1965 (IMP-3) to 1967-68 (Explorer-33).

It has been shown earlier that during IMP-1 period the K. E. density is correlated with $(\Delta H_A)^2$. Data for density

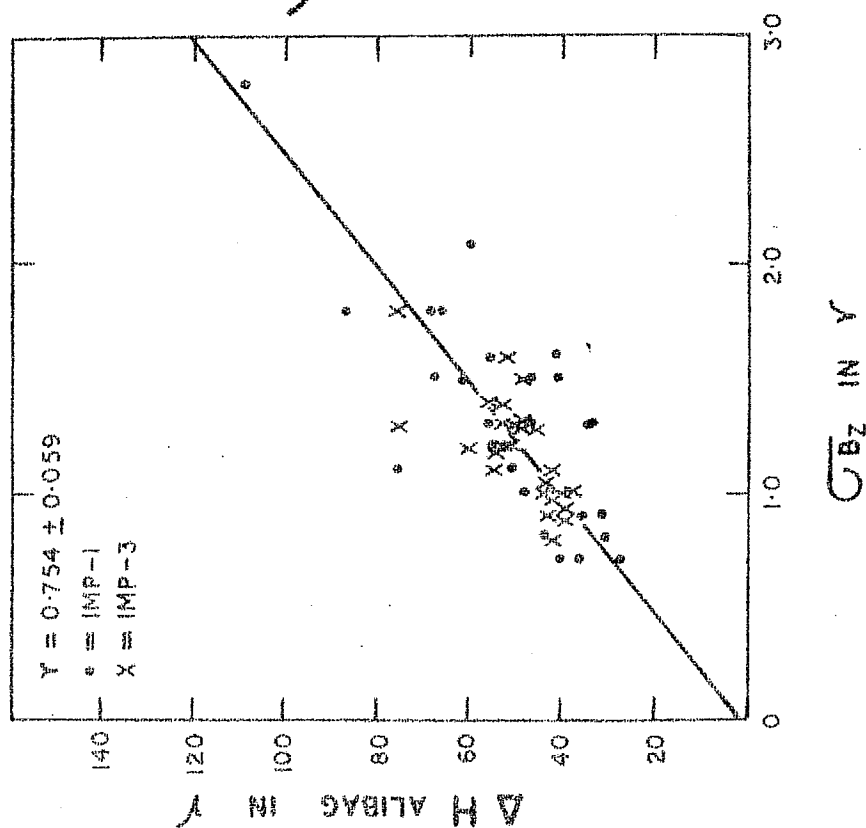


Fig. 4.20 Scatter diagram of the average 27-day values of ΔH_A and G_{BZ} , during IMP-1 and IMP-3 periods. (combined)

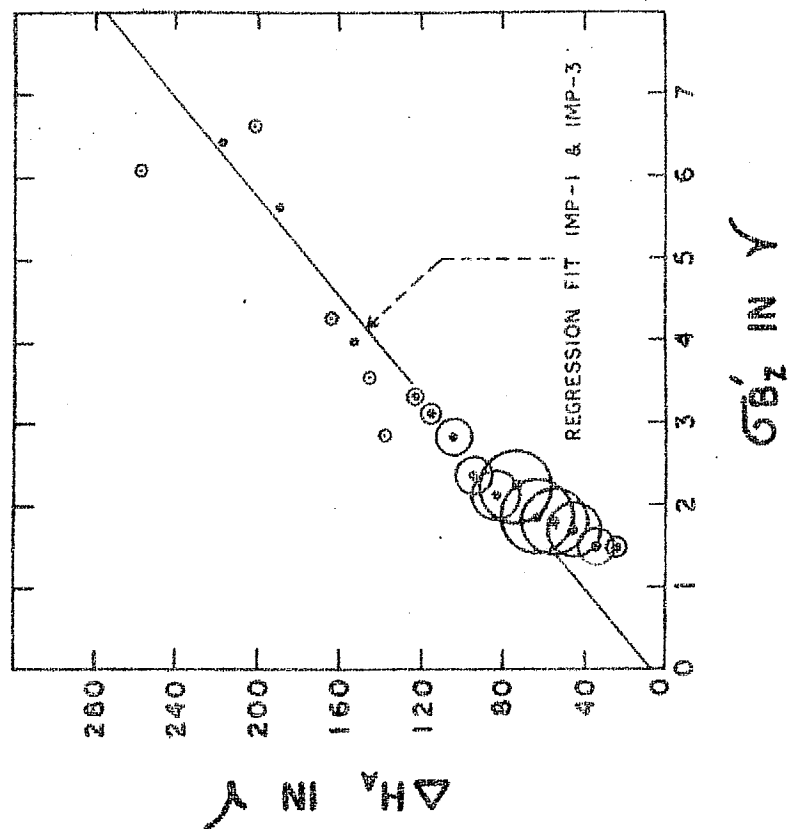


Fig. 4.21 Scatter plot of the mean values of ΔH_A and G'_{BZ} for different ranges of ΔH_A , during Explorer-33 period (1967 and 1968).

and velocity of interplanetary plasma from IMP-3 and Explorer-33 are not available with the author, but during IMP-1 period it is possible to study the relative contributions of the K.E. density and $\overline{B_z}$ of interplanetary plasma and other causes such as ionospheric currents, to ΔH_A . The multiple correlation of the average 27-day values for $(\Delta H_A)^2$, the observed kinetic energy density of the solar wind and the variance of B_z for IMP-1 period shows that while 61% of the variation in $(\Delta H_A)^2$ is attributable to changes in K.E. density alone and 58% only to $(\overline{B_z})^2$, 66% can be explained by referring to both K.E. density and $(\overline{B_z})^2$. This leaves 34% of the variance of $(\Delta H_A)^2$ attributable to other causes such as ionospheric currents.

In the light of these experimental evidences, it is shown in Chapter V that the time dependent azimuthal electric field in the magnetosphere play a very important part in populating the inner shells of the magnetosphere. These enhance the eccentric and the partial ring currents, and the tail currents lowering H during night time and contributing to an increase in ΔH .

4.8 Conclusions

The studies reported in this chapter indicate that ΔH , the daily variation of the horizontal component of the earth's magnetic field for a low latitude station away from the effects of the equatorial electrojet, is largely due to a reduction of the field on the night side. Since E-region currents are very weak during night time, the reduction of H on the night side

should be caused by an asymmetric ring current in the magnetosphere. For a normal day it has been shown that 2/3rd of the observed amplitude of ΔH is due to such an asymmetric ring current in the magnetosphere. We have proposed in section 5.1, a conceptual representation of the effects of various processes contributing to ΔH . It has been shown that currents in the magnetosphere which give major contribution to ΔH , are controlled by temporal changes in the solar wind. These findings enable one to use ΔH for probing the electromagnetic state of the interplanetary space.

CHAPTER V

5.1 Morphology of ΔH .

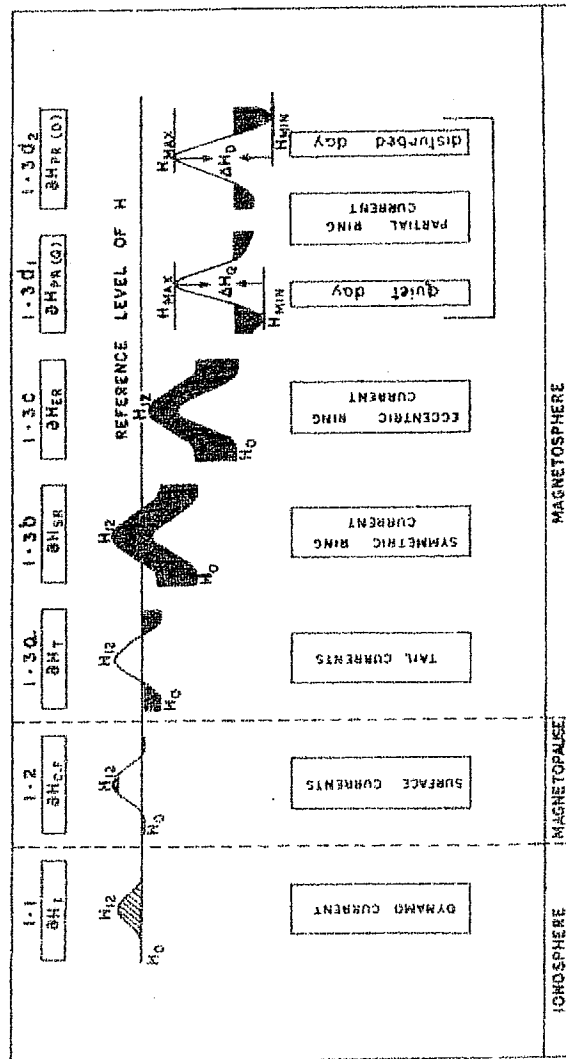
If one wishes to use geomagnetic field changes to probe interplanetary plasma, one should have an appreciation of the various current systems in the ionosphere, magnetosphere and at the magnetopause, which could affect the unperturbed geomagnetic field. Evidence has been presented (Sarabhai and Nair, 1969 (a), 1969 (b), 1969 (c) and 1969 (d); Nair et al, 1970; Nair and Sarabhai, 1970 and Sarabhai and Nair, 1971) which indicates that the daily variation of the geomagnetic field at a low latitude station away from the influence of the equatorial electrojet, is dominated by current systems outside the ionosphere.

To make credible the proposition that the observed geomagnetic effect is significantly related to magnetospheric currents, it is necessary to demonstrate that experimental observations and theoretical studies of the drifts of particles in the magnetosphere provide an overall view which is consistent with the above assumption. Some direct observational evidence is available in respect of the currents, in the ionosphere and the magnetosphere. Moreover, from theoretical studies one can now infer the existence of currents in the magnetosphere due to the convection of the plasma driven as a result of reconnection of interplanetary and geomagnetic field lines (Dungey, 1961); due to the viscous interaction of the interplanetary plasma with the magnetosphere (Axford and Hines, 1961); and due to gradient and curvature of the field lines in the magnetosphere.

The dynamo theory suggests that the currents in the ionosphere occur in the E-regions due to the thermal winds and electric fields. The effects of the currents on the magnetopause, in the magnetosphere and the ionosphere, and their progressive contributions to the unperturbed geomagnetic field at a low latitude station such as Alibag can be conceptually and diagrammatically depicted as shown in figure 5.01 (Sarabhai and Nair, 1969 d ; Sarabhai and Nair, 1971). For the time being the effects due to the induced earth currents is neglected. The darkened portions indicate the contribution of ΔH , due to decreases, and the hatched portions due to enhancements. H represents the assumed value of the surface unperturbed dipole field as would obtain if the sources of electromagnetic and particle radiations from the sun were cut off. The different effects can be summarized as follows: It is suggested that the various processes are all operative on each day, though their relative importance varies depending on solar, terrestrial and interplanetary conditions in the neighbourhood of the earth.

5.11 Dynamo current.

The effect of the ionospheric current in the equatorial electrojet has been measured with rocket-borne magnetometers (Maynard and Cahill, 1965; Sastry, 1968). Moreover, Nair et al (1970) have demonstrated the high correlation between the drift speeds of the ionospheric irregularities at Trivandrum (dip equator) and the differences between the daily range, of the H component of the geomagnetic field at Trivandrum and Alibag. It has been estimated that on an average day the ionospheric contribution to ΔH at Alibag represents a day time increase of about 17 γ , while at Trivandrum it is about 50 γ . This effect is shown in figure 5.01 as δH_I .



H_{MAX} = MAXIMUM VALUE OF H ∂H_I = EFFECT OF IONOSPHERIC CURRENT
 H_{MIN} = MINIMUM VALUE OF H ∂H_{CF} = " " MAGNETOPAUSE CURRENTS
 $\Delta H = [H_{MAX} - H_{MIN}]$
 [] = FIELD DECREASE ∂H_T = " " TAIL CURRENTS
 [] = FIELD ENHANCEMENTS ∂H_{SR} = " " SYMMETRIC RING CURRENT
 [] = " " ∂H_{ER} = " " ECCENTRIC RING CURRENT
 [] = " " ∂H_{PR} = " " PARTIAL RING CURRENT

Fig. 5.01 Hypothetical representation of the development of ΔH for low latitude station away from the effects of the equatorial electrojet, from various current systems.

5.12 Magnetopause currents.

According to Mead (1964) the effect of the surface currents on the magnetopause due to the quiet day corpuscular flux of the solar wind would give rise to an increase of nearly 27 on the day side and a reduction by about the same magnitude during night time at the surface of the earth. This is shown in figure 5.01 as ΔH_{CF} .

5.13 Magnetospheric currents.

5.131 The tail currents

Siscoe and Cummings (1969) have reported that an increase in the tangential stress at the magnetopause which is associated with an increase in kinetic energy density of the solar wind, should increase the magnetic energy stored in the tail. In consequence the tail radius should increase and the inner edge of the neutral sheet should move closer to the earth. The effect of the neutral sheet and the θ type current system in the tail is equivalent to a small magnetic dipole, of opposite magnetic moment to that of the main geomagnetic field (Axford et al, 1965; Williams and Mead, 1965). This should cause a decrease in the field during night time shown as ΔH_T in figure 5.01.

5.132 The symmetric ring current

There should be at all times and even during quiet periods a field reduction due to a symmetric westward ring

current which is mainly situated at 3.5 earth radii. From the observed values of particle drifts in the magnetosphere, Schield (1969 a, 1969 b) has estimated that the quiet day ring current would have a magnetic moment of $0.21 M_E$, resulting in a decrease of 28.4γ at the surface of the earth at the equator. This is shown as ΔH_{SR} in figure 5.01.

5.133 The eccentric ring current

The contours of constant field magnitude in the equatorial plane have been constructed by Fairfield (1968), using the data from the satellites IMP-1, 2 and 3. The contours of constant B , with $B < 150 \gamma$ are not symmetrical in the equatorial plane and they are nearer to the earth in the anti-solar direction compared to the subsolar direction. This is due to compression of the magnetic field by the solar wind on the day-side. The eccentricity of the constant B contours is enhanced when the solar wind pressure is more. Moreover, Kavanagh et al (1968) have worked out the energy contours in the outer magnetosphere for protons and electrons which are nearer to the earth in the night side compared to the dayside. Thus particles which conserve the first adiabatic invariant and do not change their energy within the period of their drift around the earth, have to drift along contours of constant B , forming a west-ward eccentric ring current which is nearer to the earth on the night side compared to the dayside. In consequence the decrease of H during night time is more than during day time. This effect is shown as ΔH_{ER} in figure 5.01.

Nakada and Mead (1965) have examined the diffusion of protons in the outer radiation belt due to violation of the third adiabatic, invariant, when the kinetic energy of the solar wind increases in time short compared to the longitudinal drift period of these trapped particles. The net effect is an inward displacement and acceleration of particles. The above mechanism enhances the eccentric ring current, which in turn enhances the range and lowers the level of H for equatorial stations.

5.134 Partial ring current

The nature of the partial ring current can be understood in terms of the inward drift of particles from the tail. The computations due to Roederer (1969) reveal that particles mirroring at low latitudes, on the night side, are seen to abandon the magnetosphere, before reaching the noon side. Anderson (1965) and Anderson and Ness (1966) have reported experimental evidence relating to partial trapping zones, called the cusp region. During geomagnetically disturbed days, as explained by Freeman and Maguire (1967) and Cummings et al (1968) protons drift closer to the earth than electrons, even though in the tail they have the same energy. Moreover in the process, energy of protons is increased through betatron acceleration. Therefore the currents produced by the protons which drift towards dusk are stronger than those produced by electrons (Kavanagh et al, 1968), and one can expect a minimum value of H in the late evening, as is observed.

The experimentally observed shift of T_{\min} of H , from dawn hours during quiet days, to dusk hours during

disturbed days (Sarabhai and Nair 1969 b) as shown in section 4.1 is a feature of great interest. It can be understood as follows:

The drift paths of charged particles, in the equatorial plane of the earth's dipole field with convective electric field and corotational electric field superimposed have been computed by Kavanagh et al (1968), Chen (1970) and Wolf (1970).

The drift velocity of charged particles, \vec{V}_d would be the same as a pure $\vec{E} \times \vec{B}$ drift in an equivalent electric field, E_{eq} where

$$\vec{E}_{eq} = -\nabla\phi \quad \dots(5.01)$$

$$\phi = -\frac{1}{c} \Omega M_E \frac{1}{R} - E_0 R \sin\varphi + \frac{\mu M_E}{3qR} \quad \dots(5.02)$$

In equation 5.02 the first term ($\frac{1}{c} \Omega M_E \frac{1}{R} = \frac{K}{R}$) represents the potential due to corotation of the plasma with the geomagnetic field, the second term ($E_0 R \sin\varphi$) is the potential due to convective electric field and the third term $\frac{\mu M_E}{3qR}$ is the potential due to geomagnetic field gradient. M_E and Ω are the magnetic moment and angular velocity of the earth, R is the radial distance, φ is the azimuthal angle measured counter-clockwise from the solar direction, μ and q are the magnetic moment and charge of the particle

$$\vec{V}_d = c \frac{\vec{B} \times \nabla\phi}{B^2} \quad \dots(5.03)$$

$$= \left(R - \frac{R^3}{K} E_0 \sin\varphi - \frac{3\mu M_E}{qKR} \right) \hat{e}_\varphi + \left(\frac{R^3}{K} E_0 \cos\varphi \right) \hat{e}_r \quad \dots(5.04)$$

The first term on the right hand side of equation 5.04 represents the azimuthal component, $\vec{V}_d(\varphi)$ and the second term represents the radial component $\vec{V}_d(r)$ of \vec{V}_d . At 00.00 hours local time, $\varphi = 180^\circ$ and therefore

$$V_d(\varphi) = \Omega \left[R - \frac{3 \mu M_E}{q K R} \right] \quad \dots (5.05)$$

For electrons q is -ve, but for protons it is +ve. Thus the azimuthal drift for electrons is eastward irrespective of their energy, while for protons the azimuthal drift is eastward when

$$\mu < \frac{|q| K R^2}{3 M_E}$$

and westward when

$$\mu > \frac{|q| K R^2}{3 M_E}$$

At a radial distance R from the centre of the earth, protons would have a critical energy E_{pc} above which the charge and energy dependent magnetic gradient drift predominates over the charge and energy independent electric field drift.

$$E_{(pc)} = \frac{\mu}{(pc)} \cdot B(R) = \frac{|q| R^2 B(R)}{3c} \quad \dots (5.06)$$

where $B(R)$ is the magnetic field strength at R . Figure 5.02 shows the variation of E_{pc} with R .

The westward ring currents due to the drifts of protons and electrons in such a situation have different characteristics depending on the value of E_{pc} . Moreover, Kavanagh et al(1968)

THE VARIATION OF $E_{(pc)}$ WITH R AT 00.00
HOURS LOCAL TIME AT THE EQUATOR

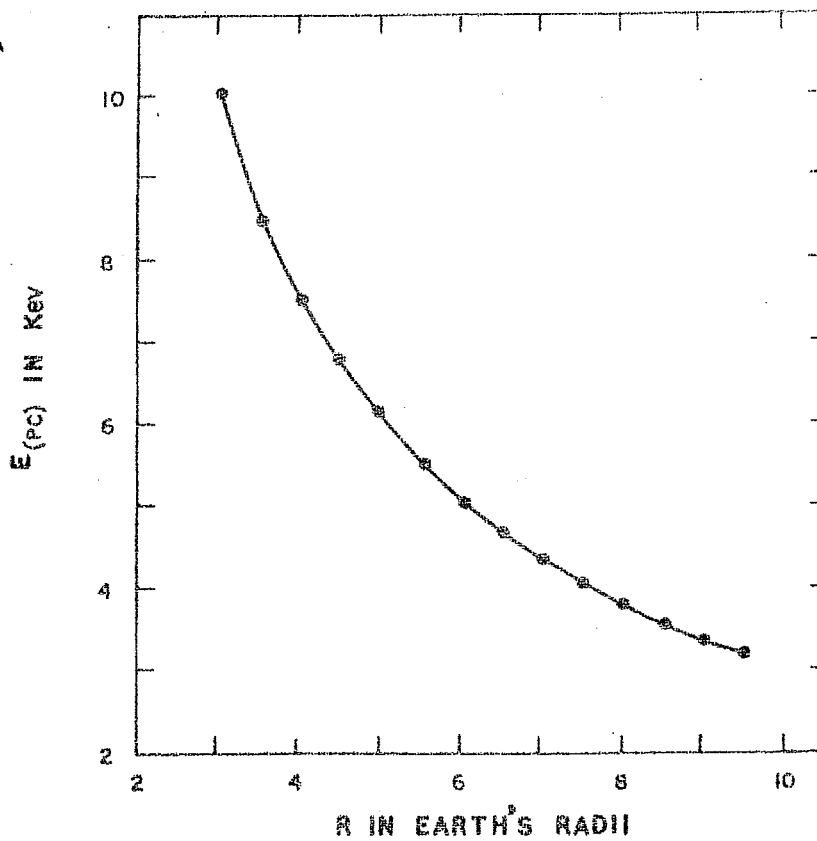


Fig. 5.02 The variation of the critical energy of protons with the radial distance at 00.00 hrs. local time at the equator.

have shown that the forbidden region for the drift of protons is nearest to the earth at 1800 hours, while for electrons it is nearest at 0600 hours local time.

During geomagnetically quiet days, the energy of protons injected from the tail of the magnetosphere must be less than E_{pc} and in consequence protons as well as electrons drift east-ward. The azimuthal component of the drift speed for electrons is more than that for protons, as a result of which relative motion of electrons with respect to protons is set up constituting a westward ring current, which is nearer to the earth on the morning side. The magnetic effect at the ground due to this asymmetric ring current is a decrease of the field during morning hours.

During geomagnetically disturbed days, the energy of protons injected from the tail of the magnetosphere must be more than E_{pc} . Electrons drift eastward and protons drift westward constituting a strong westward ring current which is nearer to the earth on the dusk side. This is so because for protons and electrons of the same energy in the tail, protons can drift closer to the earth than electrons (Kavanagh et al, 1968). The geomagnetic field depression at the ground due to this asymmetric ring current is more on the dusk side compared to the dawn side.

5.2 Solar wind effects on ΔH and K_p

5.21 ΔH_A and the deformation of the magnetosphere

In section 4.7 it is shown that during IMP-1 period

there exist a statistically significant relationship between $(\Delta H_A)^2$ and the observed kinetic energy density of the solar wind. This can be understood as follows.

Apart from an effect due to currents at the magnetopause contributing ΔH_{CF} of 4 γ during quiet days as computed by Mead (1964), Nakada and Mead (1965) have pointed out the effect of an enhancement of solar wind pressure at the magnetopause in augmenting symmetric as well as asymmetric ring currents. In consequence there should be a depression of H as well as an enhancement of ΔH through the lowering of H_{min} . Computations due to Roederer (1968) reveal that particles mirroring in low latitudes on the night side pseudo-trapping region (particles mirroring less than 180° longitudinal drift for the guiding centre) are seen to abandon the magnetosphere before reaching the noon meridian. The westward current which exists only for the night side decreases the horizontal field during night time for low latitude stations. For days with high K_p E. density the pseudo-trapping region is pronounced and with the removal of the field on the night side large values of ΔH are observed.

According to Roederer and Schulz (1969) the azimuthal asymmetry of the earth's magnetosphere enables pitch-angle scattering to violate the third adiabatic invariant of trapped particles, thereby causing radial diffusion. The radial diffusion coefficient

$$D_L \sim R_s^{-8}, L^{10} \cdot \left(\frac{K_p}{J} \right) \dots (5.07)$$

where R_s is the stand-off distance to the magnetopause given by equation (3.04)

$$\mu_o = \cos \alpha_o \quad \dots (5.08)$$

where α_o is the equatorial pitch angle at the night meridian and \mathcal{T} is the life time of the particle against pitch angle scattering.

From equation (3.04) and (5.07) it can be seen that

$$D_L \sim \left[\frac{4\pi n m v^2}{B_o^2} \right]^{4/3} L_{10} \cdot \left(\frac{\mu_o}{\mathcal{T}} \right) \quad \dots (5.09)$$

Thus

$$D_L \propto (\text{K.E. Density})^{4/3} \quad \dots (5.10)$$

The enhancement of the K.E. density of the solar wind thus enriches the inner shells of the magnetosphere and thereby promotes partial, eccentric and symmetric ring currents. In consequence there should be a depression of H as well as an enhancement of ΔH through lowering of H_{\min} .

5.22 Interplanetary magnetic field fluctuations and ΔH_A

From the study of the observed interplanetary magnetic field parameters from satellites IMP-1, IMP-3 and Explorer-33, it is shown in section 4.7 that $\overline{B_z}$, the fluctuation of the north-south component of the interplanetary magnetic field is linearly correlated with ΔH_A . The relationship between the two remains relatively unaltered during the solar cycle from 1963-64 (IMP-1)

through 1965 (IMP-3) to 1967-68 (Explorer-33). A probable mechanism for this relationship can be visualized as follows.

Falthammar (1968) has examined the consequences of the variations of the electric and magnetic fields in the magnetosphere, resulting in diffusion and acceleration of charged particles into the magnetosphere, by the violation of the flux invariant. The diffusion coefficient D_E for the particles, due to east-west electric field fluctuations is given by

$$D_E (W, L, \theta_m) = \frac{L^6}{2B_p^2} \sum (P_n (L, n\omega)) \dots (5.11)$$

where $P_n (L, n\omega)$ is the power spectrum of the time variation of the n^{th} spatial Fourier coefficient of the electric potential field in the equatorial plane. W is the energy of the particle, θ_m is the co-latitude of the mirror point, L is the McIlwain's parameter and B_p is the polar field strength of the earth's magnetic field. The term P_n is a function of $\overline{E_{ym}}$, the fluctuation of the east-west component of the electric field in the outer magnetosphere. From the field line reconnection process it is possible to understand that $\overline{E_{ym}}$ is related with $\overline{B_z}$, the fluctuations in the north-south component of the interplanetary magnetic field (Obayashi and Nishida, 1968). Thus the term P_n is a function of $\overline{B_z}$. So when $\overline{B_z}$ is high, P_n is high and in consequence D_E is more. This suggests that the radial transport of particle by the violation of flux invariant is more when $\overline{B_z}$ is high. Thus the time dependent azimuthal electric field plays a very important part, along with the azimuthal asymmetry of the outer magnetosphere in populating inner shells of the

magnetosphere, which in consequence, as explained in section 5.1 enhances the eccentric ring, partial ring and tail currents which in turn enhance ΔH .

5.23 The relationship of \vec{V}_s and \vec{B}_z with $\sum K_p$

The relationship of \vec{V}_s and \vec{B}_z with $\sum K_p$ as shown in section 4.7 can be explained in the light of the interaction of the solar wind with the magnetosphere. In Dungey's unshielded magnetospheric model, it is assumed that the interplanetary magnetic field has a south-west component. In the presence of the interplanetary magnetic field the solar wind is associated with an electric field.

$$\vec{E} = -\frac{1}{c} (\vec{V} \times \vec{B}) \quad \dots (5.12)$$

when observed in a frame fixed to the magnetosphere. This electric field is 'thought to enter the magnetosphere' (Obayashi and Nishida, 1968). The fluctuation of the east-west electric field in the magnetosphere, \vec{E}_{ym} would be high when \vec{V}_s or \vec{B}_z or both are high. \vec{E}_{ym} promotes convection of plasma from the tail of the magnetosphere. Through the above process the auroral electrojet strength gets enhanced, which should result in the enhancement of $\sum K_p$. This is so because K_p is based on magnetic records from 12 selected observatories lying between 47.7° and 62.5° geomagnetic latitudes.

5.3. Recent studies on ΔH

Until recently the daily variation of the geomagnetic field was believed to be primarily related to current systems in the ionospheric E-region, particularly in the absence of geomagnetic disturbances. However, in terms of the dynamo theory a number of anomalies were seen to occur and much evidence has been accumulating recently to indicate that the classical representation of dynamo currents on a thin spherical shell is inadequate to explain the observed variations, even during geomagnetically quiet days (Price, 1968 and Matsushita, 1969).

With a growing understanding of the solar wind interaction with the magnetosphere, it became clear that a small contribution to ΔH even on quiet days could arise from currents at the magnetopause. This as well as the dynamo effect should produce an increase of H near noon, compared to night. On the otherhand evidence reported here has been presented by Sarabhai and Nair which indicates that the dominant effect at low latitude stations outside the influence of the equatorial electrojet has the character of a decrease of the field at night time. Since the E-region current system is very weak during night time, an ionospheric contribution to ΔH in the form of reduction of the field during night time is not significant and one must look to current systems in the magnetosphere to understand the observations. Their study has stimulated further investigations (Sarabhai and Nair, 1969d and 1971; Bhargava and Yacob, 1970; Matsushita, 1970; Olson, 1970; Nair et al, 1970; Hutton, 1970 and Kane 1970).

Bhargava and Yacob (1970) using data from Alibag for a period of 37 years have computed the variation in \bar{H} , the mean daily horizontal intensity (after removing secular variation in H , applying a high-pass digital filter) and ΔH , the daily range of H . They have shown that for very quiet days ($A_p \sim C$) to moderately disturbed days, \bar{H} decreases linearly, while ΔH increases as A_p increases. They have pointed out that "this is inconsistent with the dynamo theory and that a depression of the field during night time is necessary to account for the above, as suggested by Sarabhai and Nair (1969)". Bhargava and Yacob (1971) have further shown that ΔH is composed "primarily of a northward directed field of the dynamo currents in the day time and southward directed field in the evening or night sector". The southward field occurs between 1900 to 2100 hours local time and accounts for an appreciable part of ΔH . The magnitude of the southward field increases with increase in A_p .

Matsushita (1970) has reported that "at low latitude stations such as Guam, the H component at night decreases 10 to 20 gammas as A_p increases from 1 to 10, although the H component around noon remains almost the same or shows a very slight decrease (less than five gammas)". He has argued that "since the electrical conductivity of the dynamo region during night on quiet days is extremely small, westward ring current (instead of ionospheric currents) in the night side of the magnetosphere even on quiet days need to be assumed to explain this night time decrease".

The results from synchronous ATS-1 satellite (Coleman and Cummings, 1967; Cummings et al, 1968, 1971 and

Coleman, 1970) show that on the night side even at an altitude of 6.6 earth's radii at the equator on geomagnetically quiet days, the magnetic field in the anti-solar direction is less than the field in the subsolar direction by about 35 to 45 gammas. Sugiura et al (1969) using data from OGO satellites 1, 2 and 3 have computed contours of ΔB , the constant deviation of the measured field magnitude from the reference field. It can be seen that even during geomagnetically quiet days, at an altitude of 6 Earth's radii in the equatorial plane, there is a field depression of about 30% on night side compared to day side. A variation of this type cannot be due to ionospheric currents.

A semi-empirical description of the geomagnetic field intensity at the equator, reasonably good in the region of $1.5 < r < 7R_e$ is given by Roederer (1970) as

$$B = \frac{K_0}{r^3} + K_1 - K_2 r \cos \varphi \quad \dots (5.13)$$

here φ is the longitude east of midnight and $K_0 = 31100$ gammas. The values of K_1 and K_2 based on ATS-1 magnetometer surveys, are $K_1 = 12 \left(\frac{10}{R_b} \right)^3$ gammas and $K_2 = 2.77 \left(\frac{10}{R_b} \right)^4$ gammas R_e^{-1} . R_e is the earth's radius and R_b is the stand off distance of the magnetosphere in units of R_e .

According to relation 5.13, even during quiet period (i.e. for a stand off distance of $10 R_e$) currents outside $6.6 R_e$ could produce $(B_{\text{day}} - B_{\text{night}}) = 8.3\gamma$ in the form of night decrease at $1.5 R_e$. This effect should be more pronounced when there is enhancement in the kinetic energy density of the solar wind. Thus equation 5.13 can explain part of the daily variation in H.

Recently Olson (1970) has reported that the calculations done with models of the magnetopause, asymmetric ring, and neutral sheet current systems show that they all produce variations in the earth's surface magnetic field similar to the observed Sq. pattern and that, after giving allowance for the induced earth currents, the combined fields of these three non-ionospheric current systems account for more than 10% to the Sq. variation. He has concluded that "because of the large observed fluctuations in solar wind parameters (which determine the strength of these currents), it is suggested that magnetospheric currents may make a significant contribution on the day-to-day variability in Sq. " Olson has ignored the effect of the partial ring current, the existence of which is now well accepted.

Hutton (1970) has reported from the analysis of geomagnetic field data from M'Bour that " when the hourly H values are corrected for D_{st} , it is found that, for all days, there is a significant positive correlation between ΔH and H_{max} and a significant negative correlation between ΔH and H_{min} . Table 5.01 shows the correlations between ΔH and H_{max} and between ΔH and H_{min} for the years 1959 to 1961 for M'Bour reported by Hutton (1970).

TABLE 5.01

Correlation between ΔH and H_{\max} and between ΔH and H_{\min} for
M'Bour (Hutton, 1970)

Year	Data	Number of days	Correlation between ΔH and H_{\max}	Correlation between ΔH and H_{\min}
1959	All days	365	0.15 ± 0.05	-0.76 ± 0.02
	Quiet days	59	0.71 ± 0.07	-0.18 ± 0.13
1960	All days	366	0.09 ± 0.05	-0.80 ± 0.02
	Quiet days	60	0.68 ± 0.07	-0.13 ± 0.13
1961	All days	363	0.29 ± 0.05	-0.76 ± 0.02
	Quiet days	57	0.67 ± 0.07	-0.36 ± 0.12

It has been suggested by Hutton (1970) that "in general, it is clear both from the comparison of quiet and disturbed days and from the solar cycle dependence that H_{\min} is very sensitive to the degree of magnetic disturbances. Also, the contribution of changes in H_{\min} and H_{\max} to changes in ΔH is approximately 2:1".

From the analysis of quiet day daily variation of H on 213 days ($A_p = 0$ to 8) at Alibag for the year 1964, Kane (1970) has suggested that "it is caused mainly by day time increases (in mid and low latitudes) and not by night time depletions as proposed by Sarabhai and Fair (1969). It does not follow, however,

that the source of these variations is necessarily the ionospheric current system. Large day to day fluctuations in ΔH even during quiet periods are still a mystery. As pointed out by Piddington (1968), K_p or A_p are not adequate indices of the measure of disturbance, particularly at low values and it is suspected that solar wind interaction with geomagnetic field is not fully reflected in these indices. Results of Cummings et al (1968) indicate that even at 6.6 earth radii, ΔH can be about 25-30 gammas, indicating possible magnetospheric contributions to ΔH observed at ground. Such effects need further quantitative studies".

The contention of Kane (1970) to have a magnetospheric contribution to ΔH in the form of a day enhancement cannot be easily understood. This is so because as pointed out by Roederer (1970), the net contribution to ΔH from magnetopause currents, tail currents and partial and eccentric ring currents outside 6.6 R_e is in the form of a decrease during night time rather than an enhancement during day time. Moreover, it is difficult to understand how a ~~westward~~ asymmetric ring current can give rise to a day time enhancement in H for low latitudes. The reason for this is that the geomagnetic field gradient increases towards the earth and consequently protons drift westward and electrons eastward constituting a westward ring current.

Kane's result is analogous to the positive correlation between ΔH and H_{max} during geomagnetically quiet days as reported by Hutton. The results of Hutton considering all the days in a year, are similar to those reported by Sarabhai and Nair, and show that there is only a quantitative rather than a

qualitative change of phenomena with increasing degree of geomagnetic disturbance.

In summary the results of Bhargava and Yacob, Matsushita, Olson, Hutton and of Kane are consistent with the picture presented in section 5.1, wherein it has been suggested that ΔH , the daily variation of the horizontal component at a low latitude station outside the influence of the equatorial electrojet is caused by (1) the dynamo current, mainly at the ionospheric E-region, (2) the surface currents at the magnetopause and (3) the tail currents, the eccentric ring current and the partial ring current in the magnetosphere. It is suggested that all the processes are generally operative on each day, though their relative importance varies depending on solar, terrestrial and interplanetary conditions in the neighbourhood of the earth.

The capability which now exists, of simultaneously measuring the daily variation of H at ground stations in low latitudes away from the effect of the equatorial electrojet and at synchronous altitude with geostationary satellites, should make it possible in the years to come to estimate with refinement the relative contributions of the different mechanisms under varying conditions.

5.4 Summary of the results and the conclusions

5.41 Cosmic-ray studies with directional meson telescopes at Trivandrum

(a) Computation of the variational coefficients for deriving the effect related to the primary component of cosmic rays,

from the observed variations of the secondary intensity has been made by the author. The calculated difference in the time of maximum between west and east telescopes ($\phi_{IW} - \phi_{IE}$) is between 4.3 to 6.3 hours for values of β between -1.2 to +1.0, where β is the exponent in the relation, representing the energy spectrum of variation of the anisotropy of galactic cosmic rays.

(b) Patel et al (1968) and Patel (1970) have reported the direction and amplitude in space, of the diurnal and semi-diurnal anisotropy and the value of β on a day-to-day basis. Using their values the author has evaluated the amplitude and phase of the diurnal and semi-diurnal components due to primary anisotropy at the respective instruments (along east, vertical and west directions) at Trivandrum, on a day-to-day basis for the period 1964 to 1966. Comparison of the computed daily variation of the cosmic ray μ meson intensity with the observed pressure corrected daily variation shows a residual effect. It is observed that the diurnal time of maximum of the residual effect along east, vertical and west directions remains practically constant within statistical errors and is around 0500 hours local time, which is in agreement with the observations of Quenby and Thambyapillai (1960), Mori et al (1966) and Bercovitch (1968). However, the diurnal amplitude of the residual effect along west shows larger value compared to vertical and east ($\gamma_{IE} < \gamma_{IV} < \gamma_{IW}$) suggesting that the effect is energy dependent. This residual effect can be attributed to temperature variations in the upper atmosphere. Comparison of this residual effect with the temperature effect derived by Dorman's method suggests the possibility of a local source of non-meteorological origin.

5.42 Geomagnetic plasma probe for solar wind

- (a) The time of maximum of the daily variation of H for a low latitude station, outside the effects of the equatorial electrojet such as Alibag, is relatively unaffected by the degree of geomagnetic disturbance and is around 1100 hours local time. The time of minimum of H occurs at 0500 hours significantly more often on geomagnetically quiet days than on all other groups of days. The shift of the time of minimum of H , from dawn hours during quiet days to dusk hours during disturbed days, is explained in section 5.1, as a consequence of the drift-motion of charged particles injected from the tail of the distorted magnetosphere in the presence of corotational electric field and geomagnetic field gradients.
- (b) For low latitude stations such as Alibag, Honolulu and Guam, which are away from the effects of the equatorial electrojet ΔH , the daily range of H is negatively correlated with H_{\min} , the minimum value of H during the day with a fairly good correlation and there is no significant qualitative difference in the relationship between the two with increasing degree of geomagnetic disturbance. On the other hand the correlation between ΔH and H_{\max} , the maximum value of H during the day, is positive but not highly significant. These observations suggest, that ΔH is largely due to a decrease of the ambient field on the night side along with a small enhancement during day time.
- (c) . It is shown, that on a day-to-day basis, ΔH_A is more or less independent of the purely ionospheric contribution

namely ($\Delta H_T - \Delta H_A$). Moreover the mean drift speeds of the ionospheric irregularities in the E and F regions at Thumba, very near to Trivandrum, during the mid-day hours (1100-1300 hours) measured by the spaced aerial technique correlates well with ($\Delta H_T - \Delta H_A$). While at Trivandrum the ionospheric contribution is similar in magnitude to the magnetospheric contribution on a normal day, at Alibag the ionospheric contribution is only about a third of ΔH_A . A well pronounced equinoxial maximum in equatorial electrojet strength is seen in the seasonal variation of ($\Delta H_T - \Delta H_A$). A probable mechanism for the enhancement of the equatorial electrojet strength during equinoxes is discussed. The study of the variability of H at different hours related to day-to-day changes of the daily variation of H, confirms the view that there are two independent processes contributing to ΔH_A even during quiet days and that the variance, due to both the factors, is larger during years of high solar activity than when the sun is quiet.

(d) It is shown that during IMP-1 period there exist a statistically significant and physically meaningful relationship between $(\Delta H_A)^2$ and the observed kinetic energy density of the solar wind. This is attributed to asymmetric ring currents in the magnetosphere due to deformation of the magnetosphere by the solar wind.

(e) From the study of the observed interplanetary magnetic field parameters from satellites IMP-1, IMP-3 and Explorer-33, it is shown that $\overline{CB_z}$, the fluctuation of the north-south component of the interplanetary magnetic field is linearly correlated with ΔH_A . The relationship between the two remains

relatively unaltered during the solar cycle from 1963-64 (IMF-1) through 1965 (IMP-3) to 1967-68 (Explorer-33). It is suggested that time dependent azimuthal electric fields in the magnetosphere along with the azimuthal asymmetry of the outer magnetosphere play an important part in enhancing ΔH , through lowering of H during night time.

(f) It is suggested that ΔH , the daily variation of the horizontal component at a low latitude station outside the influence of the equatorial electrojet is caused by (1) the dynamo current, mainly at the ionospheric E-region, (2) the surface currents at the magnetopause and (3) the tail currents, the eccentric ring current and the partial ring current in the magnetosphere.

Studies reported in this thesis reveal that ΔH , provides an index for probing the electromagnetic state of the interplanetary space in the neighbourhood of the earth.

REFERENCES

- | | | |
|--|------|---|
| Ables, J.G.,
K.G. McCracken
and U.R. Rao | 1968 | Proc. 9th Int. Conf. London, 1,
208 |
| Ahluwalia, H. S.
and A. J. Dessler | 1962 | Planet. Space Sci., 9, 195 |
| Akasofu, S. I.
and S. Chapman | 1963 | J. Geophys. Res., 68, 3155 |
| Alfven, H. | 1939 | Kgl. Sv. Vet. Akad. Handl.,
Ser. 3, 18, No. 3. |
| Alfven, H. | 1950 | Cosmic Electro-dynamics
Oxford Press, London |
| Alfven, H. | 1954 | Tellus, 6, 232 |
| Alfven, H. | 1958 | Tellus, 11, 106 |
| Alfven, H. | 1963 | Space Science Rev., 2, 862 |
| Alfven, H. | 1964 | Space Sci., Rev., 2, 867 |
| Alfven, H. | 1967 | Space Sci. Rev., 7, 1440 |
| Alfven, H. | 1968 | Ann. de Geophys., 24, 1 |
| Alfven, H.
and Falthammar | 1971 | To be published in Cosmic
Electrodynamics |
| Axford, W. I. | 1968 | Space Science Rev., 8, 331 |
| Anderson, K. A. | 1965 | J. Geophys. Res., 70, 4741 |
| Anderson, K. A.
and N. F. Ness | 1966 | J. Geophys. Res., 71, 3705 |
| Angerami, J. J.
and D. L. Carpenter | 1966 | J. Geophys. Res., 71, 711 |

- | | | |
|---|---------|---|
| Antonova, A. E.
and V. P. Shabansky | 1968 | Geomagnetism i Aeronomiya,
8, 801. |
| Axford, W. I. | 1962 | J. Geophys. Res., 67, 3721. |
| Axford, W. I. | 1965(a) | Planet Space Sci., 13, 115. |
| Axford, W. I. | 1965(b) | Space Res., 5, 612 |
| Axford, W. I., | 1968 | Physics of Geomagnetic Phenomena,
Academic Press, New York, 1243 |
| Axford, W. I. and
C. O. Hines | 1961 | Canad. J. Phys. 39, 1433 |
| Axford, W. I.,
H. E. Petschek
and G. L. Siscoe | 1965 | J. Geophys. Res., 70, 1231 |
| Ballif, J. R.,
D. E. Jones,
P. J. Coleman Jr.
L. Davis, Jr. and
E. J. Smith | 1967 | J. Geophys. Res., 72, 435 |
| Ballif, J. R.,
D. E. Jones and
P. J. Coleman, Jr | 1969 | J. Geophys. Res., 74, 2289 |
| Beard, D. B. | 1960 | J. Geophys. Res., 65, 3559. |
| Beard, D B | 1964 | Rev. Geophysics, 2, 335 |
| Beard, D. B. and
E. B. Jenkins | 1962 | J. Geophys. Res., 67, 3361. |
| Beyers, N. J.,
B. T. Miers and
R. J. Reed | 1966 | J. At. Sciences, 23, 325 |
| Beisser, A. | 1958 | J. Geophys. Res., 63, 1 |
| Behannon, K. W.,
and N. F. Ness | 1966 | J. Geophys. Res., 71, 2327 |

- | | | |
|---|----------------|---|
| Bercovitch, M. | 1963 | J. Geophys. Res., 68, 4366 |
| Bercovitch, M. | 1966
(1965) | Proc. 9th Int. Cosmic Rays,
London, 1, 495. |
| Bercovitch, M. | 1968 | Proc. 10th Int. Conf. Cosmic
Rays(Calgary), Part A, 269. |
| Bhargava, B.N.
and A. Yacob | 1969 | J. Geomag. and Geoelect., 21,
1, 385 |
| Bhargava, B N.
and A. Yacob | 1970 | (under publication) |
| Biermann, L. | 1951 | Z. Astrophys, 29, 274. |
| Biermann, L. | 1952 | Z. Naturf., 7a, 127 |
| Birmingham, T.J. | 1969 | J. Geophys. Res., 74, 2169 |
| Block, L.P. | 1967 | Space Sci. Rev., 7, 198 |
| Bonetti, A.,
H.S. Bridge ,
A.J. Lazarus;
B. Rossi and
F. Scherb | 1963 | J. Geophys. Res, 68, 4017 |
| Brice, N. | 1967 | J. Geophys. Res. 72, 5193 |
| Bridge, H.S.,
A.J. Lazarus,
E.F. Lyon,
B. Rossi and
F. Scherb | 1962 | Space Research, Pro. Intern.
Space Sci. Symp. 3rd,
Washington, 1962, North-
Holland, Publishing Company,
Amsterdam. |
| Burger, J.J. | 1971 | To be published in Astrophys. J. |
| Burnberg, E.A.
and Dattner | 1953 | Tellus, 5, 135 |
| Carpenter, D.L. | 1963 | J. Geophys. Res., 68, 1675 |
| Carpenter, D.L. | 1966 | J. Geophys. Res., 71, 693 |

- | | | |
|---|---------|---|
| Carpenter, D. L. | 1970 | J. Geophys. Res., 75, 3837 |
| Chandra H. and
R. G. Rastogi | 1969 | J. Atmosph. Terres. Phys.
31, 1205 |
| Chapman, S. | 1917 | Terrest. Magn. Atmosph. Elec.,
22, 121. |
| Chapman, S. | 1919 | Phil. Trans. Roy. Soc. A 218, 1. |
| Chapman, S. | 1940 | Terr. Mag. Atmos. Elec., 46, 245 |
| Chapman, S and
J. Bartels | 1940 | Geomagnetism Oxford Univ. Press,
London |
| Chapman, S
and V. C. A. Ferraro | 1930 | Nature, 126, 129 |
| Chapman, S. and
V. C. A. Ferraro | 1931 | Terr. Mag. Atmos. Elec., 36, 77 |
| Chapman, S., and
V. C. A. Ferraro | 1932 | Terr. Mag. Atmos. Elec., 37, 147 |
| Chapman, S and
V. C. A. Ferraro | 1933 | Terr. Mag. Atmos. Elec., 38, 79 |
| Chen, A. J. | 1970 | J. Geophys. Res., 75, 2458 |
| Coleman, P. J., Jr. | 1966 | J. Geophys. Res., 71, 5509 |
| Coleman, P. J., Jr. | 1970 | Intercorrelated satellite
observations to solar events,
Page 251, ed. by V. Manno and
D. E. P ge D. Reidel Publishing
Company, Holland. |
| Coleman, P. J.
and W. D. Cummings | 1967 | Conjugate point symposium IV-15-1 |
| Coleman, P. J., Jr
L. Davis, Jr. and
C. P. Sonett | 1960(a) | Physical Rev. Lett., 5, 43 |

- | | | |
|---|---------|-------------------------------------|
| Coleman, P. J., Jr.
C. P. Sonett, D. L.
Judge, and E. J.
Smith | 1960(b) | J. Geophys. Res., 65, 1856 |
| Coleman, P. J., Jr.
C. P. Sonett, and
L. Davis | 1961 | J. Geophys. Res., 66, 2043 |
| Compton, A. H.
and I. A. Getting | 1935 | Phys. Rev., 47, 817 |
| Cummings, W. D. | 1966 | J. Geophys. Res., 71, 4495. |
| Cummings, W. D.
J. N. Barfield and
P. J. Coleman, Jr. | 1968 | J. Geophys. Res. 73, 6687 |
| Cummings, W. D.,
P. J. Coleman, Jr.
and G. L. Siscoe | 1971 | J. Geophys. Res., 76, 926 |
| Daniel, R. R.
and S. A. Stephens | 1966 | Proc. Ind. Aca. Sci. A., 63,
276 |
| Dattner, A., and
Venkatesan, D. | 1958 | Tellus, 11, 239 |
| Davis, L., Jr. | 1947 | Phys. Rev., 72, 632 |
| Davis, L. Jr. | 1948 | Phys. Rev., 73, 536. |
| Davis, L. | 1955 | Phys. Rev., 100, 1440 |
| Dessler, A. J. | 1967 | Rev. Geophys., 5, 1 |
| Dessler, A. J.
and E. N. Parker | 1959 | J. Geophys. Res., 64, 2239 |
| Dessler, A. J.
and J. A. Fejer | 1963 | Planet. Space Sci., 11, 505. |
| Dhanju M. S.
and V. A. Sarabhai | 1967 | Phys. Rev. Letters, 19, 252 |

- | | | |
|---|------|--|
| Dorman, L.I. | 1957 | Cosmic ray variations, Moscow State Publishing House, |
| Dorman, L.I. | 1963 | Progress in Ele. Par. and Cosmic Ray Phys., Vol.7 (New York), John Wiley & Sons). |
| Dorman, L.I. | 1969 | Proceedings of the 11th International Conference on Cosmic rays Budapest, 381. |
| Dorman, L.I. and E. L. Feinberg | 1958 | Suppl. Nuovo Cim., 8, 258 |
| Duggal, S.P. and M.A. Pomerantz | 1962 | Phys. Rev. Letter, 8, 215 |
| Duggal S.P. S. E. Forbush and M. P. Pomerantz | 1967 | Nature, 214, 154 |
| Dungey, J.W. | 1961 | Phy. Rev. Letters, 6, 47 |
| Dungey, J.W. | 1963 | Geophys: The earth's environment, edited by De Witt, Heiblot and Lebean gorden and Breack, Science Publishers, New York, 526 |
| Dungey, J.W. | 1965 | Space Sci. Rev., 4, 199 |
| Dungey, J.W. | 1967 | Solar Terr. Phys , Academic Press, London, 91 |
| Ehmert, A. | 1960 | Proc. Moscow Cosmic Ray Conf. 4, 142 |
| Elmore, C.W. and M. Sands | 1949 | Electronics, McGraw Hill Book Company, New York. |
| Elliot, H. and P. Rothwell | 1956 | Phil. Mag., 1, 699 |
| Fairfield, D.H. | 1968 | J. Geophys. Res., 73, 5511 |
| Fairfield, D.H. | 1970 | Int. Sym. Sol. Terr. Phys. Leningrad, 1970 |

- | | | |
|---|------|--|
| Fairfield, D.H.
and L.J. Cahill, Jr. | 1966 | J. Geophys. Res., 71, 155 |
| Faller, A.M.
and P.L. Marsden | 1966 | Proc. 9th Int. Conf. Cosmic
Rays, London, 1, 231 |
| Falthammar, C.G. | 1965 | J. Geophys. Res., 70, 2503 |
| Falthammar, C.G. | 1966 | J. Geophys. Res., 71, 1487 |
| Falthammar, C.G. | 1968 | Earth's particles and Fields,
ed. B.M. McCormac Reinhold
Book Corp., 157 |
| Falthammar, C.G. | 1970 | Int. Symp. on Solar Terr. Phy.,
Leningrad. |
| Falthammar, C.G.
and M. Walt | 1969 | J. Geophys. Res., 74, 4184 |
| Frank, L.A.,
J.A. Van Allen
and J.D. Craven | 1964 | J. Geophys. Res., 69, 3155 |
| Frank L.A. | 1967 | J. Geophys. Res., 72, 3753 |
| Fejer, J.A. | 1961 | Can. J. Phys., 39, 1409 |
| Fejer, J.A. | 1964 | J. Geophys. Res., 69, 123 |
| Fisk, L.A. | 1970 | NASA Pre-Print X-660-70-180 |
| Freeman, J.W. Jr. | 1968 | J. Geophys., Res. 73, 4151 |
| Freeman, J.W. Jr.
and J.J. Maguire | 1967 | J. Geophys. Res., 72, 5257 |
| Forbush, S.E. | 1967 | J. Geophys., Res., 72, 4937 |
| Forbush, S.E.
D. Venkatesan
and C.E. McIlwain | 1961 | J. Geophys. Res., 66, 2275 |
| Forbush, S.E.
G. Pizzella
and D. Venkatesan | 1962 | J. Geophys. Res., 67, 3651 |
| Greenstadt, E.W. | 1961 | Nature, 191, 329 |

- | | | |
|--|------|---|
| Gringauz, K.I. | 1961 | Space Research, II, 539, North Holland Publ. Co., Amsterdam. |
| Gringauz, K.I. | 1969 | Reviews of Geophysics, 7, 339 |
| Gringauz, K.I.
and M. Khokhlov | 1965 | Space Research, Transactions of All-union conference on Space Physics NASA Tech. Transl. F-389. |
| Gringauz, K.I.
V. G. Kurt,
V. I. Moroz
and I. S. Shklovsky | 1961 | Soviet Astron. A. J., 4, 680 (English Trans) |
| Gringauz, K.I.
V. V. Bezrukikh,
L. S. Musatov,
R. Ye. Rybchinsky,
and E. K. Solomatina | 1966 | Space Res., 6, 850 |
| Gleeson, L. J. | 1969 | Planet. Space Sci., 17, 31 |
| Gleeson, L. J.
and W. I. Axford | 1967 | Astrophys. J., 149, L., 115 |
| Gleeson, L. J.
and W. I. Axford | 1968 | Astrophysics and Space Sci., 2, 431 |
| Gloeckler, G.
and J. R. Jokipii | 1967 | Ap. J., 148, L., 41 |
| Gosling, J. T.
R. T. Hansen
and S. J. Bame | 1971 | J. Geophys. Res., 76, 1811 |
| Harries, M. F.,
F. G. Finger
and S. Teweles | 1962 | J. Atmospheric Sciences, 19, 136 |
| Hasim, A.,
D. S. Peacock
J. J. Quenby and
T. Thambyahpillai | 1969 | Planet. Space Sci., 17, 1749 |

Hashim, A. and T. Thambyahpillai	1969	Planet. Space. Sci., 17, 1879
Heppner, J. P.	1967	Space Science Rev., 7, 166
Herlofson, N.	1960	Phys. Rev. Lett. 5, 411
Hirshberg, J.	1963	J. Geophys. Res., 68, 6201.
Hoffman, R. A. and P. A. Brachen	1967	J. Geophys. Res., 72, 6039
Hones, E. W.	1963	J. Geophys. Res., 68, 1209
Hones, E. W., Jr. and J. E. Bergeson	1965	J. Geophys. Res., 70, 4951
Hundhausen, A. J.	1968	Sp. Science Rev., 8, 690
Hundhausen, A. J.	1970	Rev. Geophys. and Space Physics, 8, 729.
Hutten, R.	1970	Upper Atmospheric Currents and Electric Fields Symposium, Boulder, Colorado.
Jacchia, L. G.	1966	Annales de Geophys., 22, 75
Jacchia, L. G. J. Slowey and F. Verniani	1967	J. Geophys. Res., 72, 1423
Jacklyn, R. M. and J. E. Humble	1965	Australian J. Phys., 18, 451
Janossy, L.	1937	Zeit. Phys., 104, 430
Jensen, D. C. and J. C. Cain	1962	J. Geophys. Res., 67, 3568
Jokipii, J. R.	1966	Astrophys. J. 146, 480
Jokipii, J. R.	1967	Astrophys. J., 150, 675
Jokipii, J. R.	1968	Can. J. Phys., 46, S 950

- | | | |
|---|---------|---|
| Jokipii, J.R. | 1969 | Astrophys. J 156,1107 |
| Jokipii, J.R. | 1971 | Reviews of geophysics and
Space Physics, 9, 27. |
| Jokipii, J.R.
and L. Davis, Jr. | 1969 | Astrophys. J. 156, 1101 |
| Jokipii, J.R.
and E.N. Parker | 1969 | Astrophys. J., 156 ,777 |
| Jory, F.S. | 1956 | Phys. Rev., 103, 1068 |
| Kane R. P. | 1966 | Nuovo Cimento, 48,8 |
| Kane R.P. | 1970 | J Geophys. Res.,75, 4350 |
| Kane R.P. | 1970(a) | Planet. Space Sci., 18,1834 |
| Kane R.P. and
U.R. Rao | 1958 | Proc. Ind. Aca Sci.,A,47,30 |
| Kane R.P. and
U.R. Rao | 1960 | Current Science,11,29,425 |
| Katzman, J
and D. Venkatesan | 1960 | Canad. J. Phys., 38,1011 |
| Kavanagh, L.D.,
J.W. Freeman
and A.J. Chen | 1968 | J. Geophys. Res.,73,5511 |
| Kellogg, P.J | 1959 | Nature, 183, 1295 |
| Kellogg, P.J. | 1962 | J. Geophys. Res., 67, 3805 |
| Korff, S.A. | 1955 | Electron and Nuclear Counters
D. Van Nostrand Co. Inc. |
| Krymskiy, G.F. | 1964 | Geomagn. and Aeronomy,4,763 |
| Krimskiy, G.F | 1966 | Proc. 9th Int. Conf. Cosmic Rays,
London,1,197 |
| Levy, R. H.,
H. E. Petscheck and
G. L. Siscoe | 1964 | A I A A J. 2, 2065 |

- | | | |
|--|---------|---|
| Lin, R.P. | 1968 | J. Geophys. Res., 73, 3066 |
| Lin, R.P. and
K.A. Anderson | 1966 | J. Geophys. Res., 71, 4213 |
| Leitti, B. and
J. J. Quenby | 1968 | Can. J. Phys., 46, S., 942 |
| Lust, R. | 1967 | Solar. Terr. Phys., ed., by
J. W. King and W. S. Newman
Academic Press, London-1 |
| Lust R.,
A. Schluter
and K. Kallerback | 1965 | Nachr. Akad. Wiss Gottingen
Math. Phy K. L., 119, 8 & 128 |
| Malmfors, K.G. | 1945 | Ark. Mat. Astr. Phys., 32A, 473 |
| Marsden, P. L. | 1968 | Electromagnetic radiation in
space J. G. Emming (ed) |
| Methew, T.,
D. Venkatesan
and B. G. Wilson | 1969 | J. Geophys. Res., 74, 1218 |
| Matsushita, S and
W. H. Campbell | 1967 | Physics of geomagnetic
Phenomena, Academic Press,
New York, 1967 |
| Matsushita, S. | 1970 | Quiet time ring current,
Symp. on Qualitative
magnetospheric models,
Colorado. |
| Maer, K. Jr.
and A. J. Dessler | 1964 | J. Geophys. Res. 69, 2846 |
| Mayer, R. and
J. A. Simpson | 1958 | Nuovo Cim. 8(Suppl) 233 |
| Maynard, N. C.
and L. J. Cahill | 1965 | J. Geophys. Res., 70, 5923 |
| McCracken, K. G. | 1962 | J. Geophys. Res., 67, 423 |
| McCracken, K. G. | 1962(a) | J. Geophys. Res., 67, 477 |

- | | | |
|---|------|--|
| McCracken, K. G. and
U. R. Rao | 1966 | Proc. 9th Int. Conf. Cosmic
Rays, London, 1, 213. |
| McCracken, K. G.
U. R. Rao and
M. A. Shea | 1962 | MIT, Laboratory for Nuclear
Science, Tech Rep. 77. |
| McCracken, K. G.,
U. R. Rao,
B. C. Fowler,
M. N. Shea
and D. F. Smart | 1965 | IQSY, Ins. Manual (London),
No. 10 |
| McIlwain, C. E. | 1961 | J. Geophys. Res., 66, 3681 |
| Mead, G. D. | 1964 | J. Geophys. Res., 69, 1181 |
| Mead, G. D. and
D. B. Beard | 1964 | J. Geophys. Res., 69, 1169 |
| Meada, H. | 1953 | J. Geomagn. Geoelect., 5, 94. |
| Mihalov, J. D.
D. S. Collurn
R. G. Currie
and C. P. Sonett | 1968 | J. Geophys. Res., 73, 948 |
| Montgomery, C. G.
and G. D. Montgomery | 1940 | Phys. Rev. 57, 1030 |
| Mori, S., H. Ueno
and K. Nagashima | 1966 | Proc. 9th Int. Conf. Cosmic
Rays, London, 1, 498 |
| Morrison, P. | 1956 | Phys. Rev., 101, 1397 |
| Nagashima, K. | 1951 | J. Geomagn. and Geoelect., 3,
100. |
| Nair, K. N. | 1937 | Proc. Cosmic Rays, Ele. Part,
phys., and Astrophys., Aligarh,
149. |
| Nair K. N. and
V. Sarabhai | 1937 | Proc. Cosmic Rays, Ele. Part,
Phys., and Astrophys., Aligarh,
152. |

- | | | |
|---|------|--|
| Nair K.N.
and V.Sarabhai | 1970 | Int. Symposium on solar-terrestrial Physics., M1-8 |
| Nair, K.N.,
R.G. Rastogi
and V.Sarabhai | 1970 | Nature, 1970, 226, 740 |
| Nakada, M.P.
and G.D.Mead | 1965 | J. Geophys. Res., 70, 4777 |
| Neher, H.V. | 1952 | Progress in Cosmic Rays, Phys. Vol. 1, Int. Sci., Publishers, 245 |
| Ness, N.F. | 1965 | J. Geophys. Res., 70, 2989 |
| Ness, N.F. | 1967 | Solar Terr. Phys., ed by J.W.King and W.S. Newman, Academic Press, London, 89. |
| Ness N.F. | 1969 | Reviews of Geophys., 7, 97 |
| Ness N.F.
C.S. Scearce
and J.B. Seek | 1964 | J. Geophys. Res., 69, 3531 |
| Ness, N.F. and
J. M. Wilcox | 1965 | Science, 148, 1592 |
| Ness, N.F.
and J. M. Wilcox | 1966 | Astrophys. J., 143, 23 |
| Neugebauer, M.
and C.W. Snyder | 1963 | Science, N.Y., 138, 1095 |
| Neugebauer, M.
and C.M. Snyder | 1966 | J. Geophys. Res., 71, 4469 |
| Nishida, A., | 1966 | J. Geophys. Res., 71, 5669 |
| Nishida, A., | 1968 | J. Geophys. Res., 73, 5549 |
| Nishida, A.
and L.J. Cahill, Jr. | 1964 | J. Geophys. Res., 69, 2243 |
| Obayashi, T
and A. Nishida | 1968 | Space Science Review, 8, 3 |

- | | | |
|---|---------|---|
| O'Brien, B. J. | 1967 | Solar Terr Phys. ed. J.W.King
and W.S. Newman, Academic Press,
London 1 |
| O'Gallagher, J. J. | 1967 | Astrophys J. 150, 675 |
| Olson, W. P. | 1969 | J. Geophys. Res., 74, 5642 |
| Olson, W. P. | 1970 | Trans. Am. Geophys. Union, 51,
401 |
| Osborne, D.G. | 1963 | J. Geophys. Res., 68, 2435 |
| Osborne, D.G.
and N. J. Skinner | 1963 | J. Geophys. Res., 68, 2441 |
| Pai, G. L. | 1962 | Ph.D. Thesis, Kerala University. |
| Pai, G. L. and
V. A. Sarabhai | 1964 | Planet. Space Sci., 12, 855 |
| Pai, G. L.
H. S. Bridge,
E. F. Lyon and
A. Egidi | 1967 | Trans. Am. Geophys. Union, 48, 176 |
| Parker, E. N. | 1958 | Astrophys J 128, 664 |
| Parker, E. N. | 1958(a) | Phy. Rev. 110, 1445 |
| Parker, E. N. | 1958(b) | Phys. Fluids, 1, 171 |
| Parker, E. N. | 1960 | Astrophys J., 132, 821 |
| Parker, E. N. | 1963 | Interplanetary Dynamical Processes
(Inter Science Publishers, New York) |
| Parker, E. N. | 1964 | Planet Space Sci., 12, 735 |
| Parker, E. N. | 1965 | Planet. Space Sci., 13, 9. |
| Parker, E. N. | 1965(a) | Space Science Rev., 4, 666 |
| Parker, E. N. | 1966 | Proc. Int. Con Cosmic Rays
(London), 1, 26 |

- | | | |
|--|---------|---|
| Parker, E.N. | 1967 | Planet Space Sci., 15, 1723 |
| Parker, E.N. | 1969 | Space Science Rev., 9, 325 |
| Parker, E.N. | 1969(a) | Reviews of Geophys., 7, 3 |
| Parker, E.N.
and V.C.A. Ferraro | 1969 | Handbuch der Physik 49 (3)
Springer Verlag, Heidelberg |
| Parsons, N.R. | 1957 | Aust. J. Phys., 10, 327, 462 |
| Patel, D.M. | 1970 | Ph.D. Thesis, Gujarat University. |
| Patel, D,
V. Sarabhai
and G. Subramaniam | 1968 | Planet. Space Sci., 16, 1131 |
| Pfitzer, K.A.,
T.W. Lezniak
and J.R. Winckler | 1969 | J. Geophys. Res., 74, 4687 |
| Piddington, J.H. | 1968 | Geophys. J. R. Astr. Soc., 15, 39 |
| Pizzella, G,
C.E. Van Allen
and J.A. Van Allen | 1962 | J. Geophys. Res., 67, 1235 |
| Quenby, J.J. | 1967 | Hand b d. Phys. Vol. 46/2 (Berlins
Springer Verlag) |
| Quenby, J.J.
and W.R. Webber | 1959 | Phil. Mag., 4, 654 |
| Quenby, J.J.
and W.R. Webber | 1962 | (Phil. Mag., 7, 1457 |
| Quenby, J.J. and
T. Thambyahpillai | 1960 | Phil. Mag., 5, 585 |
| Quenby, J.J. and
B. Leitti | 1968 | Planet. Space Sci., 16, 1209 |
| Quenby, J.J.
and G.J. Wenk | 1962 | Phil. Mag., 7, 1457 |
| Rao, U.R. and
Agarwal, S.P. | 1970 | J. Geophys. Res., 75, 2391. |

- | | | |
|--|---------|--|
| Rao, U R.
and V. Sarabhai | 1961 | Proc. Roy Soc., A, 263, 101 |
| Rao, U.R. and
V. Sarabhai | 1964 | Planet. Space Sci., 12, 1055 |
| Rao, U.R.,
McCracken, K.G.
and Venkatesan, D | 1963 | J. Geophys. Res., 68, 345 |
| Roederer, J. G. | 1967 | J. Geophys Res., 72, 931 |
| Roederer, J. G. | 1968(a) | Earth's Particles and Fields,
ed. B.M. McCormac, Reinhold
Book Corp., 143. |
| Roederer, J. G. | 1968(b) | Earth's Particles and Fields,
ed. B.M. McCormac Reinhold,
Book Corp., 193 |
| Roederer, J. G. | 1969 | Reviews of Geophysics., 7, 77 |
| Roederer, J. G | 1970 | Dynamics of geomagnetically trapped
radiation, N Y., Springer -Verlag
(Physics and Chemistry of Space
Vol. 2) |
| Roederer, J. G.,
and M. Schulz | 1969 | J. Geophys. Res., 74, 4117 |
| Rostoker, G., and
C.G. Falthammer | 1967 | J. Geophys. Res., 72, 5853 |
| Sandstrom, A.E.,
E Dyring, and
S. Lindgren | 1962 | J. Physical Soc. of Japan, 17, 471 |
| Sarabhai V. | 1963 | J. Geophys. Res., 68, 1555 |
| Sarabhai V.
and R. P. Kane | 1953 | Phys. Rev, 92, 415 |
| Sarabhai V., and
P. D. Bhavsar | 1958 | Nuovo Cim., 8, 299 |

- | | | |
|--|---------|---|
| Sarabhai, V.
and G. Subramanian | 1966 | Proc. Int. Conf. Cosmic Rays.,
London, 1, 204 |
| Sarabhai V., and
K.N. Nair | 1969(a) | Nature, 223, 603 |
| Sarabhai, V
and K.N. Nair | 1969(b) | Proc. of Indian Academy of
Sciences, Vol. LXIX, 291 |
| Sarabhai, V
and K.N. Nair | 1969(c) | III Int. Symp. on Equatorial
Aeronomy, Vol. II |
| Sarabhai, V
and K.N. Nair | 1969(d) | IAGA Bulletin No. 26 ed. by L.R.
Alldredge Madrid, 304 |
| Sarabhai, V.,
U.D. Desai and
R.P. Kane | 1953 | Proc. Indian Ac. Sci., 37, 287 |
| Sarabhai V.,
U.D. Desai
and D. Venkatesan | 1955 | Pays. Rev., 99, 1490 |
| Sarabhai, V
and K.N. Nair | 1970 | Proc. of the seminar on problems
of the equatorial electrojet,
Ahmedabad, 14. |
| Sarabhai, V
and K.N. Nair | 1971 | To be published in Cosmic Electro-
dynamics. |
| Sarabhai, V.,
and L. V. Kargathra | 1971 | To be published in Proc. of XII
Int. Con Cosmic Rays, Tasmania. |
| Sarabhai, V, G. L. Pai
and M. Wada | 1965 | Nature, 206, 705 |
| Sastry, T.S.G | 1938 | J. Geophys. Res., 73, 1789. |
| Schild, M A. | 1969(a) | J. Geophys. Res., 74, 1275 |
| Schild, M.A. | 1969(b) | J Geophys. Res , 74, 5189 |
| Schild, M.A ,
J.W. Freeman
and A. J. Dessler | 1969 | J. Geophys. Res , 74, 247 |

- | | | |
|---|------|---|
| Schuster, A | 1889 | Phil. Trans. Roy. Soc., London
A, 180, 467, 1889. |
| Schuster, A. | 1908 | Phil. Trans. Roy. Soc., London
A, 208, 163 |
| Shea, M.A.,
D. F. Smart
and McCracken | 1965 | J. Geophys. Res , 70, 4117 |
| Siscoe, G. L.
and W. D. Cummings | 1969 | Planet. Space Sci., 17, 1795 |
| Singer, S. F. | 1957 | Trans. Am Geophys Union,
38, 175 |
| Singer, S. F. | 1958 | Nuovo Cim., 8, Suppl. II, 334 |
| Simpson, J. A.,
W. Fonger
and S. B. Treiman | 1953 | Phys. Rev., 90, 934 |
| Snyder, C.,
M. Neugebauer
and U. R. Rao | 1963 | J. Geophys. Res., 68, 6361. |
| Sonett, C. P. | 1960 | Phys. Rev. Lett., 5, 46 |
| Somogyi, A. | 1969 | Proc. of the 11th Int. Conf. on
Cosmic Rays, Budapest, 357 |
| Spreiter, J. R.
and B. R. Briggs | 1962 | J Geophys. Res., 67, 37 |
| Spreiter, J. R.
and A. Y. Alksne | 1969 | Reviews of Geophysics, 7, 11. |
| Spreiter, J. R.,
and W. P. Jones | 1963 | J. Geophys Res. 68, 3555 |
| Stewart, B. | 1882 | Encyclopaedia, Britanica
9th ed. 16, 159 |
| Stern, D. | 1964 | Planet. Space Sci , 12, 973 |
| Stormer, C. | 1936 | Astrophys. Norveg, 2, No. 1 |
| Subramanian, G.
and V. Sarabhai | 1967 | Astro Physical J 149, 417 |

- | | | |
|---|------|---|
| Subramanian, G. | 1971 | J. Geophys. Res. 76, 1093 |
| Sugiura, M. | 1969 | G.S.F.C. Pre-Print X-612-69-12 |
| Sugiura, M.,
T. L. Skillman,
B. G. Ledley and
J. P. Heppner | 1969 | G.S.F.C. Pre-Print X-612-69-359. |
| Sugiura, M
and J. P. Heppner | 1965 | Space Science, ed. W. N. Hess,
Blackie and Sons Limited, London. |
| Thambyahpillai, T
and E. Elliot | 1953 | Nature, 171, 918 |
| Taylor, H. E. | 1966 | J. Geophys. Res., 71, 5135 |
| Taylor, H. E.
and E. W. Hones, Jr. | 1965 | J. Geophys. Res., 70, 3605 |
| Treiman, S. B. | 1952 | Phys. Rev., 86, 917 |
| Van Allen, J. A. | 1959 | J. Geophys., Res., 64, 1683 |
| Van Allen, J. A. | 1969 | Rev. of Geophys. 7, 233 |
| Van Allen, J. A.
and L. A. Frank | 1959 | Nature, 183, 219 |
| Van Allen, J. A.
and W. C. Lin | 1960 | J. Geophys. Res., 65, 2998 |
| Van Allen, J. A.
and N. F. Ness | 1968 | University of Iowa, Reprint,
68-46 |
| Vasybiunas, V. M. | 1968 | J. Geophys. Res., 73, 2529 |
| Vernov, S. N.
E. V. Gorchakov,
S. N. Kuznetsov,
Yu I. Logachev,
E. N. Sosnovets and
V. G. Stolpovsky | 1969 | Reviews of Geophys. 7, 257 |
| Verzariu, P.,
I. B. Strong and
M. Sugiura | 1969 | Trans. Am. Geophys. Union, 50,
STM-22, 279 |

- | | | |
|--|------|--|
| Wada, M. | 1960 | Inst. Phys. Chem. Res., 54, 335 |
| Wada, M. | 1961 | Sci. Inst. Phys. Chem. Res.,
Tokyo, 55, 7 |
| Wada, M. and
S. Kudo | 1956 | J Sci. Res. Inst. 50, 415 |
| Wada, M. and
S. Kudo | 1968 | Canad J. Phys., 46, 5934 |
| Walt, M. | 1971 | Reviews of Geophys. and Space
Phys., 9, 11. |
| Webb., W.L. | 1966 | Problems of Atoms, Circulation
ed R.V. Garcia and T.F. Malone,
Mac Millan and Co, 127 |
| Webber, W.R. | 1962 | Progress in Ele. Par. and
Cosmic Ray Phys. Vol. 6,
(North-Holland Public
Amsterdam) |
| Webber, W.R. | 1968 | Proc. Int. Conf. Cosmic Rays
(Calgary), Part A, 148 |
| Webber, W.R.
and J. J. Quenby | 1959 | Phil. Mag. 4, 645 |
| Wilcox, J.M. | 1968 | Space Sci. Reviews, 8, 258 |
| Wilcox, J. M.
and N. F. Ness | 1965 | J. Geophys. Res. 70, 5793 |
| Wilcox, J. M.
K. Schatten
and N. F. Ness | 1967 | J. Geophys. Res., 72, 19 |
| Wilkinson, D. H. | 1950 | Ionisation chambers and
counters, cambridge Univ Press. |
| Williams, D. J
and G. D. Mead | 1965 | J Geophys. Res., 70, 3017 |

- Willets, A. C., 1969 Pre-print, University of
W. K. Griffiths, Leeds, England
C. J. Hatton
and P. L. Marsden
- Wolfe, J. H., 1966 J. Geophys. Res., 71, 3329
R. W. Silva,
D. D. McKibbin
and R. H. Mason
- Wolfe, J. H. 1970 Space Science Rev., 10, 511
and D. S. Intriligator
- Wolf, R. A. 1970 J. Geophys., 75, 4677